

**Primary and immortalized
murine alveolar epithelial cells
as novel *in vitro* systems
for preclinical studies**

Dissertation

zur Erlangung des Grades des
Doktors der Naturwissenschaften
der Naturwissenschaftlich-Technischen Fakultät
der Universität des Saarlandes

vorgelegt von

Sandra Sapich
Saarbrücken 2018

Tag des Kolloquiums: 20. November 2018

Dekan: Prof. Dr. Guido Kickelbick

Berichterstatter: Prof. Dr. Claus-Michael Lehr

Prof. Dr. Robert Bals

Vorsitz: Prof. Dr. Marc Schneider

Akad. Mitarbeiter: Dr. Jessica Hoppstädtter

Eidesstattliche Erklärung

„Hiermit versichere ich, Sandra Sapich, an Eides statt, dass ich diese Arbeit ‚Primary and immortalized murine alveolar epithelial cells as novel *in vitro* systems for preclinical studies‘ selbstständig und nur unter Angabe der angegebenen Quellen und Verweise angefertigt habe. Die aus anderen Quellen oder indirekt übernommenen Daten und Konzepte sind unter Angabe der Quellen gekennzeichnet. Ich habe diese Arbeit bisher weder im In- noch im Ausland in gleicher oder ähnlicher Form in einem Verfahren zur Erlangung eines akademischen Grades vorgelegt.“

Saarbrücken, Juni 2018

Sandra Sapich

Die vorliegende Dissertation entstand unter Leitung von
Herrn Prof. Dr. Claus-Michael Lehr
in der Arbeitsgruppe „Drug Delivery“ am Helmholtz Institut für Pharmazeutische
Forschung Saarland (HIPS) in Saarbrücken.

Ich danke Herrn Claus-Michael Lehr für die Überlassung des Themas und die
Unterstützung bei der Durchführung dieser Arbeit.

Sowohl das Isolations- als auch das Immortalisierungsprotokoll muriner alveolarer
Epithelzellen wurden etabliert unter der Leitung von

Frau Prof. Dr. Dagmar Wirth
in der Arbeitsgruppe „Model Systems for Infections“ am Helmholtz Zentrum für
Infektionsforschung in Braunschweig.

Ich danke Frau Prof. Dr. Dagmar Wirth für Ihre Gastfreundschaft und die
Unterstützung bei der Durchführung dieser Arbeit.

“OUR GREATEST WEAKNESS LIES IN GIVING UP.
THE MOST CERTAIN WAY TO SUCCEED
IS ALWAYS TO TRY JUST ONE MORE TIME.”

~ THOMAS EDISON

This thesis was conducted as part of the project CILIA
("Conditional immortalization of murine alveolar epithelial cells")
funded by ZEBET ("Zentralstelle zur Erfassung und Bewertung von Ersatz- und
Ergänzungsmethoden zum Tierversuch")
at the BfR ("Bundesagentur für Risikobewertung")
under the grant agreement FK 3 - 1328 - 474.

Table of Contents

Table of Contents	7
Abstract	10
Kurzzusammenfassung	11
1 Introduction.....	12
1.1 The respiratory system and its functions	12
1.1.1 Features of the alveolar epithelium.....	16
1.1.2 Pharmaceutical relevance of drug delivery through the lungs	18
1.2 Cell systems - general and lung-specific applications	20
1.2.1 Primary culture of alveolar epithelial cells.....	21
1.2.2 Cell lines featuring characteristics of the alveolar epithelium	22
1.3 Generation of cell lines and conventional immortalization approaches	23
1.3.1 Immortalization by lentivirus-mediated transduction with a defined set of proliferation-promoting genes.....	25
1.3.2 Immortalization by conditional expression of SV40 TAg.....	27
1.4 Starting point and aim of this work	28
2 Material & Methods.....	30
2.1 Buffer solutions.....	30
2.2 General cell culture	31
2.2.1 Cell lines and primary cells.....	31
2.2.2 Cell cultivation	32
2.2.3 Freezing and thawing of cells	33
2.2.4 Cell counting.....	33
2.3 Mouse strains and ethical statement	34
2.4 Isolation procedure of primary alveolar epithelial cells	34
2.1 Immortalization of primary mAEpC	37
2.1.1 Production of lentiviral vector systems	37
2.1.2 Lentiviral gene transfer to transduce mAEpC	38

2.1.3	Cultivation of mELVi cells.....	38
2.1.4	Analysis of gene integration pattern of mELVi cells	39
2.2	TEER measurement.....	41
2.3	Morphological characterization	42
2.3.1	Histology.....	42
2.3.2	Confocal Laser Scanning Microscopy (C-LSM).....	42
2.3.3	Transmission electron microscopy (TEM)	43
2.4	Flow cytometry	43
2.5	RNA extraction and cDNA synthesis to analyze marker expression	44
2.6	Paracellular transport studies.....	46
2.7	Cytotoxicity assay.....	47
2.8	Statistics	48
3	Results & Discussion	49
3.1	Towards an optimized isolation procedure to obtain primary mAEpC	49
3.1.1	Magnetic beads mAEpC cell separation versus flow cytometric cell sorting methods.....	50
3.1.2	Purity and yield of isolated primary mAEpC	50
3.2	Characterization of primary mAEpC	52
3.2.1	Trans-differentiation and ultrastructure of mAEpC.....	52
3.2.2	Barrier properties of primary mAEpC upon different cultivation conditions	54
3.2.3	Comparison of primary mAEpC and hAEpC cultures	58
3.3	Towards an optimized immortalization approach to generate cell lines originating from mAEpC	60
3.3.1	Lentiviral-mediated transduction of mAEpC with a vector system conditionally expressing the Simian Virus 40 Large T antigen	60
3.3.2	Lentiviral-mediated transduction of mAEpC with the CI-SCREEN immortalizing gene library.....	62
3.3.3	Gene integration pattern and minimal set of immortalizing genes	63
3.3.4	Transduction of wildtype mAEpC with the defined minimal set of immortalizing genes.....	66

3.4	Characterization of mAELVi cell populations.....	67
3.4.1	Morphological characterization of mAELVi cells.....	68
3.4.2	Expression of alveolar epithelial characteristics of mAELVi cells	69
3.4.3	Expression of TJ proteins and barrier properties of mAELVi.E and mAELVi.wt cells	73
3.4.4	Characterization of mAELVi.J cells.....	78
3.4.5	Tabular characterization summary of mAELVi populations	80
3.5	Transport studies.....	81
3.6	Cytotoxicity studies.....	85
4	Conclusion & Outlook.....	88
5	Appendix	93
5.1	List of abbreviations	93
5.2	List of figures	96
5.3	List of tables	99
References.....	100	
Scientific output.....	116	
Curriculum vitae.....	117	
Danksagung.....	118	

Abstract

To deliver drugs via the lungs, compounds must overcome the air-blood barrier, which is, *inter alia*, being tested in mice during early stage drug development. To help meet the 3R principle ('refine, reduce replace') and potentially reduce the number of mice used in this context, this study aimed at the generation of novel murine cell lines displaying features of the alveolar epithelium.

As an initial step, reliable and efficient protocols for the isolation and cultivation of primary murine alveolar epithelial cells (mAEPc) were established. Like the human equivalent (hAEpC), mAEPc trans-differentiate *in vitro* from an alveolar epithelial type II (ATII) to an ATI-like phenotype and build a thin monolayer with high transepithelial electrical resistance (TEER_{max} ~1900 Ωcm²) when grown on permeable filter supports (Transwells®) demonstrating tight junction functionality. To generate cells with unlimited growth capacity, primary mAEPc from different mouse strains were lentivirally transduced with a library consisting of 33 *bona fide* proliferation-promoting genes. Upon the integration of certain genes in to the mAEPc genome, 10 genetically distinct maelvi (murine alveolar epithelial lentivirus immortalized) cell populations could be expanded, of which the most promising ones – maelvi.E and maelvi.wt – were further characterized regarding their potential use in drug transport and inhalation toxicity studies.

Kurzzusammenfassung

Um eine gewünschte Wirkung über die pulmonale Route erzielen zu können, müssen potentielle Arzneistoffe die Blut-Luft-Schranke in der tiefen Lunge überqueren, was u.a. im Rahmen der frühen Medikamentenentwicklung an Tieren getestet wird. Unter Berücksichtigung des 3R-Prinzips (‘refine, reduce, replace’) zielte diese Arbeit darauf ab, neuartige murine Zelllinien mit Eigenschaften des Alveolarepithels zu generieren, um dazu beizutragen die Zahl der in vorklinischen Studien eingesetzten Mäuse zukünftig reduzieren zu können.

Hierfür wurden geeignete Methoden zur Isolation und Kultivierung primärer alveolarer Epithelzellen der Maus (mAEPc) etabliert. Diese trans-differenzieren *in vitro* und bilden eine dünne Schicht aus alveolaren Typ I-ähnlichen Epithelzellen mit hohem transepithelialen elektrischem Widerstand und folglich funktionalen ‚Tight Junctions‘. Um Zelllinien mit unbegrenzter Teilungsfähigkeit zu erhalten, wurden mAEPc mit Hilfe einer aus 33 lentiviralen Expressionsvektoren bestehenden Bibliothek verschiedener proliferationsfördernder Gene transduziert. Aufgrund der Lentivirus-vermittelten Integration potentieller Immortalisierungsgene in das mAEPc-Genom, entstanden 10 genetisch unterschiedliche, expandierbare mAELVi-Zellpopulationen (‘murine alveolare Epithelzellen Lentivirus-immortalisiert’), deren Eignung als *in vitro* Systeme für vorklinische Studien anhand von Transport- und Zytotoxizitätsstudien im Rahmen der vorliegenden Arbeit untersucht und beurteilt wurde.

1 Introduction

1.1 The respiratory system and its functions

Few processes in biology are as ancient and pivotal for life as respiration, the mechanisms of transporting oxygen and carbon dioxide between the cells of an organisms and the external environment to ensure energy generation in terms of adenosine triphosphate (ATP) by oxidative phosphorylation. Animals exhibit specialized systems that enable an efficient exchange of gasses through respiratory membranes driven by passive diffusion (Weibel, 2011).

In mammals, the respiratory system comprises the conducting airways which direct the inhaled oxygen-rich air through branching structures of the lung finally guiding the airflow into the deep lung, the so-called respiratory zone, where the gas exchange with the blood takes place. During expiration the carbon dioxide-enriched air moves in the opposite direction. Both areas exhibit different structures consisting of different types of specialized cells comprising the respiratory epithelium whose thickness decreases the deeper the air is inhaled. Concurrently, the morphology of the epithelial lining changes from a complex pseudostratified ciliated one in the upper airways to columnar and cuboidal in the lower parts to a simple squamous epithelium on the respiratory surface within the deep lung (Bur & Lehr, 2008; de Souza Carvalho *et al.*, 2014; Steimer *et al.*, 2005). Figure 1 shows a simplified scheme of the structure and occurring cell types of the airway epithelia at the three principal levels of the respiratory system covering the trachea and bronchi, bronchioles as well as alveoli (Klein *et al.*, 2011). Furthermore, figure 2A highlights the organization and anatomy of the human lung.

The **conducting airways** begin with the nasal cavities followed by the trachea which divides into the bronchi. In this area, the pseudostratified epithelium is covered by a thick layer of high viscous lining fluid, the mucus, which is produced by secretory goblet cells (Sanders *et al.*, 2009). Moreover, it is mainly composed of basal and ciliated epithelial cells which are necessary for mucociliary clearance, the self-cleaning mechanism of the upper airways (Barton & Lourenco, 1973).

Furthermore, each bronchus branches into smaller bronchi which further divide into numerous bronchioles which represent the margin between the conducting and the

respiratory zone (also see figure 2). These conducting tubes are the first part of the airways that is no longer supported by cartilage and mainly consists of ciliated epithelial cells as well as non-ciliated cells, known as Club or Clara cells (McDowell *et al.*, 1978). The main functions of these bronchiolar exocrine cells include the secretion of glycosaminoglycans, the participation in xenobiotic metabolism, the modulation of inflammatory responses and the regeneration of both themselves and ciliated cells (Rokicki *et al.*, 2016; Roth *et al.*, 2013).

In general, the main functions of these upper airways are to filter, warm and moisten the airflow as well as to build a physical barrier against inhaled xenobiotics.

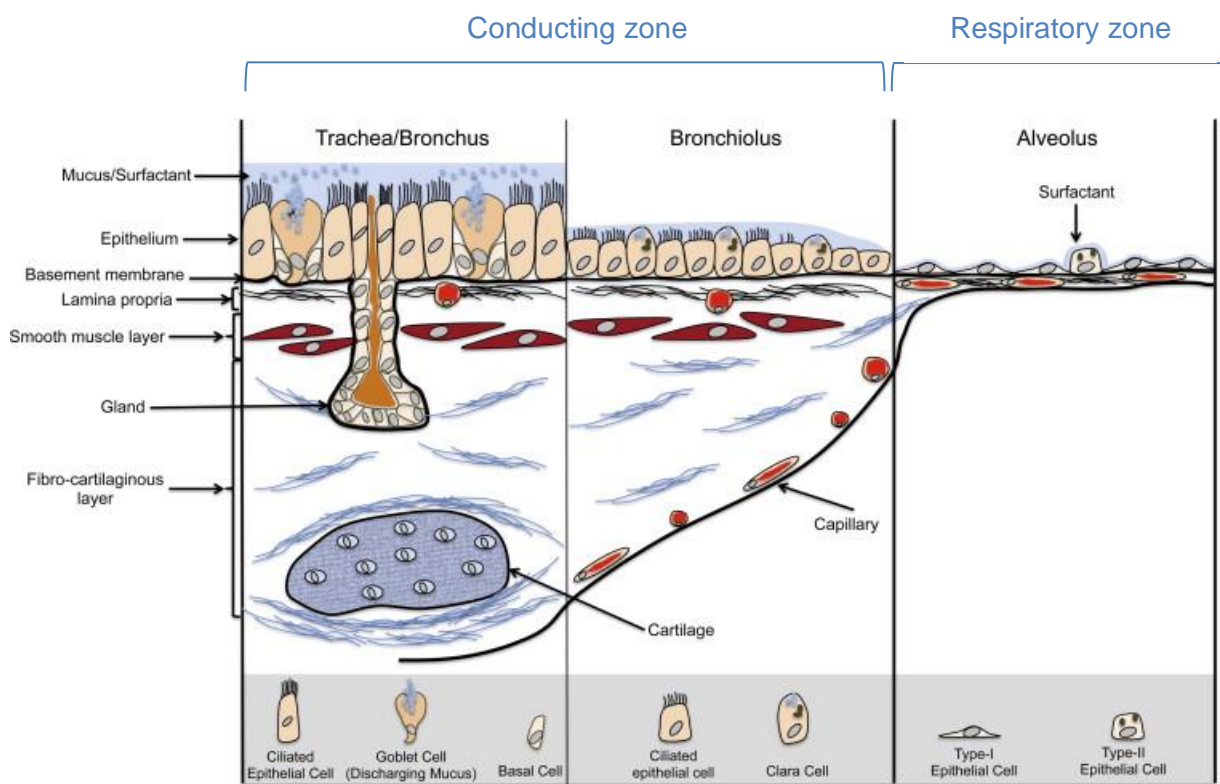
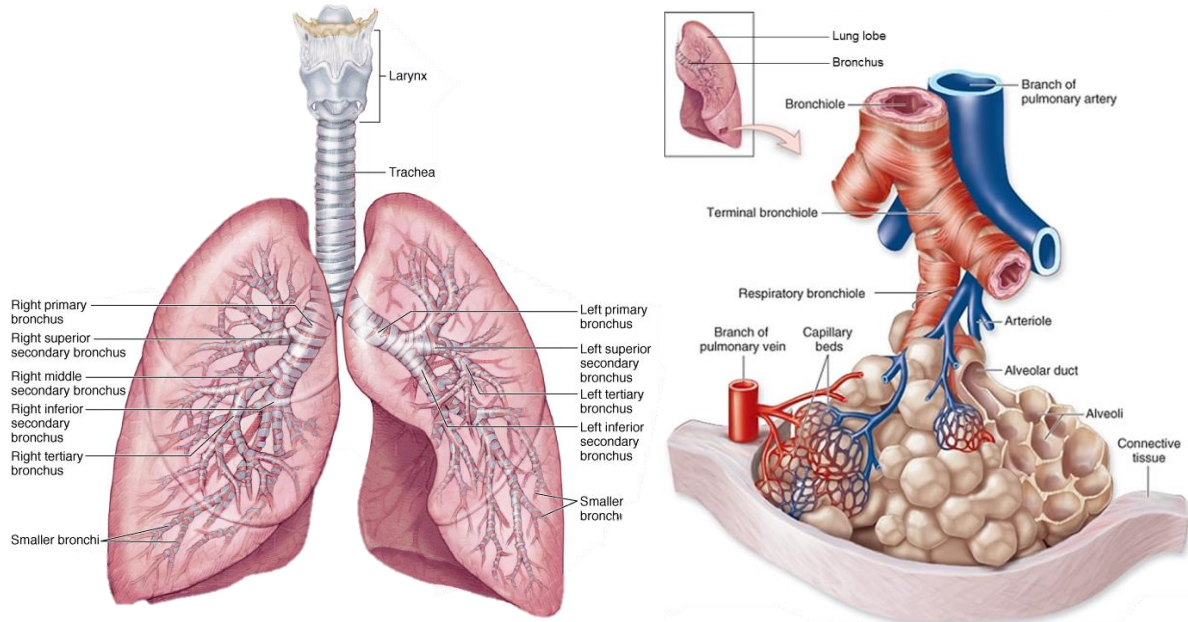


Figure 1: Structure of the airway epithelia and main cell types occurring at the 3 principal levels of the respiratory system: the trachea/bronchi, bronchioles and alveoli; adapted and modified from Klein *et al.* (2011).

The **respiratory zone** begins with the extension of terminal bronchioles into respiratory bronchioles, which further divide into alveolar ducts. Here, the number of alveoli, tiny air-containing sacs, increases and finally the airways end in grapelike clusters consisting entirely of alveoli (~300 million in an adult human lung). The lining alveolar epithelium has the total surface area of a tennis court (~ 140 m²) (Weibel, 2011) and consists of mainly two different types of pneumocytes, alveolar type I (ATI) and type II (ATII) epithelial cells. Besides, alveolar macrophages are present in the alveoli as part of the residing innate immune system.

As the basement membranes of the alveolar-surface epithelium and the capillary-wall endothelia fuse in many places within an alveolus, the blood stream is separated from the air only by the 100 - 500 nm thin monolayer of alveolar epithelial cells representing the so-called air-blood barrier. The alveolar epithelium and the comprising cell types are illustrated in figure 2B and described in more detail in the following section.

A. The organization of the human respiratory system



B. The alveoli – the site of gas exchange

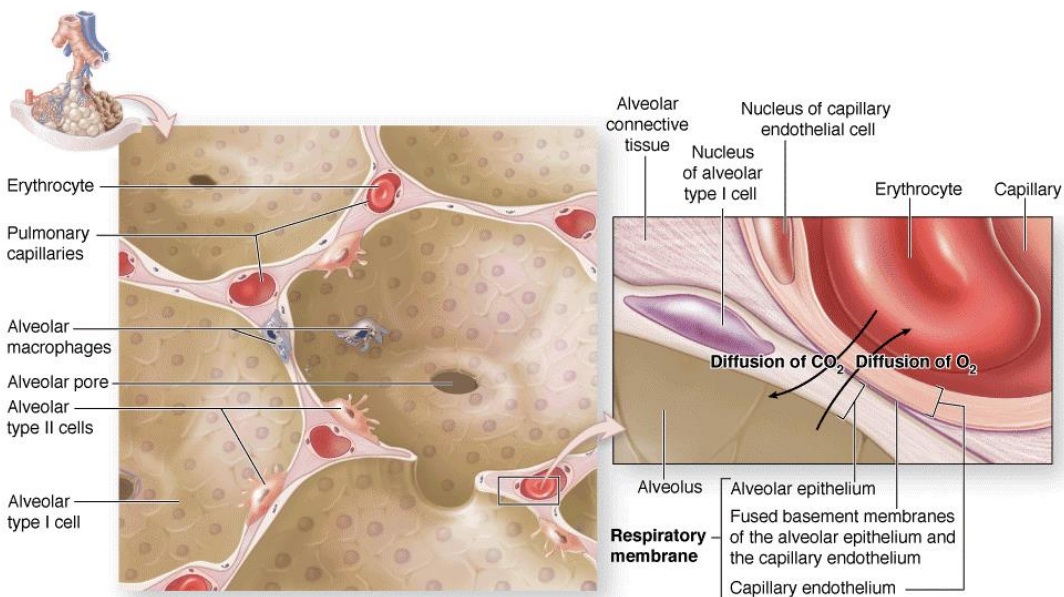


Figure 2: A - Organization of the human respiratory system emphasizing the anatomy of the lung and the air-conducting structures terminating in alveolar sacs; **B - The alveoli and comprising cell types** of the area of the alveolar epithelium and capillary endothelium displaying the air-blood barrier as the site of gas exchange; illustrations were adapted and modified from Mescher (2016).

1.1.1 Features of the alveolar epithelium

At the site of gas exchange, the alveolar lining comprises cellular and connective tissue components such as extracellular matrix. Cellular components encompass endothelial capillary wall cells lining the surrounding blood vessels as well as the two types of alveolar epithelial cells (ATI and ATII) and alveolar macrophages (see figure 1 and 2B).

The squamous **ATI** cells are very thin (50 – 100 µm in diameter, volume of 2000 - 3000 µm³) with broad cytoplasmic extensions forming a barrier sealed with tight junction complexes across which gas exchange occurs (Crandall & Matthay, 2001; Crapo *et al.*, 1982).

ATI cells also adhere to each other through dynamic intercellular junctions called desmosomes which form a linkage between the intermediate filaments of two cells (Garrod & Chidgey, 2008). Additionally, they exhibit the highest known water permeability of any mammalian cell type indicating an important role in the maintenance of alveolar fluid homeostasis (Schmidt *et al.*, 2017). Although the ATI population covers up to 98% of the total alveolar surface area, it only represents ~ 10% of cells being present in the lung (Dobbs *et al.*, 2010).

The highly specialized **ATII** cells are smaller (10 - 20 µm in diameter, volume of ~450 – 900 µm³), cuboidal in shape and cover the remaining ~2 - 4% of the surface region (Crapo *et al.*, 1982). ATII cells exhibit progenitor potential and can recover the alveolar epithelium after lung injuries or upon primary culture of isolated ATII cells (Daum *et al.*, 2012; Elbert *et al.*, 1999), respectively, by trans-differentiating into ATI-like cells (Bhaskaran *et al.*, 2007). In addition, ATII cells play a role in defense mechanisms, e.g. against viral infections, by expressing Toll-like receptors and MHCII (class II major histocompatibility complex) molecules as well as responding to cytokines and chemokines (Qian *et al.*, 2013; Steimer *et al.*, 2005; J. Wang *et al.*, 2011). However, their main function entails the production, secretion and recycling of **surfactant** ('surface active agent'), the complex alveolar lining fluid consisting of phospholipids and proteins which reduces the surface tension and stabilizes the alveoli. Therefore, ATII cells possess unique secretory organelles, termed lamellar bodies, which synthesize and store the four surfactant proteins (SP-A, -B, -C and -D) and surfactant lipids (Wright, 2005).

Type I and II cells are coupled by both tight junctions (TJ) and gap junctions providing dynamic, selectively permeable barrier functions and pathways for intercellular communication (Crandall & Matthay, 2001; Isakson *et al.*, 2001a). Two main ways of transepithelial transport across the air-blood barrier have been described: the paracellular and the transcellular route (see figure 3).

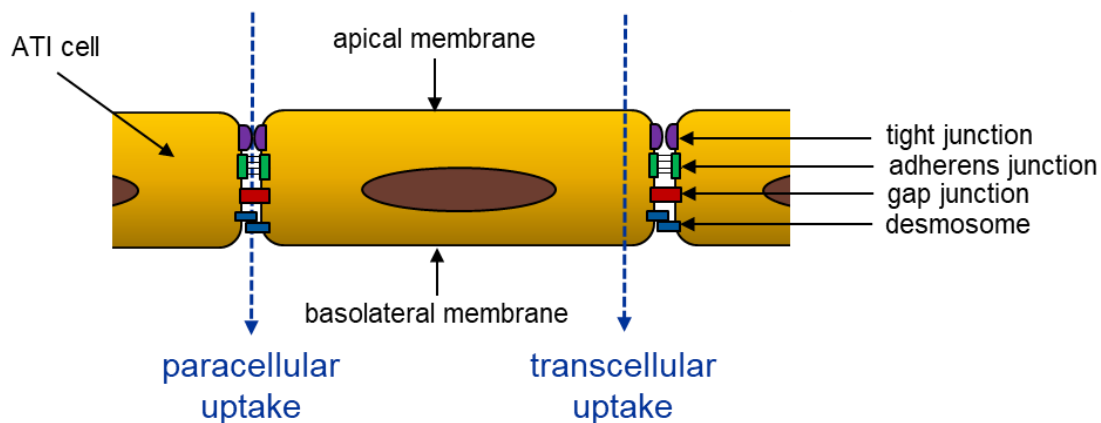


Figure 3: Scheme of the two main ways of transport across the air-blood barrier –the paracellular and the transcellular route. Paracellular uptake into the bloodstream occurs through the intercellular space of adjacent ATI cells and is regulated by junctional complexes (tight junctions, adherens junctions, gap junctions and desmosomes, shown schematically). In contrast, transcellular uptake through the cell membranes is mediated either by transporter proteins or transcytosis.

TJ and associated protein complexes have been identified to regulate the passive transport of solutes, ions and small molecules (molecular weight ≤ 40 kDa) between the alveolar and interstitial space of adjacent epithelial cells (Gunzel & Yu, 2013; Schneeberger & Lynch, 2004). The complexes are composed of various TJ transmembrane proteins (e.g. occludin, claudins, junctional adhesion molecules), cytoplasmic adaptors linked to the actin cytoskeleton (e.g. ZO-1, -2, 3) and signaling molecules (e.g. protein kinase C, PKC) enabling the dynamic regulation of the paracellular transport (Mária A. Deli, 2009b). Together, they form a boundary between the apical and basolateral domains of epithelial (and endothelial), which seals the intercellular spaces of neighboring cells and contributes to the maintenance of the cell surface polarity (Balda & Matter, 2000). This mechanical barrier function can, in part, be measured as transepithelial electrical resistance (TEER) reflecting the tightness of a cell monolayer, and is a prerequisite for directional paracellular flux (Gunzel & Yu, 2013). Calcium chelators, such as EDTA (ethylenediaminetetraacetic acid), serve as

absorption enhancers through the disassembly of TJ (and adherens junctions) which is triggered by the activation of PKC resulting in higher cell monolayer permeability and decreased barrier integrity (M. A. Deli, 2009a; Tomita *et al.*, 1996).

Transcellular transport can either depend on the polarized distribution of ion channels (e.g. epithelial Na⁺ channels, ENaCs) and drug transporters (for more detail refer to chapter 1.1.2) or be mediated vesicular by transcytosis (Hollenhorst *et al.*, 2011; Van Driessche *et al.*, 2007).

Although the main function of the air-blood barrier entails the exchange of oxygen and carbon dioxide between the air-facing (apical) and blood-facing (basolateral) surfaces, it also exhibits a defense mechanism to prevent harmful particles from entering the blood system (Tam *et al.*, 2011). Therefore, alveolar macrophages, as the residing part of the innate immune system, keep the alveolar lining under guard and phagocytose inhaled toxins or microorganisms, a mechanism described as alveolar clearance (Bur & Lehr, 2008).

Finally, the efficiencies of gas exchange and host defense rely on the integrity of the alveolar epithelium and its dynamic interaction with the surrounding (Barkauskas *et al.*, 2013; Ganesan *et al.*, 2013). Dysregulation or malfunction of the pathways involved in maintaining the barrier function of these cells can result in a loss of integrity and thus, can lead to the first signs of many pulmonary diseases such as acute lung injury (Herold *et al.*, 2013), lung fibrosis (Camelo *et al.*, 2014), asthma (Tsicopoulos *et al.*, 2013) or cystic fibrosis (Castellani *et al.*, 2012).

1.1.2 Pharmaceutical relevance of drug delivery through the lungs

Delivering drugs through the lung not only provides the possibility to target local diseases such as asthma or COPD (Chronic obstructive pulmonary disease), but also offers great potential for rapid, non-invasive systemic delivery of therapeutics. Due to the huge alveolar absorptive surface, high permeability and a low concentration of local drug-metabolizing or -degrading enzymes, particles of highly dispersed aerosols deposited in the lungs by inhalation are absorbed into the blood circulation with high bioavailability avoiding hepatic and intestinal first-pass effects (Patton & Byron, 2007).

Particularly for drugs with poor oral absorption, such as peptides and proteins (e.g. inhaled insulin to treat diabetes), the pulmonary route of administration is a promising alternative to reach the systemic circulation. In this context, two groups of transport systems can be distinguished: cell membrane-associated transporters for ions or small molecules (e.g. the cystic fibrosis transmembrane conductance regulator CFTR) and vesicle- or Caveolae-mediated translocation of macromolecules. The latter is particularly interesting for an increasing number of biopharmaceutics such as nucleic acid-based polymers or hormones (Steimer *et al.*, 2005; Uchenna Agu *et al.*, 2001).

Besides, a variety of drug transporters including peptide transporters, the P-glycoprotein (P-gp), multidrug resistance-related proteins (MRP) and organic cationic transporters were found to be present in the lung offering potential targets for either local or systemic drug delivery (Groneberg *et al.*, 2002; Salomon & Ehrhardt, 2012). Among these, the impact of the ATP-dependent efflux pump P-gp, also known as multidrug resistance protein 1 (MDR1), on pulmonary absorption and disposition has been studied most extensively. P-gp substrates are excreted back into the alveolar space, whereby the efficacy of a potential drug substance is significantly reduced (Nickel *et al.*, 2016).

However, the current understanding of what happens to a specific drug formulation after depositing in the deep lung is still limited and requires extensive investigations of the interactions between the compound, the delivery or carrier system and the air-blood barrier (Agrahari *et al.*, 2016; Patil & Sarasija, 2012; R. Mathias *et al.*, 1996). Therefore, novel *in vitro* approaches to mimic the air-blood barrier are needed to elucidate drug delivery via the lung regarding the ADMET principle and risk assessment in order to prove the safety and effectiveness of a pharmaceutical formulation before entering clinical trials (Hittinger *et al.*, 2015).

1.2 Cell systems - general and lung-specific applications

Since the first human cell line HeLa was established in the 1950s (Leighton & Kline, 1954), *in vitro* cell cultures of mammalian cells have become indispensable tools in research, biotechnology and medicine disciplines with numerous applications. These include basic research, where cell systems are used to analyze individual gene functions and regulation as well as to elucidate complex signaling pathways or immunological questions. In the field of biotechnology, cell systems are used to produce therapeutic proteins (e.g. antibodies) (Lindl, 1996), to screen for novel drugs or potential drug targets (Yin & Kassner, 2016) or to predict the effectiveness, properties and toxicology as part of preclinical studies during early drug development. In addition, cell cultures have recently been utilized for therapeutic purposes including cell-based therapies in regenerative medicine (Gerlach & Zeilinger, 2002), tissue engineering (Lee *et al.*, 2009) and some diagnostics. For each of these applications, different cellular features and characteristics are required with the foremost aim to mimic the *in vivo* physiology as closely as possible.

Accordingly, primary cells are often the first choice and represent the gold standard, but at the same time their usability is narrow due to limited availability, limited lifespan and cell heterogeneity caused by different donors or varieties in batch-to-batch isolations. Thus, immortalized cells or cell lines are the preferred tools for many routine applications because they can overcome most of the difficulties of primary cells. This results from the fact that cell lines offer unlimited availability, display homogenous cell populations and enable the possibility of controlled genetic manipulation. Nevertheless, cell lines exhibit one major drawback which is their restricted physiology and the loss or lack of cell type specific functions (Lipps *et al.*, 2013). For that reason, scientists focus on the maintenance of such characteristics and investigate novel approaches for the generation of cell lines featuring cell-specific attributes.

In this context, primary and cell line-based *in vitro* systems of the alveolar epithelium have been established which are described in the following sections. Upon ADMET investigations, animal testing is still the most common model applied for risk assessment, disease research and the development of novel drugs. To eventually reduce the number of animals used in this context according to the 3R principle (Balls *et al.*, 1995), alternative systems such as cell culture models of the air-blood barrier

became of utmost investigational interest. However, such *in vitro* systems, especially those based on cell lines, often consign unresolved questions in relation to the realistic *in vivo* situation (Horvath *et al.*, 2015), but concurrently provide simplicity, robustness, cost-effectiveness and advanced control in data acquisition.

1.2.1 Primary culture of alveolar epithelial cells

During the last decades, primary alveolar epithelial cells from various species, including mouse (Corti *et al.*, 1996), rabbit (Saha *et al.*, 1996), rat (J. Chen *et al.*, 2004; Gonzalez *et al.*, 2005; S. Wang & Hubmayr, 2011) and pig (Steimer *et al.*, 2006), have been isolated to probe structure as well as to characterize morphological and functional changes upon varying cultivation conditions.

Since they were first described (Elbert *et al.*, 1999) and consistently optimized (Daum *et al.*, 2012), primary human alveolar cells (hAEpC) are still the most mimetic cell model reflecting features of the air-blood barrier like high transepithelial electrical resistance (TEER) and as a consequence, functional tight junctions. This is why hAEpC have been deployed for many investigations such as pulmonary absorption and transport studies of xenobiotics or nanoparticles (Bur *et al.*, 2006; Endter *et al.*, 2007; B. Forbes & Ehrhardt, 2005; Thorley *et al.*, 2014; Yacobi *et al.*, 2010) and virus infection research (J. Wang *et al.*, 2011). Recently, hAEpC have also been co-cultured with primary alveolar macrophages isolated from the same donor tissue to establish an advanced model of the air-blood barrier applicable for investigations of aerosol deposition of pharmaceutical formulations (Hittinger *et al.*, 2016a; Hittinger *et al.*, 2016b).

Similar to hAEpC, primary murine alveolar epithelial cells (mAEpC) also mimic the air-blood barrier (Demaio *et al.*, 2009) and can be utilized as an *in vitro* model to study respiratory virus infections (Kebaabetswe *et al.*, 2013) or immune responses upon *Pseudomonas aeruginosa pneumonia* infection (Wolf & Sapich *et al.*, 2016). As an advantage over hAEpC, murine data from mApC can be generated from a specific knock-in or knockout mouse strains which offers the possibility to compare both *in vitro* and *in vivo* findings, as recently demonstrated.

1.2.2 Cell lines featuring characteristics of the alveolar epithelium

Alveolar epithelial cell lines are useful tools to study biochemical aspects of healthy and diseased conditions, but concurrently exhibit dedifferentiated characteristics like impaired tight junction providing only limited application for barrier-dependent investigations. As an example, the human alveolar type II-like cell line A549, derived from an adenocarcinoma, is widely applied for toxicity studies (Foldbjerg *et al.*, 2011; Kreja & Seidel, 2002; Lestari *et al.*, 2012) but lacks high TEER and is thus, not well suited for drug adsorption studies (Foster *et al.*, 1998). The human alveolar type I-like cell line TT1 ('transformed type-1') was obtained through immortalization of primary ATII cells which were retrovirally transduced with hTERT and a temperature sensitive mutant of the Simian Virus 40 (SV40) large T antigen (Kemp *et al.*, 2008; O'Hare *et al.*, 2001). Immortalization methods and genes are addressed in the following chapter (see 1.3). In fact, TT1 cells have been used to study nanoparticle uptake (Kemp *et al.*, 2008) as well as inflammatory responses and barrier properties (van den Bogaard *et al.*, 2009). In the latter study, it was shown that TT1 did not develop high TEER limiting their applicability to barrier-independent experiments. This example illustrates that the genomic alterations upon cellular transduction might cause a loss of functional properties.

Recently, a breakthrough in the immortalization of primary hAEpC could be achieved by which hAELVi (human alveolar epithelial lentivirus immortalized) cells were obtained (Kuehn *et al.*, 2016). The hAELVi cell model represents the first described human alveolar epithelial cell line featuring the development of high TEER due to functional tight junctions. By now, the cell line, referred to as 'huAEC', is commercially available from InSCREENeX GmbH (Braunschweig, Germany) providing a suitable tool to mimic the air-blood barrier. This approach offers great potential to bridge the gap between the scientific limitations of *in vitro* systems and preclinical applications, especially regarding the replacement or reduction of animal testing used in these premises. Considering that cell culture systems are more and more considered as alternatives to animal testing, thereby overcoming ethical concerns, the interest in the development of cell lines has emerged in recent years.

1.3 Generation of cell lines and conventional immortalization approaches

As the application of primary cells is bounded by several limitations (e.g. ethical concern, limited availability and life span, genetic heterogeneity, batch-to-batch variations), the need for novel cell lines, which can overcome these drawbacks, has led to the development of various cell immortalization approaches in recent years (Lipps *et al.*, 2013).

On the one hand, the generation of cell lines could be achieved by spontaneous immortalization. In this context, murine embryonic fibroblasts (MEF) were immortalized by continuous low-density passaging of primary cells *in vitro* according to a cultivation method that became known as '3T3 protocol' (Todaro & Green, 1963) which yielded numerous infinitely growing NIH3T3 cell lines. Furthermore, immortal cells can be isolated from tumors such as HeLa cells representing the most ancient human cell line originally derived from a cervical carcinoma in 1951. However, tumor-derived cells are often characterized by chromosomal instability, non-defined (epi-)genetic alterations and aberrant growth control (Castro-Gamero *et al.*, 2013; Damia & D'Incalci, 2010; Stevens *et al.*, 2013) eventually causing dedifferentiation processes.

On the other hand, cell lines could be generated by vectored transfer of specific genes or viral DNA *in vitro*. As a prominent example for the latter, the human cell line HEK293T was generated by transfer of a mix of sheared adenovirus type 5 DNA into primary human embryonic kidney cells (Graham *et al.*, 1977). In subsequent years it was shown that the immortalization of HEK293T was most likely to be triggered by the genome integration of the viral genes E1A and E1B (Louis *et al.*, 1997). Another distinguished virus associated with immortalization of particularly B lymphocytes is the Epstein-Barr virus (EBV). Although the responsible EBV-genes are not yet fully characterized, the EBV-mediated generation of B-cell lines is being routinely applied for the production of human monoclonal antibodies (Traggiai, 2012).

Aside from that, immortalization of primary cells could be achieved by transduction of viral immortalizing genes. In this context, the Simian Virus 40 (SV40) large T antigen (TAg) was shown to be a broadly acting immortalizing gene due to its binding capacity to the tumor suppressor p53 and the subsequent inhibition of p53-dependent pathways (Hubbard & Ozer, 1999). In addition, TAg modulates the activity of numerous other cellular proteins causing inactivation of cell cycle control mechanisms which results in

an extended cell life span. However, immortalization attempts of human primary cells with TAg alone resulted in cell lines exhibiting dramatically altered phenotypes (Gazdar *et al.*, 2002).

Other viral oncogenes shown to be able to facilitate immortalization are the human papillomavirus (HPV) proteins E6 and E7 which interfere with host cell mechanisms associated with cell cycle control and the regulation of apoptosis. Upon transduction of primary amniotic epithelial cells with both E6 and E7, expandable cell lines were obtained which could not be confirmed in the case of single-gene transfer (Munger *et al.*, 2004).

Another well-known immortality gene is the human Telomerase reverse transcriptase (hTert) encoding the catalytic subunit of the telomerase enzyme which maintains the length of telomeres *in vivo*, thus abating the senescence process known as the ‘Hayflick limit’. Upon recombinant expression of hTert the repetitive telomer DNA-sequences are transcribed enabling the cell to undergo infinite cell divisions. With this approach, successful immortalization of many cell types could be established including human corneal epithelial cells (Robertson *et al.*, 2005) and mesenchymal stem cells (Bocker *et al.*, 2008). As another example, the continuously replicating human bronchial epithelial cells (HBEC) could be obtained by transduction of primary cells from non-cancerous and cancerous lung tissue with a combination of hTert and Cdk4, cyclin-dependent kinase 4 (R. D. Ramirez *et al.*, 2004). By this procedure HBEC retained epithelial characteristics, an intact p53 checkpoint and the cells did not form tumors upon engraftment into mice. However, the continuous expression of hTert over a longer period may induce changes in gene expression eventually resulting in a premalignant phenotype (Milyavsky *et al.*, 2003).

Although it may often be desirable to generate cell lines with unlimited capacities, it is even more important to ascertain that immortalization attempts do not cause structural or functional changes. In theory, the ideal cell line would be characterized by infinite growth, maintenance of genome integrity and retained cell-specific functions – challenges which could not be mastered in an adequate manner by any of the above-mentioned immortalization strategies. Therefore, cell type-specific and growth-controlled immortalization approaches are the subject of recent and ongoing investigations which are described in the following sections.

1.3.1 Immortalization by lentivirus-mediated transduction with a defined set of proliferation-promoting genes

As existing cell line-based *in vitro* models most commonly are not sufficiently reflecting desired *in vivo* properties, cell lines overcoming this problem are of high interest for the realistic elucidation of molecular and biochemical processes. It has been demonstrated by many conventional immortalization attempts (see previous chapter) that the major limitation upon the generation of cell lines entails the unpredictability of potentially occurring cellular changes. These findings also revealed that the single gene transfer of prominent immortalizing genes such as SV40 TAg or the HPV oncogenes E6/E7 mostly resulted in cell lines with inappropriate applicability. Thus, until today no universal system or immortalizing gene exists that would enable the generation of cell lines of any given cell type in unison with the maintenance of cell-specific functions. Taken together, it is highly probable that defined gene combinations could preferentially support the immortalization of specific cell types providing higher possibilities to retain both the natural physiology and function.

In this context, an advanced approach to immortalize primary cells by lentivirus-mediated transduction with a defined set of proliferation-promoting genes has recently been patented (May, Hauser, Klein, Zauers, & Schucht, 2016). This gene library (CI-SCREEN library, International patent US9453203 B2, InSCREENeX GmbH) consists of 33 distinct genes with immortalizing potential which were cloned into lentiviral expression systems under the control of the constitutively active SV40 promotor. Lentiviruses as member of the retrovirus family, with HIV (Human Immunodeficiency Virus) representing the most prominent example, exhibit the ability to integrate viral DNA into the genome of the infected host cell providing an efficient method for gene delivery (Stevenson, 2002). Upon ectopic transduction of primary cells with the above lentiviral library, a certain combination of immortalizing genes will most likely be integrated into the host's genome. If so, effectively transduced cells will form proliferating cell colonies which can further be expanded, while non-transduced cells would become senescent. It might also eventuate that cells will indeed be transduced, but the integrated gene combination could not trigger any proliferation-inducing mechanisms causing senescence, too. Thereby, the pattern of integrated genes in proliferating colonies can be assessed by basic PCR analysis revealing a potential set of cell-specific immortalizing genes. Based on the function-orientated characterization

of the obtained cell colonies, cell lines with the desired phenotype can eventually be established.

As proof of concept, this advanced immortalization strategy could efficiently be applied for the generation of murine small intestinal epithelial cell lines reflecting *in vivo* characteristics of the intestinal epithelium (Schwerk *et al.*, 2013).

Furthermore, the recently described human alveolar epithelial hAELVi cells, representing the first human cell line exhibiting *in vivo* properties of the air-blood barrier, was obtained by transduction of primary cells with the lentiviral gene library, as mentioned before (Kuehn *et al.*, 2016). These breakthroughs in cell immortalization offer great potential for pharmaceutical applications. Furthermore, the results demonstrate that physiological properties of primary cells could be maintained upon the outlined immortalization strategy, which was accordingly applied for this work to immortalize alveolar epithelial cells isolated from mice (see figure 4 for illustration).

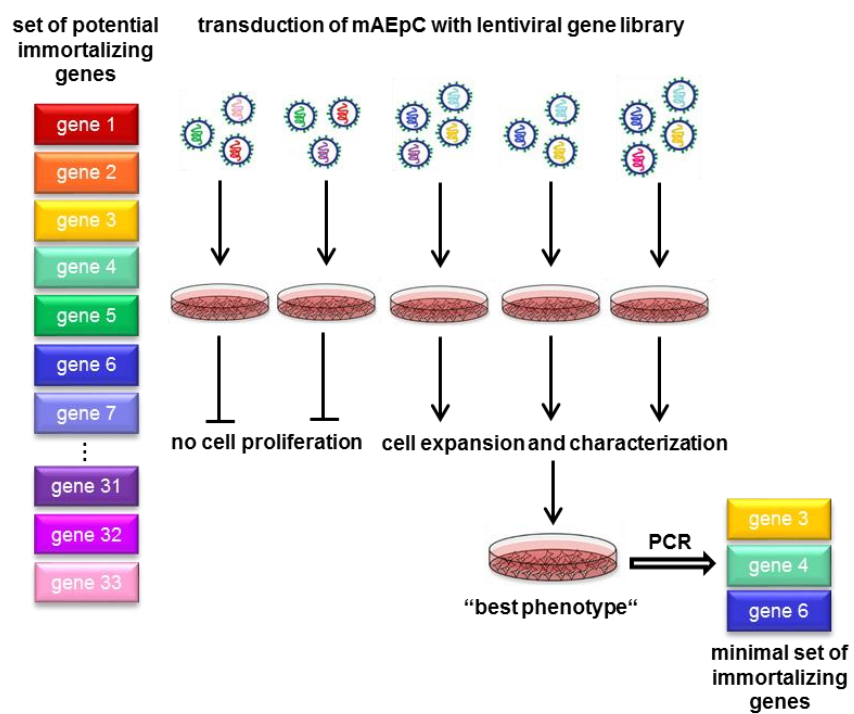


Figure 4: Scheme of immortalization strategy using 33 different lentiviral vector, each constitutively expressing a potential immortalizing gene (CI-SCREEN gene library; Lipps *et al.*, 2018) to transduce primary mAEpC. Upon transduction, the random integration of certain genes triggered cell proliferation while other integrated gene combinations had no growth-inducing effect. Proliferating cells were expanded and characterized in terms of the integration pattern and alveolar epithelial features.

1.3.2 Immortalization by conditional expression of SV40 TAg

As outlined in previous chapters, the clear majority of existing cell lines lack cell type-specific features due to gross cellular changes caused by the integration of immortalizing genes. Because of the correlating narrow applicability of such insufficient cell lines, alternative strategies enabling the conditional expression of introduced immortalizing genes to generate transcriptionally-controlled cell lines were investigated (Mignotte *et al.*, 1990). Such transgene regulation systems do not interfere with endogenous activities of the host cell's regulatory network. As an example, an improved version of the original tetracycline system (Gossen & Bujard, 1992) has been developed to enable conditional expression of immortalizing genes such as the SV40 Large T antigen (TAg). Thereby, not only the immortalizing but also the transgenic reverse transactivator gene (rtTA) are expressed under the control of a tetracycline-dependent promotor, building an autoregulated system. Only in the presence of the inducer tetracycline or its more stable analogue doxycycline (Dox), rtTA binds to the tetracycline-operator region of the promotor inducing a positive expression feedback loop (May *et al.*, 2006; Urlinger *et al.*, 2000).

Using such an autoregulated TAg expression cassette, transduced mouse embryo fibroblasts could be conditionally immortalized. In fact, proliferating cell clones were isolated in the presence of Dox whose growth-inducing effects could be completely reversed into growth arrest upon its absence in the cultivation medium. However, it has been shown that the expression of TAg changes the expression levels of more than 100 cellular genes. In absence of the inducer, these gene deregulations could be fully rescued providing an essential advantage over constitutively expressing immortalizing systems (Anastassiadis *et al.*, 2010; May *et al.*, 2004; May *et al.*, 2005).

1.4 Starting point and aim of this work

Before a potential drug will be approved for clinical trials by health authorities, the compound must proof its effectiveness and safety in numerous preclinical studies at several instances. During these studies, the efficient delivery of a drug is always dependent on its ability to cross the biological barrier it will face upon administration. To date, animal testing is indispensable in early ADMET studies prompting the need for alternative cell-based methods to reduce the number of mice consistent with the 3R principle.

Addressing the pulmonary route, thorough investigations of the air-blood barrier are the center of attention. Whereas primary human (Elbert *et al.*, 1999; Fuchs *et al.*, 2003) and rat (Hansen *et al.*, 2006; Yacobi *et al.*, 2007) *in vitro* cell models of the air-blood barrier are well characterized in the literature demonstrating their applicability for many areas in pulmonary research, little was known about murine alveolar epithelial cells (mAEpC). Despite isolation protocols for murine ATII have been described before (Corti *et al.*, 1996; Messier *et al.*, 2012), these primary cells were not characterized with regard to barrier properties. Nevertheless, the *in vitro* trans-differentiation of murine ATII into ATI-like cells alongside with an improved isolation protocol could be outlined by Demaio *et al.* (2009). It could further be demonstrated that isolated mAEpC form tight, polarized monolayers when grown on laminin 5-coated permeable filter supports, thus featuring characteristics of the air-blood barrier. However, no murine alveolar cell line exhibiting similar *in vivo* attributes yet exists.

For these reasons, and to help meet the 3R principle, this work aimed at the generation of novel *in vitro* systems of the murine alveolar epithelium originating from primary cells.

As a starting point to generate novel cell lines featuring ATI-like functions, an efficient and reliable isolation procedure to obtain mAEpC was established based on existing human (Daum *et al.*, 2012) and murine (Demaio *et al.*, 2009) protocols. These primary cells were isolated either from wildtype or transgenic ROSAConL mice exhibiting a luciferase gene under the control of the ubiquitously active ROSA26 promotor (Sandhu *et al.*, 2011). The luciferase activity might be useful as a cell tracker upon *in vivo* studies, e.g. engraftment experiments to investigate lung cell regeneration after injury,

as previously outlined for murine ATII cells (Hoffman & Ingenito, 2012; P. M. Wang & Martin, 2013), but was not further addressed.

Proceeding from previous findings (Demaio *et al.*, 2009), the Transwell® cultivation conditions for mAEpC were optimized with the aim to achieve the best possible formation of an ATI-like monolayer with high TEER. In this context, it was demonstrated that the cell seeding density, the medium composition and the presence of specific cell attachment proteins have a strong impact on the development of integer monolayers (Isakson *et al.*, 2001b). To mimic the *in vivo* situation of the alveolar epithelium as closely as possible, submerged cultures of mAEpC (equals liquid-covered conditions, LCC) were lifted to the air by removing the cultivation medium from the apical Transwell® compartments setting up air-liquid-interface (ALI) conditions.

In a next step to generate novel cell lines of the murine alveolar epithelium, primary mAEpC exhibiting barrier properties were transduced with a lentiviral library consisting of 33 different proliferation-promoting genes (see figure 4 for a scheme of the immortalizing strategy). Based on this immortalization approach (Lipps *et al.*, 2018; May *et al.*, 2016), 10 distinct **mAELVi** (murine alveolar epithelial lentivirus-immortalized) cell populations with a prolonged lifespan compared to untreated mAEpC were obtained and characterized regarding their alveolar epithelial features and barrier properties. Besides, the overall pattern of integrated genes was analyzed with the objective to identify cell type-specific immortalizing genes and define a minimal set of genes applicable for the generation of mAELVi populations isolated from a specific knock-in or knock-out mouse strain.

Based on these findings, mAELVi.E (originating from ROSAConL mice) and mAELVi.wt (originating from wildtype mice) populations were selected and applied for the assessment of absorption rates in comparison with primary cells, and the prediction of acute inhalation toxicity to evaluate their potential to eventually reduce the number of mice used during preclinical studies.

2 Material & Methods

2.1 Buffer solutions

The compositions of different buffer solutions and the respective application are listed in table 1. All mentioned buffers are water-based (Millipore Milli-Q® purified water). For the adjustment of pH levels either hydrochloric acid or sodium hydroxide solution, respectively, was used.

Table 1: Composition of buffer solutions and respective applications.

BSSB, pH 7.4 <i>Balanced Salt Solution Buffer was used for the isolation procedure of mAEpC.</i>	137 mM NaCl 5.0 mM KCL 0.7 mM Na ₂ HPO ₄ * 7 H ₂ O 10 mM HEPES 5.5 mM D-glucose 1.2 mM MgSO ₄ * 7 H ₂ O 1.8 mM CaCl ₂ * 2 H ₂ O 1% penicillin/streptomycin
HEBS, pH 7.1 <i>HEPES Buffered Saline was used for transient transfection of HEK293T as part of the production of lentiviruses.</i>	280 mM NaCl 50 mM HEPES 1.5 mM Na ₂ HPO ₄
KRB, pH 7.4 <i>Krebs Ringer Buffer was used for the assessment of transport rates of model compounds through cell monolayers.</i>	142.03 mM NaCl 2.95 mM KCl 1.49 mM K ₂ HPO ₄ * 3 H ₂ O 10.07 mM HEPES 4.00 mM D-Glucose 1.18 mM MgCl ₂ * 6 H ₂ O 4.22 mM CaCl ₂ * 2 H ₂ O

2.2 General cell culture

2.2.1 Cell lines and primary cells

In these studies, different cell lines and primary cells have been used, which are listed and described in table 2.

Table 2: Origin and description of cell lines and primary cells in alphabetical order.

Cells	Species	Origin	Description
A549 cell line	Human	Epithelial lung carcinoma cells	ATCC® CCL-185™; derived from a lung carcinoma of a 58-year-old Caucasian male; used as negative control and reference cell line.
hAEpC primary cells	Human	Alveolar epithelial cells	Isolated from healthy patient tissue from lung lobectomies according to Daum <i>et al.</i> (2012).
hAELVi cell line	Human	Alveolar epithelial lentivirus immortalized cells	Derived from primary hAEpC by transduction with lentiviral CI-SCREEN gene library according to (Kuehn <i>et al.</i> , 2016).
HEK293T cell line	Human	Embryonic kidney cells	ATCC® CRL-3216™; transformed by transfection with sheared DNA from adenovirus Ad5 (Graham <i>et al.</i> , 1977); used to produce lentiviral vectors.
mAEpC primary cells	Murine	Alveolar epithelial cells	Isolated from either C57Bl/6 wildtype or ROSAConL hetero mice according to (Wolf & Sapich <i>et al.</i> , 2016)
mAELVi cell line	Murine	Alveolar epithelial lentivirus immortalized cells	Derived from primary mAEpC by transduction with lentiviral CI-SCREEN gene library (InSCREENeX GmbH) according to May <i>et al.</i> (2016).
MLE12 cell line	Murine	Lung epithelial cells	ATCC® CRL-2110™; Established from pulmonary tumors from a mouse transgenic for the SV40 large T antigen under the control of the promotor region of the human surfactant protein C (Wikenheiser <i>et al.</i> , 1992; Wikenheiser <i>et al.</i> , 1993); used as a reference mouse cell line.
NIH3T3 cell line	Murine	Embryonic fibroblast cells	Spontaneously immortalized cells established from primary mouse embryonic fibroblasts cultured according to the '3T3 protocol' (Todaro & Green, 1963); used for titer determination of produced lentiviruses.

2.2.2 Cell cultivation

Cell culture plastic and inserts have been used by Costar Corning (well-plates, Transwells®, cultivation dishes or flasks). In general, cells were cultivated at 37°C (5% CO₂, 95% relative humidity) and the medium was changed every two to three days. At 70 – 80% confluence, cells were passaged according to the experimental needs, as described in the appropriate sections.

Table 3: Composition of cell cultivation media for cells of murine and human origin.

Medium	Composition and supplements	Application
Complete Mouse Medium (CMM) adapted from a previous publication (Demaio <i>et al.</i> , 2009)	DMEM/F12 50:50 (Dulbecco's Modified Eagle Medium/ Nutrient Mixture Ham F-12) + 1 mM glutamine (Gibco) + 0.25% BSA (Sigma-Aldrich) + 0.1 mM NEAA (Gibco) + 0.05% insulin-transferrin-sodium selenite supplement (Roche) + 100 µg/ml Primocin (Antimicrobial Reagent for primary cells, InvivoGen) + 10% FBS (optional)	CMM was used for the isolation of mAEpc. CMM10 (CMM+10%FBS) was used for the cultivation of mAEpc, mAELVi and MLE cells.
Small Airway Growth Medium (SAGM)	SABM™ (Small Airway Epithelial Cell Basal Medium; Lonza) + SAGM™ SingleQuots™ Kit (Lonza) + 10% FBS + 1% penicillin/streptomycin	SAGM was used for the isolation and cultivation of hAEpc and hAELVi cells. Here, it was also used to test its suitability for the cultivation of murine cells.
Dulbecco's Modified Eagle medium (DMEM)	DMEM + 10% FBS + 1% glutamine + 1% penicillin/streptomycin	DMEM was used for the cultivation and transient transfection of HEK293T and NIH3T3 cells.

For the cultivation of primary (mAEpc, hAEpc) and immortalized (mAELVi, hAELVi) cells, cell culture devices were coated with different extracellular matrix proteins to improve cell attachment or differentiation, respectively. Cells from murine origin were seeded on cell culture devices treated with a coating solution consisting of laminin 5

(1 µg/cm² Laminin from Engelbreth-Holm-Swarm murine sarcoma basement membrane, Sigma-Aldrich) and fibronectin (2 µg/cm² from human fibroblasts, BD Biosciences), whereas human cells were seeded on collagen-fibronectin-coated (rat tail collagen I and human fibronectin, both from BD Biosciences) cultivation surfaces. The compositions of the different applied cell culture media are listed in table 3.

2.2.3 Freezing and thawing of cells

Aliquots of used cell lines could be stored in liquid nitrogen by freezing the cells at a controlled cooling rate of about -1°C per minute in an appropriate cryoprotectant. This method allows the indefinite preservation of cell lines. Vice versa, the freezing process can be reversed by rapid thawing and subsequent seeding of the cells.

Freezing was performed by resuspending 1 – 2 x 10⁶ cells in 0.5 – 1 ml cryoprotective medium (10% DMSO in FBS) and subsequent transfer of the cell suspension into a freezing vial (ThermoFisher). Freezing vials were put into a Mr. Frosty™ Freezing Container (ThermoFisher) which was placed at -80°C for at least 24 hours before the cells were transferred to liquid nitrogen.

Thawing was performed by placing the vials from liquid nitrogen directly into a 37°C-water bath until the cell suspension was slightly defrosted. Subsequently, the cell suspension was transferred into 10 ml of cooled cultivation medium. After centrifugation (5 min, 300g at 4°C), the cell pellet can be resuspended in fresh medium and cells can be seeded as required.

2.2.4 Cell counting

For cell counting, determination of viability and purity of cells from cell culture or isolation two different approaches were used.

2.2.4.1 Neubauer cell counting chamber

Cell suspensions of primary murine and human AEPC were diluted in trypan blue solution in a 1:10 ratio. Subsequently, 10µl of the prepared dilution were pipetted into the Neubauer chamber. Cells that appeared white within the large grid squares were

counted manually using a light microscope. If N cells were counted in one large square, the number of cells can be determined by calculating:

$$\text{Cell number in cells/ml} = N \times 10^4$$

2.2.4.2 CASY® - Roche Innovatis

CASY® technology combines the resistance measurement principle with pulse area analysis. In brief, cells are diluted in CASY®ton and aspirated through a precision capillary in which a change of electrical resistance is recorded. The electrical signal is scanned, and the data from each particle is processed into a series of values that can be interpreted by pulse area analysis. This allows a particle size range to be recorded for each sample that can be interpreted as viable cells, dead cells, cell debris and cell aggregates.

2.3 Mouse strains and ethical statement

In these studies, murine alveolar epithelial cells (mAEpC) were isolated from lungs harvested either from the recombinant mouse strain ROSAConL (Sandhu *et al.*, 2011) or wildtype mice (C57Bl/6), which were obtained from Janvier Labs (Le Genest-Saint-Isle, France). The ROSAConL line exhibits a luciferase gene under the control of the ubiquitously active ROSA26 promoter and was established by backcrossing ROSALUC male mice with Balb/c (Sandhu *et al.*, 2011). All animal experiments were performed in accordance with the national guidelines of the German Animal Welfare Law and approved by the local government of Lower Saxony and the “Landesamt für Soziales, Gesundheit und Verbraucherschutz” of the Saarland, Germany, respectively.

2.4 Isolation procedure of primary alveolar epithelial cells

Primary murine alveolar epithelial cells (mAEpC) were isolated from 7 to 12 weeks-old female ROSAConL hetero (Sandhu *et al.*, 2011) or C57Bl/6 wildtype mice. Hereby, the procedure for the isolation of mAEpC was established by adaption to existing human and murine protocols (Daum *et al.*, 2012; Demaio *et al.*, 2009), and published in the course of this work (Wolf & Sapich *et al.*, 2016).

Material & Methods

For each isolation procedure 3 to 5 animals were slightly euthanized by an i.p. injection of 2.6 mg ketamine hydrochloride (Ketanest®; Pfizer) and 0.18 mg of xylazine hydrochloride (Rompun; Bayer) per mouse, or by CO₂ asphyxiation, respectively. To remove the lung from the animal, the peritoneum was carefully cut open from the abdomen to the jaws, and the jugular veins within the armpits as well as the renal artery were cut through. In a next step, the diaphragm was punctured so that the lung lobes collapse. To expose both lung and heart, the diaphragm and parts of the rib cage were removed. Subsequently, the lung was perfused by intracardiac injection of 2 x 5 ml PBS to remove erythrocytes from pulmonary blood vessels. Then, lungs were instilled intratracheal with 2 ml dispase solution (50 U/ml; Corning), harvested and incubated in dispase solution for 45 min at 37°C. After dispase digestion, lungs were transferred into a culture dish (Ø 10cm²) containing 10 ml CMM (see table 4 for medium composition) plus 1 ml DNase I (from bovine pancreas, Sigma-Aldrich). Bronchi were removed, the lung tissue was cut into small pieces with the help of scissors and forceps, and incubated for 45 min at 37°C.

To obtain a homogenous cell suspension, the tissue pieces were carefully resuspended for at least 15 min and filtered through 100 µm and 40 µm cell strainers (Corning). After centrifugation (5min, 300g at RT), the cell pellet was resuspended in 20 ml CMM + 1 ml DNase I, seeded on 10cm²-culture dishes and incubated for 90 min at 37°C. During this incubation step, macrophages adhere to the plastic surface, whereas the epithelial cells remain in the supernatant, which was collected and spun down. The cell pellet was resuspended in 1.3 ml BSSB buffer (see table 2 for the manufacturing protocol) and incubated with a monoclonal anti-mouse EpCAM-PE antibody (PE-conjugated monoclonal rat anti-mouse CD326 antibody G8.8; 1:200 in BSSB; eBiosciences™, Cat.no. 14-5791-81) for 30 min at 4°C on a rotating device. After washing with BSSB, the cells were incubated with magnetic PE-Microbeads (Miltenyi) for 30 min at 4°C.

Afterwards, the cell suspension was transferred to an equilibrated magnetic column (LS column, MACS® Cell separation, Miltenyi), which was subsequently rinsed twice with 6 ml washing buffer (PBS, pH 7.2, supplemented with 0.5% BSA and 2 mM EDTA). Finally, EpCAM-PE labeled cells were eluted with 5 ml CMM plus 10% FBS (PAA Laboratories). Freshly isolated cells were seeded in a density of 0.5 x 10⁶ 24-well plastic plates (for immortalization) or porous membranes of the apical Transwell®

compartments (0.33cm^2 , pore size $0.4\ \mu\text{m}$, Corning), respectively. Prior to cell seeding, cell cultivation devices were coated with a combination of human fibronectin ($2\ \mu\text{g}/\text{cm}^2$; Sigma-Aldrich) and laminin-5 ($1\ \mu\text{g}/\text{cm}^2$; Laminin from Engelbreth-Holm-Swarm murine sarcoma basement membrane, Sigma-Aldrich). For air-liquid-interface (ALI) conditions, the medium within the apical compartment was removed after 48 hours. Figure 5 illustrates the crucial steps of the isolation and purification of murine alveolar cells.

Primary human alveolar epithelial cells (hAEpC) were isolated from lung tissue following the established protocol (Daum *et al.*, 2012). Human lung tissue samples were used with the ethical improvement of the “Ärztekammer des Saarlandes” and informed patients’ agreement. The isolation protocol of hAEpC follows the same principle as the one to obtain mAEpC. The major difference is given by the fact that the lung tissues from these two species differ from each other in terms of size and texture and must thus be processed in a species-adapted manner (e.g. use of species-specific antibodies and tissue digestion enzymes).

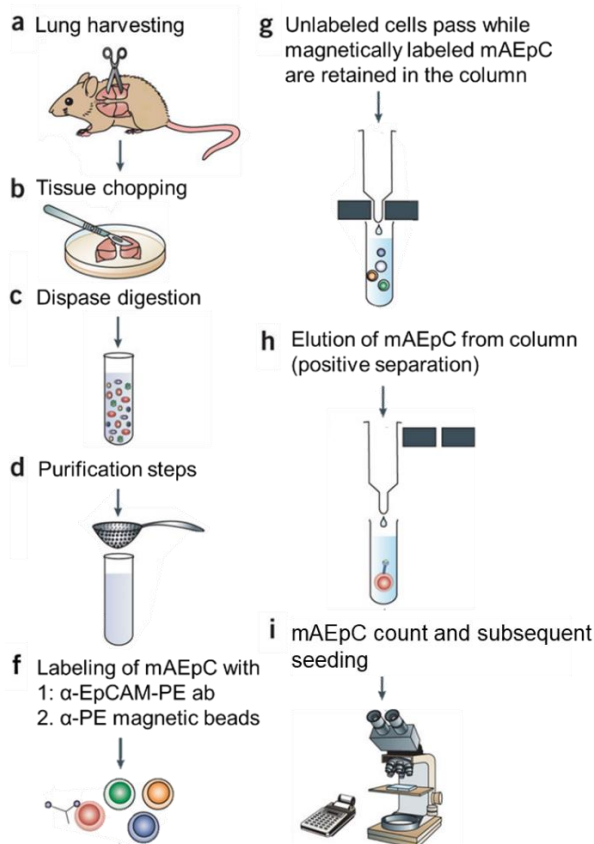


Figure 5: Illustrated overview of the mAEpC isolation procedure (Wolf & Sapich *et al.*, 2016). Images were modified from Nature Protocols (K. A. Sauer *et al.*, 2006).

2.1 Immortalization of primary mAEpC

In the following section, the lentivirus-induced immortalization of mAEpC is described. All experiments were performed in a biosafety level 2 laboratory.

2.1.1 Production of lentiviral vector systems

In total, 33 different lentiviral vector systems were produced individually by transient transfection of HEK293T cells achieved through calcium phosphate co-precipitation as described previously (May *et al.*, 2007; Spitzer *et al.*, 1999). Briefly, 5×10^6 HEK293T cells were seeded in DMEM and cultivated for 24 hours. For safety reasons, HEK293T were co-transfected with lentiviral helper plasmids (ViroPower™ Packaging Mix containing the packaging and envelope plasmids pLP1, pLP2 and pVSV-G encoding essential genes for lentivirus production) plus the lentiviral expression cassette into which the CI-SCREEN library genes (see table 5; Lipps *et al.*, 2018; May *et al.*, 2016) have been cloned before.

Therefore, the plasmids were mixed with 2.5 M CaCl₂ solution, which was subsequently dropped into a HEBS solution with simultaneous vortexing. The HEBS-plasmid-DNA solution was then added dropwise onto HEK293T cells, which were cultured in fresh medium overnight. After 24 and 48 hours, the supernatant containing replication-incompetent lentiviruses can be harvested and stored at -80°C after filtration. To evaluate the lentivirus titer of the harvested supernatants, 1×10^4 NIH3T3 were transfected with serially diluted lentivirus suspensions. After 3 days of cultivation, NIH3T3 were analyzed by flow cytometry regarding the expression of GFP, which verifies positive transduction and enables the determination of the virus titer by calculating:

$$\frac{\text{lentiviral particles}}{\text{ml}} = \frac{10^4 \text{ NIH3T3}}{\text{dilution factor}} * \text{number of positive cell counts}$$

Finally, the 33 different lentivirus suspensions were mixed in equal quantities resulting in a lentivirus “cocktail”, which was used to transduce primary mAEpC. This “cocktail” represents the CI-SCREEN gene library. Figure 6 illustrates the production procedure of lentiviral vector systems and the appropriate transduction of primary mAEpC.

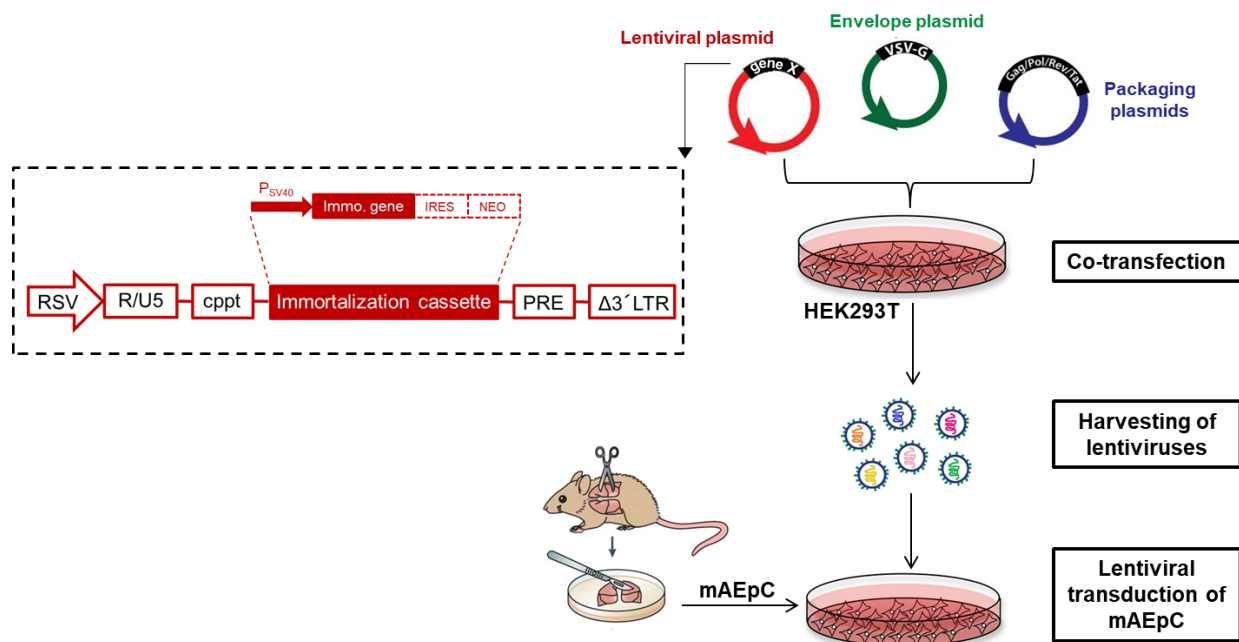


Figure 6: Schematic overview of the lentivirus production procedure by co-transfection of HEK293T cells, virus harvesting and the subsequent lentiviral transduction of primary mAEpC.

2.1.2 Lentiviral gene transfer to transduce mAEpC

To assess the optimal timepoint for lentiviral transduction, mAEpC were seeded on porous membranes to evaluate the trans-differentiation from an ATII- to an ATI-like phenotype by TEER measurement (see 2.2 for detail). When the TEER reached maximum values (5-7 days post isolation), mAEpC from the same isolation but grown on 24-well culture plates (instead of Transwells®) were transduced with a lentiviral gene library containing 33 different proliferation-promoting genes (referred to as CI-SCREEN gene library; InSCREENeX GmbH) according to a recent publication (Lipps *et al.*, 2018). Upon infection, the primary cells were incubated with CMM containing the lentiviral “cocktail” for 10 hours at 37°C in the presence of 8 µg/ml polybrene. Subsequently, the medium was replaced against fresh CMM + 10% FBS.

2.1.3 Cultivation of mAELVi cells

The lentivirally transduced cells were further cultivated in CMM + 10% FBS (CMM10), which was changed every two to three days. To achieve clonal formation, the cells were continuously expanded (1:1) in culture dishes, up to a growing area of 10 cm².

Proliferating cells, which were initially characterized in terms of the percentage of EpCAM-positive cells obtained by FACS analysis (see 2.4), were further cultured and confirmed to be polyclonal cell lines, referred to as mAELVi (murine alveolar epithelial lentivirus immortalized cells).

2.1.4 Analysis of gene integration pattern of mAELVi cells

To analyze the integration pattern of successfully integrated immortalizing genes of the CI-SCREEN library (Lipps *et al.*, 2018), total amounts of high molecular weight DNA were extracted from mAELVi cells, following the manufacturer's protocol (DNeasy Kit, Cat. no. 69504, Quiagen). Subsequently, 33 individual PCR reactions (1 µg DNA as template) were prepared using Taq PCR Biomix (Quiagen). Table 4 displays the appropriate PCR program run with Roche Light Cycler 480. The gene-specific 3' reverse primer sequences of the CI-SCREEN immortalizing gene library, which were used to detect integrated genes, are listed in table 5 with the corresponding amplicon sizes. The 5' forward primer binds within the SV40 promotor region of the immortalizing cassette and was used for all reactions (5' SV40For primer sequence: GGAGGCCTAGGCTTTGCAA). PCR reactions were analyzed by gel electrophoresis (1% agarose gel, 100 V for 20 min, BioRad Power Pac HC). As internal positive control PCR reactions for mGAPDH were carried along.

Table 4: PCR program to analyze the gene integration pattern of mAELVi cells.

Step	Temperature	Duration	No. of cycles
Initiation	94°C	5 min	1
	72°C	7 min	1
Denaturation	94°C	30 s	35
Annealing	55°C	45 s	
Elongation	72°C	4 min	
Final elongation	72°C	7 min	1
Hold	4°C	∞	

Material & Methods

Table 5: Reverse primer sequences of the CI-SCREEN library (Lipps et al., 2018) to analyze the pattern of integrated immortalizing genes in mAELVi cells performing 33 independent PCR reactions. The forward primer binds within the SV40 promotor region of the immortalizing gene expression cassette and was used for all PCR reactions (SV40-Forward primer sequence: 5' GGAGGCCTAGGCTTTGCAA 3').

#	CI-SCREEN library	3' → 5' Reverse Primer sequence	Amplicon size in bp
1	Id2	GCAGGGCTGACAATAGTGGGA	462
2	Fos	GGATGATGCTGGGAACAGGA	1054
3	NS1	ATGTCCCTGGAAGAGAAGGCA	678
4	Jun	TTCCTCATGCGCTTCCTCTC	912
5	E2F1	CAGGGTCTGCAATGCTACGA	944
6	βCat	TTATGCAAGGTCCCAGCGGT	806
7	TAg	CACCTGGCAAACCTTCCTCA	1214
8	Myb	CTTCTGGAAGCTTGTGCCA	780
9	Id3	ATGACAAGTTCCGGAGCGAG	453
10	E7	GCCCCATTAAACAGGTCTTCCA	404
11	E6	ATTCGCCCTTTACAGCTGG	636
12	Bcl2	TCTGCGAAGTCACGACGGTA	440
13	HoxA9	GTTTAATGCCATAAGGCCGG	515
14	Bmi1	GGGCCATTCTTCTCCAGGT	782
15	PymT	CATCTGGGTTGGTGTCCA	606
16	Core	ACTTTACCCACGTTGCGCGA	487
17	Oct3	GCAAAGCAGAAACCCTCGTG	846
18	Klf4	AAGATCAAGCAGGAGGCGGT	1084
19	Id1	AGAACGCCAACGTGACCA	980
20	Myc	AGTGGGCTGTGAGGGAGGTTT	1001
21	Lmo2	TTTCCGTCCCAGCTTGTAGT	822
22	Nfe2L2	GCTGCTGAAGGAATCCTCAA	1008
23	Yap1	GCCAGGATGTGGTCTGTTTC	950
24	Nanog	TATGGAGCGGAGCAGCATT	935
25	Sox2	CTCGCAGACCTACATGAACG	846
26	RhoA	AAGCATTCTGTCCAACGT	562
27	Ezh2	ACTTCGAGCTCCTCTGAAGC	1481
28	Gli1	CACCACATCAACAGCGAGCA	1144
29	v-Myc	GACACCCTGAGCGATTCAAGA	1052
30	Suz12	TACCCTGGAAGTCCTGCTTG	769
31	ZFP217	CAAGAAGGGAGCACCGACAA	1188
32	Id4	CAGCAAAGTGGAGATCCTGC	652
33	Rex	GCGAGCTCATTACTGCAGG	920

2.2 TEER measurement

The transepithelial electrical resistance (TEER; stated in Ωcm^2) measurement provides an *in vitro* method to evaluate the integrity of tight junction dynamics and cellular barrier properties of cell monolayers, respectively. The TEER of primary and immortalized cells was determined as previously described (Daum *et al.*, 2012; Srinivasan *et al.*, 2015). Briefly, cells were seeded and cultivated on permeable Transwell™ membranes under submerged conditions (LCC = liquid covered conditions) and the TEER was measured with an epithelial voltohmometer (EVOM²; World Precision Instruments, Sarasota) using a chopstick electrode. During this procedure, the Transwell® plates were kept at 37°C on a heating plate to keep the temperature at a stable level.

For the assessment of the TEER of cells kept at the air-liquid-interface (ALI), pre-warmed cultivation medium was first added to the apical and second into the basolateral compartment. The cells were then incubated at 37°C for 1 – 2 hours prior to the TEER measurement. Afterwards, the cultivation medium was first removed from the basolateral, then from the apical compartment to restore ALI growth conditions. Table 6 contains the appropriate volumes of medium for apical and basolateral Transwell® compartments depending on the size of the cell growing area. TEER was calculated by subtraction of the resistance of blank inserts without cells ($\text{TEER}_{\text{blank}}$: 37 Ω for 0.33 cm^2 / 108 Ω for 1.12 cm^2 inserts; mean values with $n = 9$) from the measured cell layer resistance (TEER_{raw}) and subsequent multiplication with the size of the cultivation area size:

$$\text{TEER in } \Omega \text{ cm}^2 = (\text{TEER}_{\text{raw}} - \text{TEER}_{\text{blank}}) * 0.33/1.12 \text{ cm}^2$$

Table 6: Volumes of cultivation medium for apical and basolateral compartments of 0.33 cm and 1.12 cm^2 Transwell® inserts to set either LCC or ALI conditions.

Transwell® insert size	volume of medium in μl			
	LCC		ALI	
	apical	basolateral	apical	basolateral
0.33 cm^2	200	800	/	200
1.12 cm^2	500	1500	/	500

2.3 Morphological characterization

For morphological and ultrastructural characterization mAEpC and mAELVi cells were grown on Transwell® membranes with a pore size of 0.4 µm and a growth area of 0.33 or 1.12 cm² (3470/3460, Corning), respectively. Cells were cultivated under LLC or ALI conditions, and analyzed by cross sections, confocal laser scanning microscopy (CLSM) or transmission electron microscopy (TEM).

2.3.1 Histology

For histology analysis cells were fixed with 3% paraformaldehyde for 30 min at room temperature. After fixation, the samples were dehydrated by an ascending ethanol series (35, 50, 70, 95, 95, 100% ethanol solutions each for 10 min) followed by a 10 min treatment with HistoClear II (Histological Clearing Agent-Fa. National diagnostics). Afterwards, the samples were embedded in paraffin (Histowax Embedding Medium – Leica Microsystems) for 1 hour and cut into 4 µm slices using a microtom (Reichert Jung 2040 Autocut). Finally, the cross-sections were stained with hematoxylin/eosin (H/E) and images were taken with a Zeiss light microscope (Zeiss Imager M1m, Zeiss) using a 100x objective.

2.3.2 Confocal Laser Scanning Microscopy (C-LSM)

Primary mAEpC were grown on 0.33 cm²-Transwell® filters (0.4 µm pore size, 3470, Corning) and fixed with 3% paraformaldehyde (PFA) at days 1, 3, 7 and 10 post isolation. Immortalized cells were grown on 1.12 cm²-0.4 µm pore size filters (3460, Corning) and fixed with 3% PFA for 30 min at room temperature at day 8 post seeding. In all samples quenching was performed using a 50 mM NH₄Cl/PBS solution for 10 min. Subsequently, the samples were blocked and permeabilized with PBS supplemented with 0.5% bovine serum albumin (BSA) and 0.025% Saponin for 30 min at room temperature (RT). Primary antibodies (rabbit anti-ZO1, Cat. No. 61-7300, Invitrogen; polyclonal anti-proSPC, AB3786, Merck Millipore) were diluted 1:200 in 0.5% BSA in PBS and incubated for 1 hour at RT or overnight at 4°C, respectively. Secondary antibodies (polyclonal Alexa Fluor 488 conjugated, goat-anti-rabbit, A-11008, ThermoFisher) were diluted 1:400 in PBS and incubated for 1 hour at 37°C. Afterwards, the filters were washed with PBS and stained with DAPI solution (1:50000).

Transwell® membranes were cut out from the carrier material, mounted in DAKO medium (Product No. S302380-2, DAKO) with a coverslip and imaged by confocal laser scanning microscopy (Zeiss LSM710, Zeiss). Images were acquired at a 1024 x 1024 resolution with a 63x water immersion objective and Z-stacks. Image analysis was performed with ZEN2012 software and ImageJ.

2.3.3 Transmission electron microscopy (TEM)

To analyze the ultrastructure, primary mAEpC grown on 0.33cm²-Transwells® at either LCC or at the ALI were fixed for 1 hours at 4°C using 1% v/v glutaraldehyde (GA) in 200 mM HEPES buffer. After fixation, the Transwell® inserts were transferred to 50 ml-tubes filled with 200mM HEPES and shipped to Dr. Urska Repnik and Prof. Gareth Griffiths at the University of Oslo, Norway, for epon embedding and image acquisition which was performed according to a previous work (Susewind *et al.*).

In brief, the cells were postfixed with 2% w/v OsO₄ solution (EMA, PA) plus 1.5% w/v potassium ferricyanide for 1 hour on ice, and stained *en bloc* with 1.5% w/v aqueous uranyl acetate (EMS, PA) for 30 min followed by an ascending ethanol series (70, 80, 90, 96, 4x 100% each for 10 min) treatment and progressive infiltration of epoxy resin (50, 75, 100%; Sigma-Aldrich) at RT. Blocks were polymerized overnight at 70°C and ultrathin sections (70 -80 nm), perpendicular to the filter plane, were prepared with a Leica ultramicrotome Ultracut EM UCT (Leica Microsystems) and an ultra-diamond knife (Diatome). Ultrathin sections were analyzed with a CM 100 transmission electron microscope (FEI). Using a Quemesa TEM CCD camera (Olympus Soft Imaging Solutions) images were recorded and analyzed with iTEM Software (Olympus Soft Imaging Solutions).

2.4 Flow cytometry

In this study, flow cytometry was applied for the determination of lentivirus titers (analysis of GFP-positive cells) after production as well as for the characterization of mAEpC and mAELVi (analysis of EpCAM-expression) following the protocol of a previous work (May *et al.*, 2007).

In general, the cells were washed twice with PBS and detached with a trypsin solution. Subsequently, the cells were suspended in FACS buffer (PBS + 2% FBS), transferred to a 15-ml capped plastic tube and spun down at 100g for 5 min using a table-top centrifuge. For each attempt, an unstained (negative control) and a stained cell sample (positive control) were prepared. For the negative controls, cell pellets were resuspended in 100 – 500 µl FACS buffer (optional: + 50 µg/ml propidium iodide to stain dead cells) and the tubes were stored on ice. The positive controls, the cell pellets were resuspended in a 1:100 FACS buffer antibody dilution and incubated for 30 min at 4°C. Subsequently, the stained cells were centrifuged with 100 g for 5 min and resuspended in FACS buffer. All samples were analyzed using a BD Biosciences FACSCalibur™ Cell Analyzer System. A side scatter (SSC)/FSC dot blot was applied to exclude cell debris (FSC < 200). The FL3 channel was used to analyze the propidium iodide staining which excludes dead cells from the analysis. The FL2 channel was used for both the acquisition of GFP and the PE-labeled anti-EpCAM antibody (PE-conjugated monoclonal rat anti-mouse CD326 antibody G8.8; 1:200 in BSSB; eBiosciences™, Cat.no. 14-5791-81), respectively. BD CellQuest™ software was used to analyze FACS data.

2.5 RNA extraction and cDNA synthesis to analyze marker expression

Total RNA amounts from freshly isolated mAEpC and mAELVi were extracted according to the manufacturer's protocols (CellAmp Direct RNA Prep Kit #3732, Takara) to assess the expression of epithelial ATI- and ATII-like marker genes. After completion of the extraction protocol, the RNA concentration was determined with a NanoDrop Spectrophotometer (Thermo Scientific) measuring the absorbance ratio 260/280 nm. Subsequently, reverse transcription of the first-strand cDNA synthesis was performed with oligo(dT)-primer following the manufacturer's protocol (Ready-to-go you-prime first strand beads, GE healthcare), where 2 to 3 ng RNA were used as template.

Primer sequences for PCR analyses were designed in a way that the sense and antisense sequences were either intron-spanning or bridging exon-exon junctions using the NCBI (National Center for Biotechnology Information) online tools RefSeq and Primer Blast. All primer sequences were purchased from Eurofins (see table 7 for

Material & Methods

nucleotide sequences and amplicon sizes). Table 8 displays the appropriate PCR program run with Roche Light Cycler 480. PCR reactions for mGAPDH were carried along as internal positive control. In a next step, the PCR reactions were analyzed by gel electrophoresis (3,5% agarose gel, 50 bp DNA ladder, 100 V, 25 min, BioRad Power Pac HC).

Table 7: Primer sequences to analyze lung cell-specific marker expression by PCR.

marker	gene	FOR primer 5' → 3'	REV primer 5' → 3'	Amplicon size
ATII	SP-A	TCCTGGAGACTTCCACTACCT	CAGGCAGCCCTTATCATTCC	101 bp
	SP-B	CTGCTTCCTACCCCTTGCTG	CTTGGCACAGGTCTTAGCTC	121 bp
	SP-C	ATGGACATGAGTAGCAAAGAGGT	CACGATGAGAAGGCCTTGAG	88 bp
ATI	AQP-5	CTCAGCAACAACACAACACCAGGC	GGGGAAAAGCAAGTAGAAAGTAGAGGATTG	86 bp
	Cav-1	CTACAAGCCCACAAACAAGGC	AGGAAGCTCTTGATGCACGGT	198 bp
	ICAM-1	GCCTTGGTAGAGGTGACTGAG	GACCGGAGCTGAAAAGTTGTA	103 bp
	T1α	GTTTGGGAGCGTTGGTTC	CATTAAGCCCTCCAGTAGCAC	101 bp
Control	mGAPDH	TCAATGAGCCCCTTCCACAATG	CCTGCACCACTGCTTA	75 bp

Table 8: PCR program to analyze the expression of lung-specific marker genes.

Step	Temperature	Duration	No. of cycles
Initiation	94°C	5 min	1
Denaturation	94°C	1 min	35
Annealing	60°C	45 s	
Elongation	72°C	30 s	
Final elongation	72°C	10 min	1
Hold	4°C	∞	

2.6 Paracellular transport studies

To evaluate the paracellular transport of fluorescent molecules of different molecular weights across monolayers, cells were seeded on Transwell® membranes. Freshly isolated mAEpC were seeded (1×10^6 cells/cm 2) on fibronectin/laminin-coated 0.33 cm 2 -inserts with 0.4 µm pore size (Corning, 3470) and cultivated for 6 to 8 days. MLE12, hAELVi, mAELVi.E and mAELVi.wt were seeded in a density of 0.1×10^6 cells/cm 2 on 1.12 cm 2 Transwell® inserts with a pore size of 0.4 µm (Corning, 3460). TEER was assessed daily. Transport experiments of sodium fluorescein (MW 400 Da, Na-Flu; Sigma-Aldrich) and FITC dextran (MW 3,000 Da, FD3000M; Sigma-Aldrich) were performed according to previous protocols (Bur *et al.*, 2006; Crandall & Matthay, 2001).

In brief, the cells were washed and equilibrated for 45 min with pre-warmed Krebs-Ringer buffer (KRB; see table 1). Then, KRB was aspirated and Na-Flu (10 µg/ml in KRB ± 8/16 mM EDTA) or FITC dextran solutions (100 µg/ml in KRB + 0.2% BSA) were added to the donor compartment while the acceptor compartment was loaded with KRB. Immediately afterwards, samples were taken from both compartments and transferred into a 96-well plate to determine the initial concentrations. Table 9 outlines the respective start and sample volumes which differ according to the size of the Transwell® membrane and the analyzed transport direction.

Subsequently, sampling from the acceptor compartment was continued every 30 min for up to 3 (Na-Flu) or 5 (FD3000) hours, respectively. Importantly, each sample volume taken from the respective acceptor compartment was replaced with the same volume of KRB. TEER was measured before the experiment, after KRB incubation and at the end of the experiment. Fluorescence was measured with a Tecan® plate reader using wavelengths of 488 nm (emission) and 530 nm (extinction). On basis of the measured fluorescence intensities and the appropriate calibration curve, the apparent permeability coefficients (P_{app}) were calculated as follows:

$$P_{app} = \frac{\Delta Q}{\Delta t * A * C_0}$$

$\Delta Q/\Delta t \triangleq$ permeation rate across cell monolayer in µg/sec
A = area of cell monolayer

Material & Methods

Table 9: Overview of start volumes (of the Transwells®) and sample/KRB volumes (to transfer to the 96-well plate) in dependence on the growing size of the Transwell® insert and the transport direction.

	Start and time points of sampling	0.33 cm² Transwell®		1.12 cm² Transwell®	
		apical	basolateral	apical	basolateral
apical-to-basolateral (a-to-b)	Start volumes Transwells®	220 µl fluorescent solution	800 µl KRB	520 µl fluorescent solution	1500 µl KRB
	Sample to determine C ₀ at the start (t _{start})	20 µl sample + 180 µl KRB	/	20 µl sample + 180 µl KRB	/
	Sampling from acceptor compartment at different time points starting at t=0	/	100 µl sample (replaced by 100 µl KRB) + 100 µl KRB	/	200 µl sample (replaced by 200 µl KRB)
	Sample to determine end concentration (t _{end})	20 µl sample + 180 µl KRB	/	20 µl sample + 180 µl KRB	/
basolateral-to-apical (b-to-a)	Start volumes Transwells®	200 µl KRB	820 µl fluorescent solution	500 µl KRB	1520 µl fluorescent solution
	Sample to determine C ₀ at the start (t _{start})	/	20 µl sample + 180 µl KRB	/	20 µl sample + 180 µl KRB
	Sampling from acceptor compartment at different time points starting at t=0	50 µl sample (replaced by 50 µl KRB) + 150 µl KRB	/	100 µl sample (replaced by 100 µl KRB) + 100 µl KRB	/
	Sample to determine end concentration (t _{end})	/	200 µl sample	/	200 µl sample

2.7 Cytotoxicity assay

The cytotoxic effects of a small set of test substances from different GHS (Globally Harmonized System) acute inhalation toxicity categories were assessed and compared, according to the methods and results of a previous study (U. G. Sauer et al., 2013). Cells (mAELVi.E, mAELVi.wt or MLE12) were seeded in 96-well plates in CMM10 at a density of 1 × 10⁵ cells/well. Serial dilutions of ethanol, acetone, lactose (1:2) as well as SDS, glutaraldehyde and formaldehyde (1:10) were prepared in medium, starting with the highest concentration of 100 mg/ml. After 48 hours, medium was replaced by 200 µl of the test substance solutions (in triplicate). Medium alone was used as 100% viability control, whereas 25% glutaraldehyde (GA) diluted in medium served as the 0% viability control. After a 4-hours incubation at 37°C on a shaker, the test substance solutions were removed, and the cells were washed twice

with HBSS (Hank's balanced salt solution; ThermoFisher). Afterwards, the cells were incubated with 200 µl/well MTT solution (1 mg/ml 3-(4,5-dimethylthiazol-2-yl)-2,5-diphenyl tetrazolium bromide in HBBS; Sigma-Aldrich) at 37°C on a shaker. After another 4-hour incubation, the MTT solution was replaced with 100 µl/well DMSO and any formed crystals were dissolved for 20 min at 37°C. Finally, the absorbance at 550 nm was measured with a Tecan[®] plate reader.

The viability was calculated as $\{(OD_{test\ substance} - OD_{0\%}) / (OD_{100\%} - OD_{0\%}) * 100\%\}$. The IC₅₀ was calculated by plotting at least three measurement points surrounding the 50% viability in logarithmic scale. If the IC₅₀ value was above 100 mg/ml, the IC₅₀ was considered to be the 100 mg/ml data point in the graph. The obtained results were then compared to the known GHS categories of the test substances.

2.8 Statistics

Data from TEER measurements, and the transport and cytotoxicity studies are representative of 3 - 6 individual experiments, each performed in triplicate, and are shown as mean ± S.D. calculated using Microsoft Excel[®] software. P values were determined by one-way ANOVA performed using Microsoft[®] Excel.

3 Results & Discussion

The results of this work can be subdivided into 5 main sections which are described and discussed in the following. First, the isolation procedure and its particularities (see 3.1) are explained followed by a characterization of the primary mAEpC model and its ability to mimic the air-blood barrier (see 3.2). In a next step, primary mAEpC were immortalized with the aim to generate novel murine alveolar cell lines by two different lentivirus-mediated approaches (see 3.3): transduction with the CI-SCREEN immortalizing gene library in accordance with Lipps *et al.* (2018) and transduction with a single vector conditionally expressing SV40 TAg. Concurrently, the DNA of mAELVi cells was analyzed to reveal the pattern of integrated immortalizing genes upon lentiviral transduction with the CI-SCREEN library. Proliferating cells obtained were expanded as mAELVi (murine alveolar epithelial lentivirus-immortalized) cell populations and characterized regarding ATI/II-specific traits and barrier properties (see 3.4). Finally, the suitability of selected immortalized cells (mAELVi.E and mAELVi.wt) for paracellular transport studies in comparison with primary mAEpC (see 3.5) and the prediction of cytotoxic effects in comparison with MLE12 cells (see 3.6) was addressed. Parts of these results have recently been published (Sapich *et al.*, 2018).

3.1 Towards an optimized isolation procedure to obtain primary mAEpC

On basis of existing methods for the isolation of primary alveolar epithelial cells from human (Daum *et al.*, 2012) and murine (Demaio *et al.*, 2009) origin, an efficient and reliable protocol to obtain primary mAEpC was established in the course of this work (Wolf & Sapich *et al.*, 2016). Thereby, the murine lung tissue is digested by dispase enzyme activity and the therein contained alveolar epithelial cells are labeled with EpCAM PE magnetic beads enabling positive cell separation (see chapter 2.4 for detail). Since this isolation protocol for mAEpC is based on the antibody-mediated selection of EpCAM-positive cells, both types of alveolar epithelial cells can be isolated. Given the fact that ATI cells form a very thin monolayer *in vivo* and are thus

extremely fragile, it is most likely that these cells will be damaged during or due to the isolation procedure, respectively. Hence, mAEpC monolayer formation is mainly performed by viable ATII cells undergoing trans-differentiation into ATI-like cells, as will be shown in the following. Furthermore, critical parameters of the isolation procedure and cultivation conditions of mAEpC are addressed below.

3.1.1 Magnetic beads mAEpC cell separation versus flow cytometric cell sorting methods

In contrast to magnetic cell separation-based methods to isolate mAEpC (Corti *et al.*, 1996; Demaio *et al.*, 2009; Messier *et al.*, 2012), alternative flow cytometric cell sorting approaches to obtain primary murine ATII cells have been described recently (Gereke *et al.*, 2012; Sinha & Lowell, 2016). The authors claim that flow cytometric isolation of mAEpC yields in highly pure and viable cell populations at lower costs enabling genomic, transcriptomic, proteomic or secretomic analyses. However, properties of the air-blood barrier of such ATII cells were not addressed in these publications. Furthermore, FACS-sorted ATII cells could be only be cultivated *in vitro* for up to 48 hours (Gereke *et al.*, 2012). Recent FACS-based attempts to isolate murine (Hasegawa *et al.*, 2017) and human (N. Fujino *et al.*, 2012) ATII cells using different marker to distinguish cell populations turned out to be incompatible with prior enzymatic digestion, as it may negatively affect the surface-antigen expression of the cells. Therefore, flow cytometry-based methods to isolate murine ATII cells cannot be taken into consideration for these studies. Nevertheless, magnetic column cell separation and FACS-based protocols can be combined to obtain endothelial, epithelial and immune cells from murine lungs in the course of a single isolation procedure enabling the analysis of molecular features of different lung cell types (Bantikassegn *et al.*, 2015). However, it is not yet possible to determine a proper ratio of isolated ATI and ATII cells using any of the abovementioned methods due to the lack of infinite markers.

3.1.2 Purity and yield of isolated primary mAEpC

To assess the purity of the isolated mAEpC, cell fractions were collected at different steps during the isolation procedure and analyzed regarding the amount of viable EpCAM-positive cells by flow cytometry (see figure 7). The total lung cell population

before MACS separation contained 21% EpCAM-positive cells which were significantly enriched after magnetic beads separation, where they represented over 90% of the cells. During the optimization of the isolation, a Percoll gradient as an additional purification step was performed, which is a regular part of the hAEpC isolation protocol. However, in case of murine cells the performance of a Percoll gradient could not increase the percentage of EpCAM-positive cells, but significantly decreased the cell yield after separation which was also observed in a previous study comparing mAEpC yields of isolation variations (Hansen *et al.*, 2014). For that reason, a gradient density purification step was excluded from further experiments.

On average, the applied mAEpC isolation protocol yields in $2 - 3 \times 10^6$ cells per mouse which equals cell yields obtained by e.g. alternative flow cytometric methods (Gereke *et al.*, 2012) or comparable methods (Demaio *et al.*, 2009). Notably, yields of individual mAEpC isolations showed marked differences which most definitely depend on the success of critical steps during lung harvesting. Namely, these key steps are the intracardial lung lavage with PBS and the intratracheal instillation with dispase solution, which require some hands-on experience. To further increase the cell yield, it is also crucial to release as many cells as possible from the digested lung tissue pieces by performing the resuspension of the cells thoroughly contributing to a reduced number of mice which must be applied for isolation procedures.

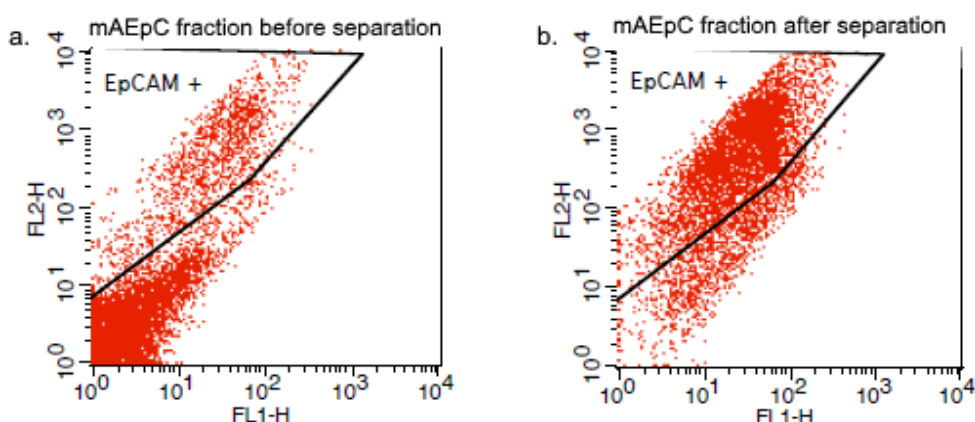


Figure 7: Flow cytometric determination of EpCAM-positive cells assessed by FACS analysis before (a, left) and after (b, right) MACS magnetic beads cell separation during the isolation procedure of mAEpC.

3.2 Characterization of primary mAEpC

To provide the basis for the generation of murine cell lines exhibiting *in vivo* functions of the alveolar epithelium, the cultivation of mAEpC was optimized in view of the best possible barrier quality. Therefore, primary cells have been characterized regarding their ability to gain ATI-like functions after isolation due to trans-differentiation processes, which is addressed in the following alongside with an ultrastructural characterization (see 3.2.1). To further improve the primary cell model, varying cultivation conditions (cell seeding density, medium composition, coating, LCC versus ALI) have been applied to evaluate the respective impact on the development of a tight mAEpC monolayer by TEER measurements (see 3.2.2). Besides, primary cultures of alveolar epithelial cells from murine and human origin are compared (see 3.2.3).

3.2.1 Trans-differentiation and ultrastructure of mAEpC

Primary AEpC of human (Daum *et al.*, 2012), rat (Gonzalez *et al.*, 2005), equine (Quintana *et al.*, 2011) or bovine (Castleman *et al.*, 1991) origin are known to trans-differentiate *in vitro* from an ATII-like phenotype into an ATI-like phenotype. This process was tracked for mAEpC by monitoring the immunofluorescence intensity and localization of pro-surfactant protein C (proSP-C; ATII marker) and Zonula occludens protein 1 (ZO-1; both ATI and TJ marker) at different time points (see figure 8).

Thereby, the expression of the ATII-marker gene proSP-C appears to be patchy and to decrease with time. Even though ZO-1 could be detected on the days 1 and 3, the characteristic distribution of ZO-1 expression restricted to the cell membranes became clearly obvious on day 7 and was maintained until day 10. These results indicate that freshly isolated mAEpC seeded at 1.5×10^6 cells/cm² attached after 24 -48 hours and form a confluent monolayer starting at day 3 after isolation, which is similar to that observed for hAEpC (Elbert *et al.*, 1999; Hittinger *et al.*, 2016a).

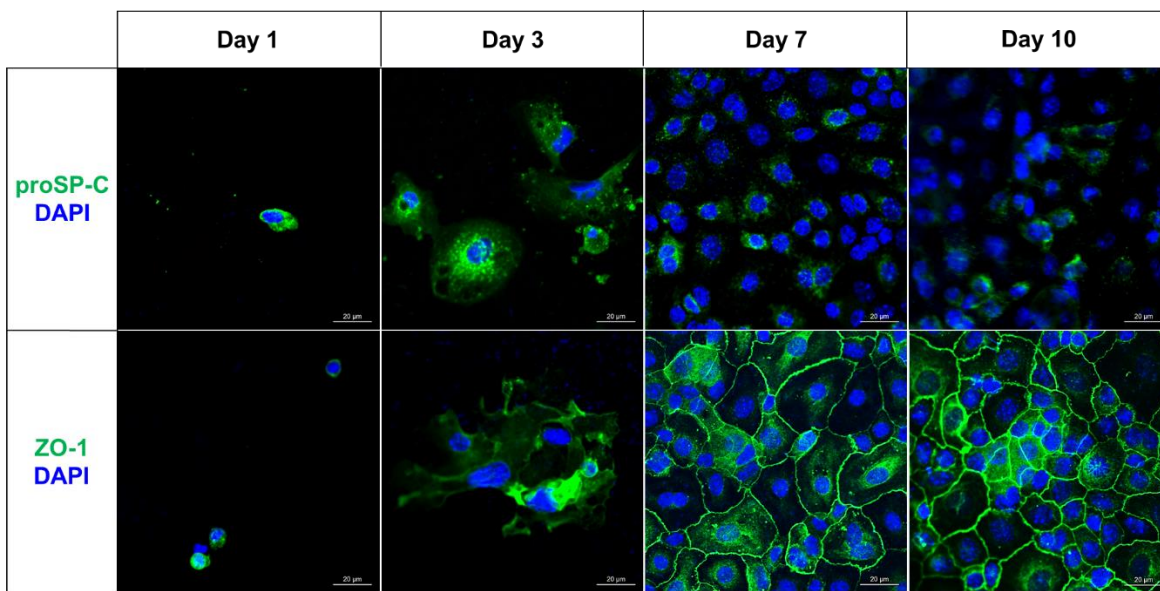


Figure 8: Trans-differentiation of primary mAEpC – immunofluorescent staining of mAEpC was performed at different time points post isolation; the expression of proSP-C protein (ATII marker) is shown in the upper panel; the expression of ZO-1 protein (both ATI and TJ marker) is shown in the lower panel (both proteins shown in green); cells were fixed on 0.33 cm²-membranes with 3% PFA and nuclei were stained with DAPI solution (shown in blue); scale bars: 20 µm.

To further confirm that mAEpC exhibit ATI-like characteristics, cells grown on Transwells® at liquid-covered conditions (LCC) or the air-liquid interface (ALI), respectively, were analyzed by TEM in collaboration with the University of Oslo (see 2.3.3 for more information).

The ultrastructure of primary mAEpC (see figure 9) grown at both conditions revealed typical ATI structures, like tight junction complexes (indicated with blue circles) and desmosomes (indicated with green circles). Under the electron microscope, TJs appear as a series of fusion points between the outer membrane of adjacent cells. At these “kissing points” the intercellular space is no longer available. The characteristic electron dense structure of desmosomes showed a central core region that spans the intracellular space between apposing cells and separated two cytoplasmic plaques associated with intermediate filaments (D. Garrod & M. Chidgey, 2008). Desmosomes, also known as maculae adhaerentes, build “intercellular bridges” between the cell membranes and the intermediate filament network by creating an anchor consisting of a scaffolding of proteins such as epithelial cadherin (E-Cad) (Hartsock & Nelson, 2008).

Taken together, these results give evidence that isolated mAEpC trans-differentiate into a monolayer of flattened ATI-like cells which exhibit structural ATI-characteristics like desmosomal structures and tight junction complexes, which could also be visualized by ZO-1 and occluding expression (see figure 8).

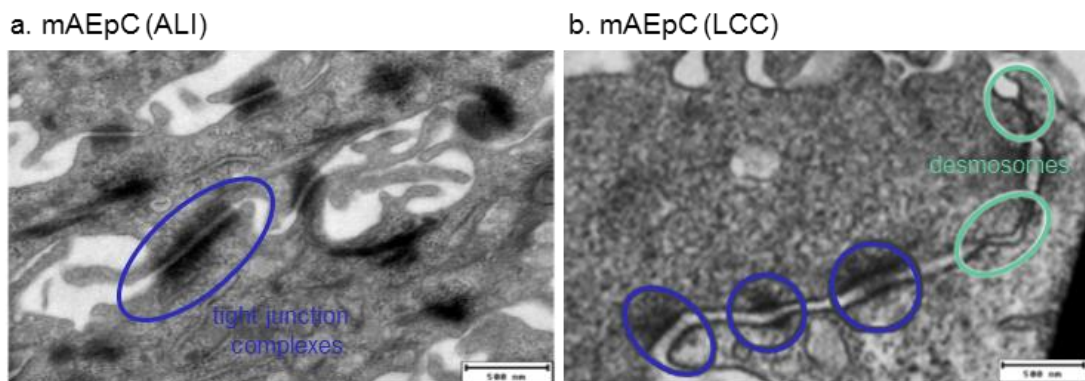


Figure 9: Ultrastructure of primary mAEpC cultivated for 8 days on Transwell® membranes at a.) the air-liquid interface or b.) liquid-covered conditions. Green circles indicate desmosomal structures, blue circles indicate tight junction complexes; cells were grown on 0.4 µm thick Transwell® filters with a pore size of 0.4 µm and stained with H/E; scale bars: 500 nm.

3.2.2 Barrier properties of primary mAEpC upon different cultivation conditions

To monitor the presence of functional tight junctions and, consequently, evaluate the barrier properties of the mAEpC monolayers grown at different cultivation conditions, the transepithelial electrical resistance (TEER) was measured daily for up to two weeks. In this context, the formation of an integer mAEpC monolayer after isolation strongly depends on the cell seeding density, as shown in figure 10A. Here, it became clearly obvious that seeding densities of $0.3 - 0.9 \times 10^6$ cells/cm² are not sufficient for the development of high TEER, whereas higher seeding densities ($\geq 1 \times 10^6$ cells/cm²) result in the formation of a mAEpC monolayer with high TEER. In this study, the highest TEER peaking at $\sim 2400 \Omega\text{cm}^2$ could be measured at the highest seeding density (3×10^6 cells/cm²). To help meet the 3R principle and reduce the number of mice, further studies were carried out at a lower mAEpC seeding density of 1.5×10^6 cells/cm², at which the maximal TEER still appeared to be high peaking at $\sim 1800 \Omega\text{cm}^2$. As the attachment of mAEpC to the cultivation device surface requires up to 48 hours,

such high seeding densities are necessary to ensure sufficient cell-cell-contact and thus, the development of a tight monolayer. Compared to a protocol described by Hansen *et al.* (2014), whereby isolated mAEpC were seeded at much higher densities (1.5×10^6 cells/24-well $\approx 4.5 \times 10^6$ cells/cm 2) on 24-well plates, the herein established procedure achieved a much higher efficiency.

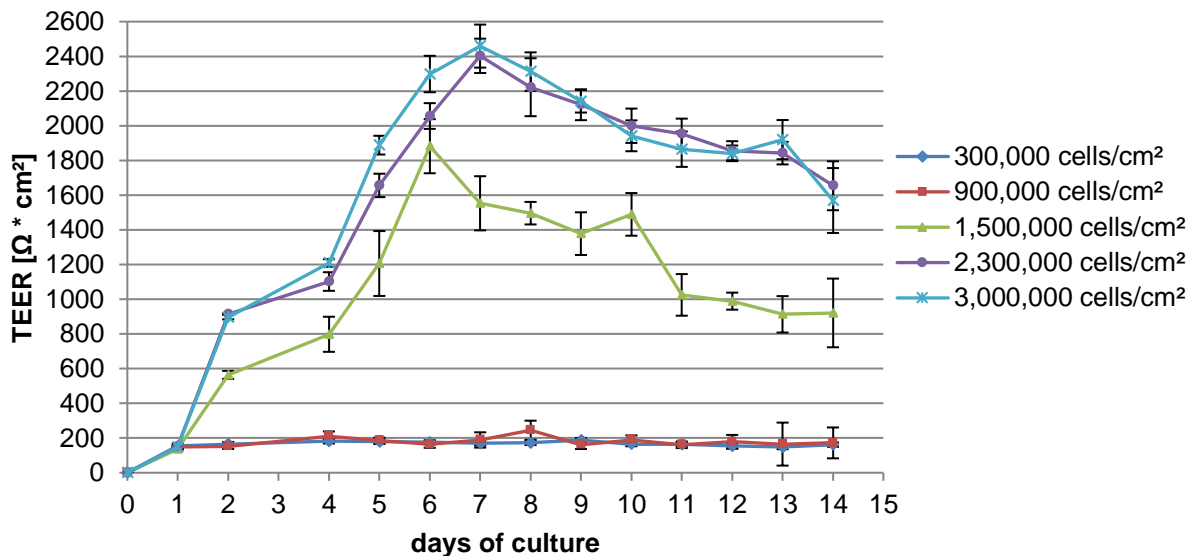
As a second key factor, cell culture devices must be subjected to a surface treatment to render the plastic suitable for cell attachment. In these studies, different extracellular matrix (ECM) proteins, such as collagen, laminin and fibronectin, were used to coat culture plates and Transwell® membranes. To determine the optimal cultivation conditions for mAEpC differentiation, TEER was assessed using different coating combinations as well as different cultivation media. Figure 10B conveys that mAEpC grown on Transwell® membranes coated with a mixture of fibronectin and laminin-5 showed higher TEER (TEER_{max} ~ 2100 Ωcm 2) than the combination of collagen and fibronectin (TEER_{max} ~ 1800 Ωcm 2) and hence, was used for all further experiments. These data suggest that mAEpC require exogenous ECM proteins for the establishment of confluent monolayers and that laminin-5 is most likely to support the tightness of the epithelial barrier. It was previously suggested that phenotypic and morphological changes of isolated mAEpC might occur due to the properties of the ECM which reflect the *in vivo* environment (Isakson *et al.*, 2001b; Rice *et al.*, 2002). Previously, it was also observed that mAEpC grown on a mixture of type I collagen and fibronectin develop into functional ATI-like monolayers, whereas the ATII phenotype was retained when the cells were grown on laminin-5 only. This result stands in contrast with the abovementioned findings and a previous work, whereby it could be shown that laminin-5 supports the formation of a high-resistance monolayer (Demaio *et al.*, 2009).

Furthermore, figure 10B shows that mAEpC grown in *Complete Mouse Medium* (CMM) revealed significantly higher TEER development than mAEpC cultivated with *Small Airway Growth Medium* (SAGM) which is generally being applied for hAEpC (Daum *et al.*, 2012). Consequently, CMM was applied for further mAEpC experiments. These data demonstrate the importance of the medium composition in terms of barrier properties. Whereas the cost-intense SAGM contains numerous supplements and growth factors, the less complex CMM is relatively cheap and its advanced suitability leads to economic benefits.

Results & Discussion

Taken together, primary mAEpC were seeded in a density of 1.5×10^6 cells/cm² in CMM10 on fibronectin/laminin-5-coated substrates for further experiments.

A. Influence of seeding density on TEER development



B. Influence of coating and cultivation medium on TEER development

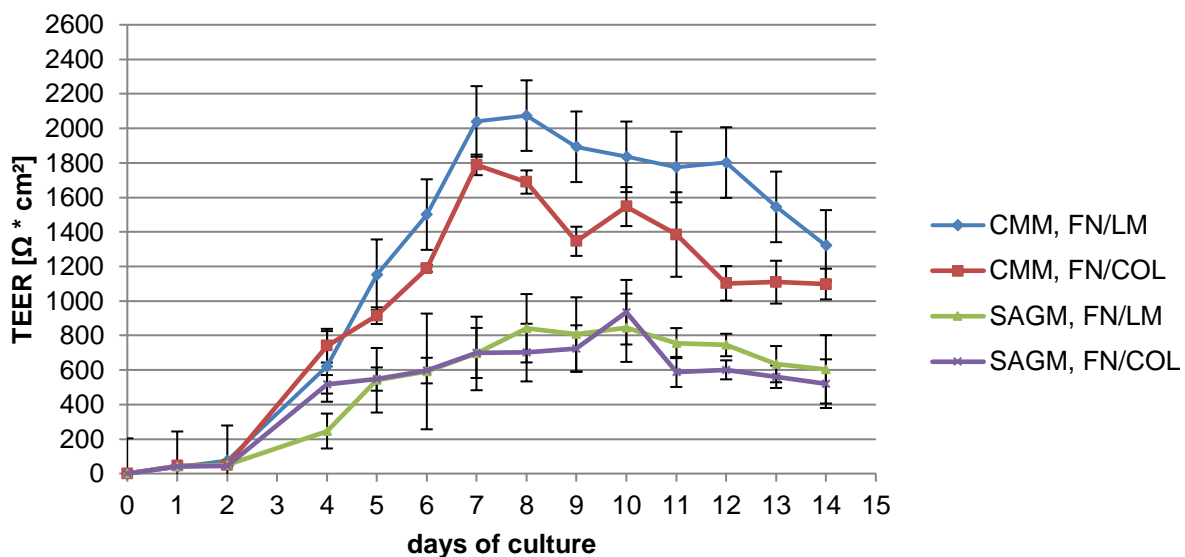


Figure 10: Influence of different cultivation conditions on the TEER development of mAEpC monolayers – A: mAEpC seeded on FN/LM-coated Transwells® at different cell densities; B: mAEpC seeded in a density of 1.5×10^6 cells/cm² on different coating combinations (FN/COL ▲ Fibronectin/Collagen or FN/LM △ Fibronectin/Laminin) and cultivated in either CMM or SAGM; values are shown as mean \pm S.D. (n = 9 from 3 independent experiments).

Results & Discussion

To reflect the *in vivo* situation of the deep lung as closely as possible, primary cultures grown on Transwells® were lifted from liquid-covered conditions (LCC) to the air-liquid interface, as described above. Figure 11 shows the mean TEER progression at both cultivation conditions as a function of time taken from six independent mAEpC isolations. At both cultivation conditions, mAEpC develop high TEER increasing with time and reaching maximum values at day 6 after isolation. Remarkably, mAEpC kept at LCC develop higher TEER ($\text{TEER}_{\max} \sim 1900 \Omega \text{cm}^2$) than cells grown at the ALI ($\text{TEER}_{\max} \sim 1100 \Omega \text{cm}^2$). This was possibly due to a less optimal nutrient supply in ALI culture, or to cellular stress caused by the measurement procedure itself which might have temporarily impaired the barrier function.

Commonly, functional alveolar epithelial *in vitro* barriers exhibit TEER values exceeding $\geq 1000 \Omega \text{cm}^2$ (Hittinger *et al.*, 2015) which goes in line with the findings of this study. Therefore, it is most likely that primary mAEpC express functional tight junction complexes and thus, build a barrier against external threats mimicking the *in vivo* situation of the air-blood barrier. For this reason, the primary mAEpC *in vitro* model fully meets the requirements to be applied for paracellular transport studies.

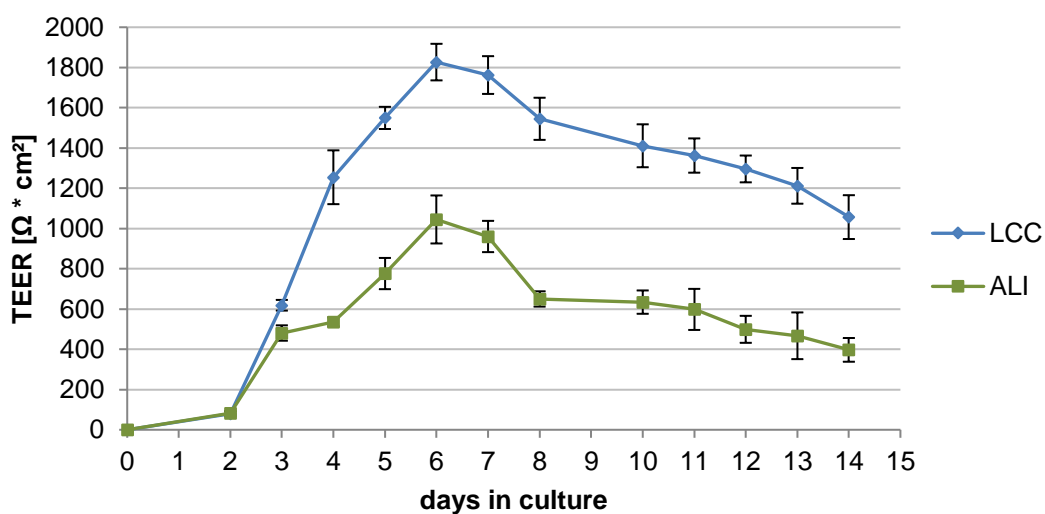


Figure 11: Comparison of the TEER development of primary mAEpC grown under liquid-covered conditions (LCC) or at the air-liquid interface (ALI); values are shown as mean \pm S.D. (n=18 from 6 independent mAEpC isolation procedures).

3.2.3 Comparison of primary mAEpC and hAEpC cultures

To evaluate if the primary murine model of the alveolar epithelium exhibits features like the human equivalent, mAEpC and hAEpC were compared addressing their barrier properties and *in vitro* differentiation after isolation (see figure 12).

Therefore, the TEER development of freshly isolated hAEpC (HIPS#629 and HIPS#631) and hence, the integrity of functional tight junctions was assessed over time (see figure 12A), whereby the cells were cultivated in SAGM (recommended for hAEpC) or CMM (recommended for mAEpC), respectively. Compared to mAEpC (see figure 10), the TEER development of human cells proceeds similarly with slightly higher TEER_{max} values. Whereas hAEpC grown in CMM show higher TEER within the first 5 days after isolation, the appropriate TEER_{max} (~2000 Ωcm²) is marginally lower as the TEER_{max} of hAEpC grown in SAGM (~2200 Ωcm²). This result suggests that primary hAEpC can develop into a tight monolayer in both tested cultivation media. Vice versa, mAEpC could only develop high TEER when cultivated in CMM and the TEER_{max} of cells cultivated in SAGM could not exceed ~800 Ωcm² (see figure 12B). From an economical point of view, it would be interesting to further investigate the suitability of CMM for other hAEpC experiments as CMM is much more cost-effective than SAGM and its usage could contribute to a cost reduction of the relatively expensive hAEpC isolation procedure (Daum *et al.*, 2012).

To monitor the differentiation of hAEpC, immunofluorescence staining on 0.33 cm²-Transwells® was performed at day 1 after isolation for the ATII marker protein proSP-C (see figure 12B) and at day 7 after isolation for the ATI marker and TJ protein ZO-1 (see figure 12C). In accordance with the findings for mAEpC and as previously described (Kuehn *et al.*, 2016), freshly isolated hAEpC express proSP-C which is being reduced by time (data not shown). Moreover, hAEpC showed an expression of ZO-1 restricted to the cell membranes starting at day 7 post isolation, as observed for mAEpC.

These data suggest that human and murine AEpC exhibit comparable *in vivo* properties of the air-blood barrier including functional tight junction complexes as expressed by high TEER and immunofluorescence staining of prominent marker proteins. The interspecies comparison also gives evidence that both primary models can be applied for the elucidation of paracellular transport mechanisms.

Results & Discussion

In this context, primary human *in vitro* cell culture models could demonstrate their suitability in manifold manner (Elbert *et al.*, 1999; I. I. Forbes, 2000; Hittinger *et al.*, 2016b), as described in detail in the course of the introducing chapters. To conclude, the herein established primary mAEpC model of the air-blood barrier can be used to complete possible applications in these premises avoiding the use of patient material.

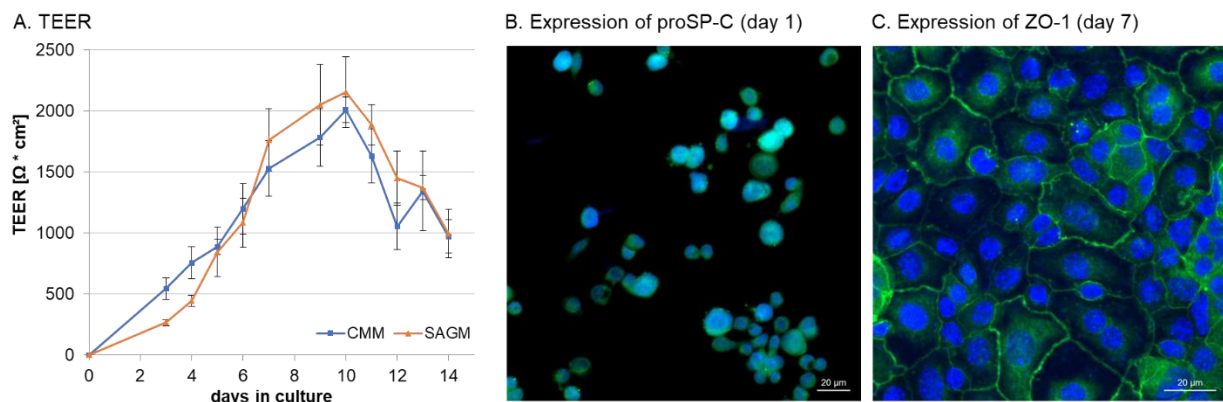


Figure 12: Barrier properties and trans-differentiation of hAEpC – A: TEER development of primary hAEpC cultivated in either CMM or SAGM; values are shown as mean \pm S.D. with (n=6 from 2 independent hAEpC isolation procedures: HIPS#629 and HIPS#631). B: Immunofluorescence of proSP-C (green) at day 1 post isolation; C: Immunofluorescence of ZO-1 (green) at day 7 post isolation; hAEpC were fixed with 3% PFA on 0.33 cm²-Transwell® membranes and nuclei were stained with DAPI solution (blue); scale bars: 20 μm .

3.3 Towards an optimized immortalization approach to generate cell lines originating from mAEpC

In these studies, two different approaches aiming at the immortalization of primary mAEpC were applied. Thereby, the focus was on a novel immortalization strategy based on the lentiviral-mediated transduction of primary cells with a recently patented library of proliferation-promoting genes (see 3.3.2 and the following), as previously described by May *et al.* (2016). In an alternative immortalization attempt, mAEpC were transduced with a single lentiviral vector system conditionally expressing the SV40 TAg, a conventional immortality gene known to cause dramatic cell alterations upon continuous expression, as outlined in the introduction (see 3.3.1).

As a starting point, primary murine alveolar epithelial cells (mAEpC) were isolated from ROSA^{ConL} hetero mice and cultivated on porous 0.33 cm²-Transwell® membranes to enable the daily assessment of the TEER to monitor the development of a tight monolayer. At the same time, primary mAEpC were seeded on 24well-plates for the lentivirus-mediated transduction. When the TEER of the Transwell®-grown cells reached its maximum (4 to 6 days post seeding), primary mAEpC grown on 24-wells were transduced with the lentiviral expression systems.

3.3.1 Lentiviral-mediated transduction of mAEpC with a vector system conditionally expressing the Simian Virus 40 Large T antigen

Previously, it has been shown in multiple cell types that the expression of the Simian Virus 40 large T antigen (SV40 TAg) leads to an extension of the cell's life span and increases the likelihood to obtain immortalized cell derivates. The explanation for the prolonged life span is attributed largely to the SV40 TAg and its binding capacity to the tumor suppressor p53 and, consequently, the inhibition of p53-dependent pathways (Hubbard & Ozer, 1999). Therefore, and as an alternative attempt to immortalize primary murine alveolar epithelial cells, a single-gene lentiviral vector conditionally expressing the Simian Virus 40 Large T antigen (TAg) was used to transduce mAEpC. This autoregulated expression system was described to feature tetracycline-dependent and, thus controllable TAg expression (May *et al.*, 2004, 2007). In theory, the key feature of cell lines established with this immortalization strategy is that their

proliferation status could be strictly controlled while the expression of relevant markers can be maintained (May *et al.*, 2010).

Due to the transduction of mAEpC with this lentiviral vector, the proliferating cell population mAELVi.J (J refers to the applied pJSARLT vector) could be obtained. When the cells could be expanded at desired densities (starting at passage 9), growth curves of mAELVi.J grown either in presence or absence of the tetracycline-analogue doxycycline (Dox) were assessed (see figure 13). Upon the presence of doxycycline in the cultivation medium, high cell division rates were observed as sigmoid growth curve, comparable to those of other standardized cell lines. However, mAELVi.J cell growth could not be arrested in the absence of doxycycline, as demonstrated by the appropriate growth curve which shows a course comparable to the results at induced conditions. In fact, induced cells grew just slightly faster than those grown without doxycycline indicating “leakiness” or dysfunction of the applied expression cassette which would have to be further analyzed in terms of functionality. Consequently, mAELVi.J cells most likely continuously express TAg and were further characterized regarding their morphology and barrier properties, which is described in the next chapter (see 3.4.3).

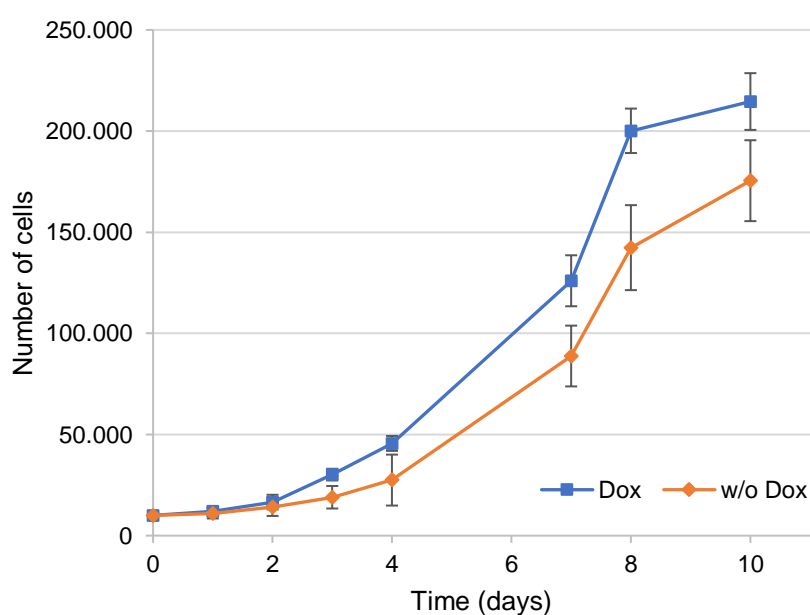


Figure 13: Growth curve of mAELVi.J cells at passage 21 assessed over 10 days either at induced conditions (Dox) or uninduced conditions (w/o Dox); numbers of cells are shown as mean \pm S.D. (n=3).

3.3.2 Lentiviral-mediated transduction of mAEpC with the CI-SCREEN immortalizing gene library

Recently, a novel human cell line of the alveolar epithelium, referred to as hAELVi (human alveolar epithelial lentivirus-immortalized) cells, could be achieved as a result of the lentiviral-mediated transduction of primary hAEpC with a patented library of 33 distinct proliferation-promoting genes (May *et al.*, 2016). Likewise, this immortalization approach was applied to transduce primary mAEpC. Upon transduction with the lentiviral gene library, certain genes were integrated into the mAEpC genome eventually inducing cell proliferation processes, while non-transduced cells remained to be inherently growth-arrested and underwent senescence or apoptosis, respectively. Subsequently, 8 genetically distinct proliferating cell populations, referred to as mAELVi.A-H (murine alveolar epithelial lentivirus-immortalized cells), were obtained. To achieve clonal formation, these mAELVi populations were continuously expanded (1:1) in culture dishes, up to a growing area of 10 cm². However, clonal cell formations could only be observed in the case of mAELVi.C and mAELVi.E and is exemplarily shown for the latter in figure 14. These light microscope images, which were captured at cell passage 6 post lentiviral transduction, clearly demonstrates a distinct morphological appearance of some mAELVi.E cells compared to the surrounding. Because of the enhanced attachment of this cell formation to the cultivation surface, it was possible to isolate the cells by passaging them in two shifted trypsinization steps. Nonetheless, it remains unclear if the cell formation emerged from a single cell or if the cells represent a heterogeneous mAELVi.E population. Thus, all mAELVi cells were treated as polyclonal cell lines.

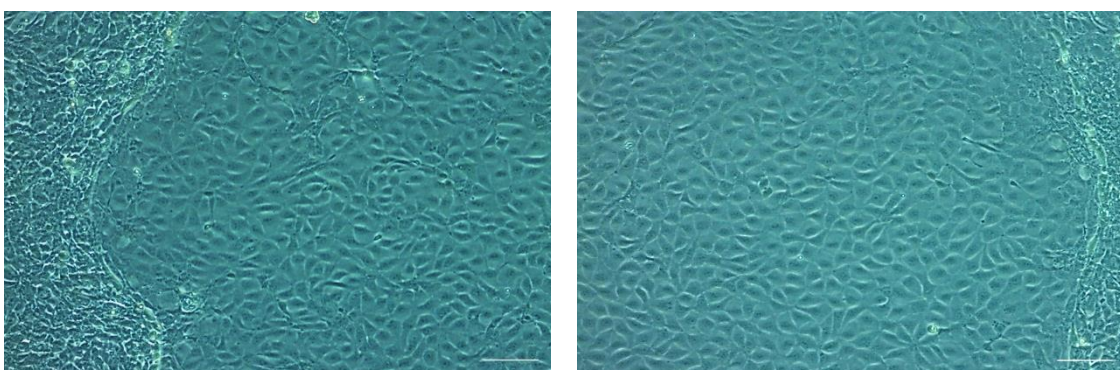


Figure 14: Formation of proliferating mAELVi.E cells at passage 6 after lentiviral transduction; cells with distinct morphology were separated from surrounding cells by a shifted two-step trypsinization and the cell population was maintained as mAELVi.E; scale bars: 100µm.

Furthermore, these expandable mAELVi populations were analyzed in terms of the integration pattern of immortalizing genes, ATI/II marker expression by PCR-based RNA-analysis and immunofluorescence staining as well as their barrier properties by TEER measurements. These experiments are described in detail for mAELVi.E and mAELVi.wt in the following (see 3.4). Table 11 (see 3.4.5) provides a summary of the obtained mAELVi cell populations and their characteristics in comparison with findings of primary mAEpC and MLE12.

3.3.3 Gene integration pattern and minimal set of immortalizing genes

Upon lentiviral-mediated transduction of mAEpC with the CI-SCREEN gene library, the resulting whole-cell RNA extracts of mAELVi.A-H cells were analyzed in respect of the pattern of integrated immortalizing genes by PCR. Table 10 provides an overview of the immortalizing gene integration pattern of the tested mAELVi cell populations. On average, 3 to 7 different genes (mean 5 ± 1) out of the total 33 genes have been integrated in the mAEpC genome which explains the outcome of the different mAELVi phenotypes.

In total, only 14 out of 33 immortalizing genes could be detected. Namely, these are Bmi1, E6, E7, Ezh2, Fos, Id2, Id3, Id4, Kfl4, Myc, Nanog, Rex, RhoA and Nfe2L2. Remarkably, some of these genes could be detected more often than others. The most prominent immortalizing genes, which could be detected in $\geq 50\%$ of the tested mAELVi populations, were Id3 (*inhibitor of differentiation protein 3*; 87,5% integration), RhoA (*Ras homolog gene family member A*; 62,5% integration) and Fos (*Fos proto-oncogene, Activating Protein-1 transcription factor subunit*; 50% integration).

The helix-loop-helix transcription factor Id3 was previously reported to be overexpressed in many types of carcinomas indicating an important role in tumorigenicity and cell cycle progression. In this context, it could be demonstrated that siRNA-mediated suppression of Id3 could significantly reduce cell proliferation suggesting Id3 as potential target for anti-cancer therapies (F. F. Chen *et al.*, 2015; Kamalian *et al.*, 2010). Similarly, the small GTP-binding protein RhoA has been found overexpressed in malignant non-small-cell lung cancer triggering cell cycle progression which could be reversed upon RhoA-knockdown (Liu *et al.*, 2017; Zhang *et al.*, 2014). The dimeric Fos transcription factor may regulate different target genes

Results & Discussion

executing distinct biological functions such as cell proliferation and transformation (Angel & Karin, 1991; Lian *et al.*, 1991).

These results suggest that some genes are more likely to be responsible for the prolongation of the cell's lifespan and that this set of proliferation-promoting genes could be applied for the cell-specific immortalization of mAEpC, which was subject of additional investigations described in the following.

Results & Discussion

Table 10: Pattern of integrated genes from CI-SCREEN gene library upon lentiviral transduction of mAEpC which resulted in expandable maelvi cells (maelvi.A-H); *maelvi.wt were transduced with a set of 9 out of 33 immortalizing genes; the results are based on PCR-analysis of maelvi whole-cell DNA extractions; green boxes indicate positive PCR products for the respective gene; mGAPDH was used as internal control of the PCR.

CI-Screen gene library	maelvi populations								
	A	B	C	D	E	F	G	H	wt*
Gli1									
Bmi1									
Core									
E6									
E7									
Ezh2									
Fos									
Bcl2									
HoxA9									
Id1									
Id2									
Id3									
Id4									
Kfl4									
Lmo2									
Myb									
Myc									
Nanog									
Rex									
RhoA									
Sez12									
Sox2									
β-Cat									
TAg									
Yap1									
ZFP217									
NS1									
Nfe2L2									
v-Myc									
Jun									
PymT									
Oct3									
E2F1									
	Ezh2 Fos Id3 Id4 Kfl4 Rex	Ezh2 Fos Id3	E7 Fos Id3 RhoA Nfe2L2	Bmi1 E7 Id2 Id3 Nanog RhoA Nfe2L2	Bmi1 Fos Id2 Id3 RhoA	Nanog RhoA Nfe2L2	Bmi1 E6 Id2 Id3 Myc	Ezh2 Id3 RhoA	E6 Fos Id2 Id3 Nanog
	6/33	3/33	5/33	7/33	5/33	3/33	5/33	3/33	5/9

3.3.4 Transduction of wildtype mAEpC with the defined minimal set of immortalizing genes

In another step towards an optimized immortalization protocol and to define a minimal set of immortalizing genes, mAEpC isolated from RosaConL hetero mice were transduced with 14 genes out of the CI-SCREEN library which could be detected in mAELVi cell populations, as described above. In total, more than 100 samples of transduced mAEpC-DNA samples were analyzed by PCR regarding the integrated immortalizing genes. Following this procedure, the number of integrated genes could be further reduced to only 9 out of the total 33 genes, which are namely E6, E7, Id2, Id3, Fos, Myc, Nanog, Nfe2L2 and RhoA. To verify that this minimal set of genes can be applied for rather “cell-specific” immortalization, mAEpC were isolated from wildtype mice providing a distinct genetic background compared to previous experiments. As soon as wildtype mAEpC developed into a tight monolayer with high TEER *in vitro*, cells were transduced with the 9 abovementioned lentiviral vectors. As a result, a proliferating cell population, referred to as mAELVi.wt (“wildtype”), could be obtained.

The immortalization attempts of wildtype mAEpC resulted in an expandable cell population, referred to as mAELVi.wt, which was included in the following characterization and application-oriented experiments. The gene integration analysis of mAELVi.wt revealed that 5 (E6, Fos, Id2, Id3, Nanog) out of 9 applied immortalizing genes were introduced.

Thus, this immortalization approach and the defined set of genes, respectively, form the basis for further experiments eventually enabling the establishment of cell lines derived from mice with a defined genetic background. This approach could be applied to compare and correlate both *in vitro* and *in vivo* data of the same mouse model, which provides an advantage over human cell culture systems.

3.4 Characterization of mAELVi cell populations

Upon various lentiviral-mediated mAEpC immortalization attempts, different mAELVi cell populations were expanded, as previously described in detail:

- **mAELVi.A-H** were achieved through transduction of mAEpC from RosaConL mice with the CI-SCREEN library
- **mAELVi.J** was obtained by transduction of mAEpC from RosaConL mice with TAg only (see 3.4.3)
- **mAELVi.wt** was achieved through transduction of mAEpC from wildtype mice with a defined set comprising 9 genes out of the CI-SCREEN library

These continuously growing cells have been characterized regarding the integration pattern of immortalizing genes (see table 10), EpCAM expression by FACS analysis, the expression of ATI/ATII-specific markers and barrier properties. Fortunately, it was possible to successfully immortalize mAEpC in a way that the resultant mAELVi cells could be easily handles and grown in almost infinite quantities. Table 11 (see 3.4.4) provides an overview of the 10 expandable mAELVi populations and their characteristics in comparison with MLE12 and primary mAEpC.

Based on these data, and particularly because of the highest TEER ($TEER_{max}$ 356 Ωcm^2) obtained, mAELVi.E cells were selected for further studies (see 3.5 and 3.6). Even though the abovementioned experiments were carried out with all mAELVi populations, the respective results presented in the following sections highlight mAELVi.E cells, unless otherwise indicated. In addition, MLE12 (*Murine Lung Epithelial*) cells were carried along in many experiments as a reference cell line (see table 2). This cell line was produced from lung tumors generated in transgenic mice expressing TAg under the control of the SP-C promotor. Upon the immortalization processes, the cells could maintain ATII-like features like lamellar bodies, but have not yet been analyzed regarding their barrier properties (Wikenheiser *et al.*, 1992; Wikenheiser *et al.*, 1993).

3.4.1 Morphological characterization of mAELVi cells

Upon mAEPc transduction with the lentiviral gene library, genetically different mAELVi populations with distinct morphological appearances were obtained, from which are some displayed in figure 15 in comparison with primary mAEPc (day 4 post isolation). Notably, cells were cultivated on fibronectin/laminin-5-coated plastic surfaces to capture these light microscopic images. Morphologies might appear different when the cells are grown on other materials or surface structures, respectively, because these parameters have been found to strongly influence the cells' behavior (Flemming *et al.*, 1999; Martinez *et al.*, 2009).

Whereas primary mAEPc, mAELVi.C, mAELVi.E and mAELVi.wt exhibit comparable morphologies displaying tight monolayers, mAELVi.H cells resembled a fibroblast-like phenotype (Seluanov *et al.*, 2010) indicating that their epithelial character got impaired due to the integration of immortalizing genes, as described previously (Moiani *et al.*, 2012; Schmitz *et al.*, 2012). Furthermore, the light microscopic appearance of mAELVi.D seems to be comparable to the human cell line A549 (Aarbiou *et al.*, 2002) displaying an ATII-like cell formation.

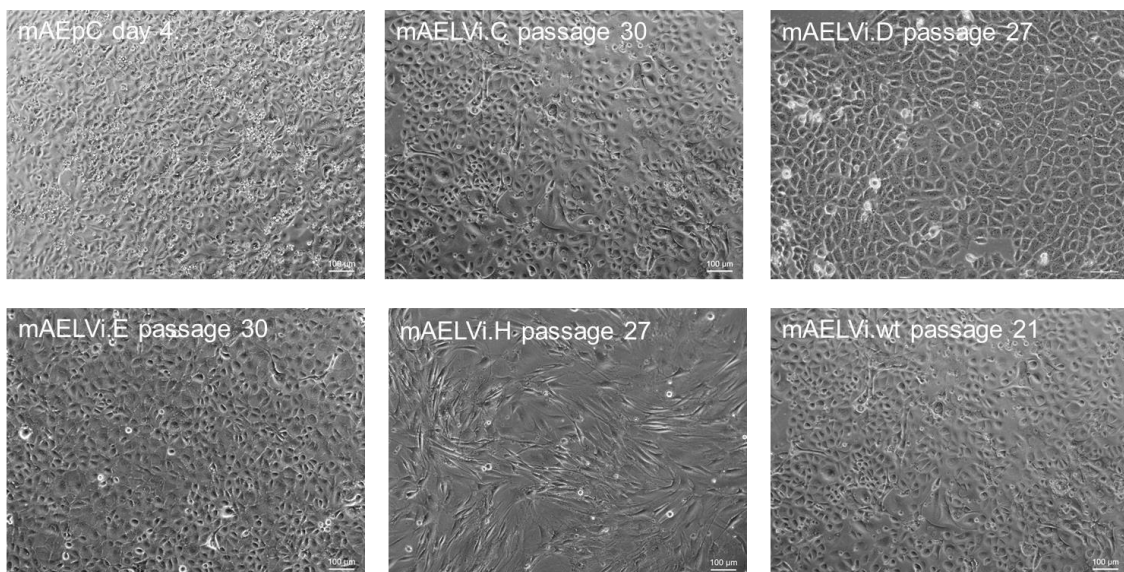


Figure 15: Light microscopic images of primary mAEPc and different immortalized mAELVi cell populations, as indicated; cells were cultured on fibronectin/laminin-5-coated plastic; scale bars: 100μm.

In addition to light microscopic analyses, the growth morphology of mAELVi.E and mAELVi.wt cells was determined by histology (see figure 16). Therefore, cells were grown on porous Transwells® for 7 days and subsequently treated for the preparation of membrane cross-sections. Both mAELVi.E (upper image) and mAELVi.wt (lower image) cells appeared to form a thin monolayer indicating an ATI-like growth behavior (Dobbs *et al.*, 2010).

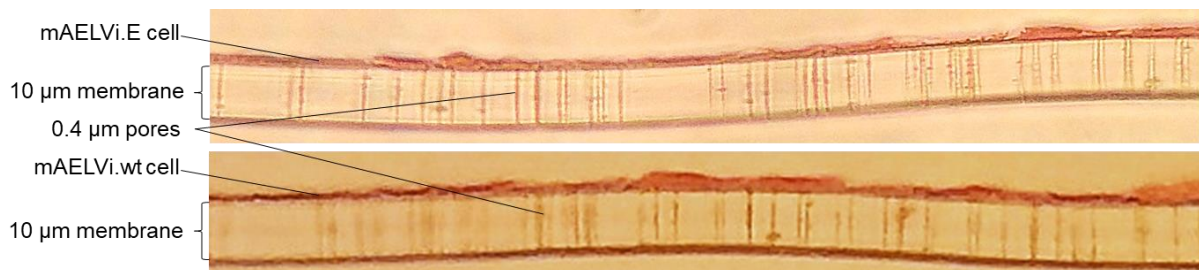


Figure 16: Histological cross sections of mAELVi.E and mAELVi.wt grown on fibronectin/laminin-5-coated 10 µm-thick Transwells® with a pore size of 0.4 µm; membrane sections were stained with H/E; images were captured with an inverted light microscope.

3.4.2 Expression of alveolar epithelial characteristics of mAELVi cells

To assess the percentage of mAELVi.A-J populations expressing the epithelial marker EpCAM, cell fractions from early (1 - 4) and late (17 - 21) passages were analyzed by flow cytometry (see figure 17). The FACS analyses revealed that the number of EpCAM-positive cells tends to increase with time, with mAELVi.C being the only exception. In all other mAELVi populations, the percentage of EpCAM-positive cells is much lower in early passages indicating that expression changes might occur upon cell expansion. In case of mAELVi.E, in early passages only 63% of the cells expressed EpCAM, whereas 90% EpCAM-expressing cells were detected in late passages. The increase in EpCAM-positive cells could be due to natural selection processes upon cultivation. This highly conserved transmembrane glycoprotein mediates cell-cell-adhesion by binding to the actin cytoskeleton. It is normally expressed at the basolateral membrane of most epithelial tissues, and thus, is widely used as marker for such cells (Trzpis *et al.*, 2007; Winter *et al.*, 2003).

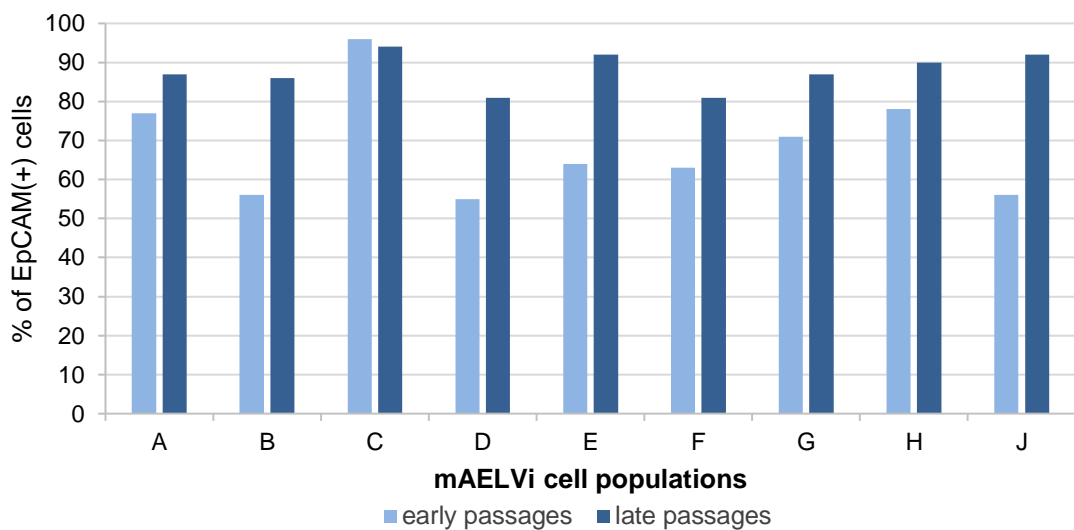


Figure 17: Percentage of EpCAM-positive cells of mAELVi cell populations assessed with a monoclonal anti-EpCAM PE antibody by FACS analyses. Results from early (passages 1 – 4) and late (passages 17 – 21) passages are compared.

Furthermore, the expression and cellular localization of the transmembrane protein EpCAM was visualized by immunofluorescence staining performed with mAELVi.E cells at passage 33. Figure 18 illustrates that EpCAM is expressed mainly in the areas of the cell membranes in all mAELVi.E cells. Thus, mAELVi.E cells display an epithelial character, since non-epithelial cells do generally not express EpCAM (Trzpis *et al.*, 2007).

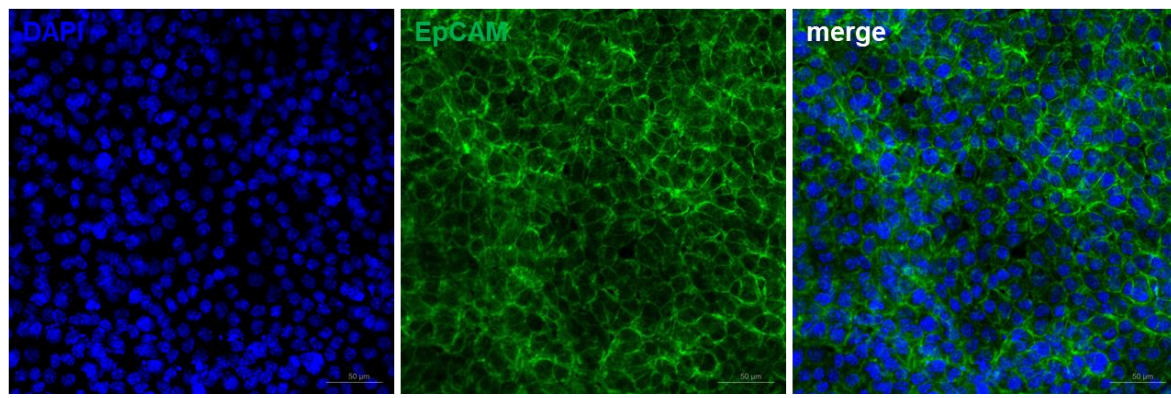


Figure 18: Expression of EpCAM in mAELVi.E cells at passage 33 (left: DAPI-stained nuclei, middle: EpCAM distribution, right: merge); cells were fixed on fibronectin/laminin-5-coated chamberslides with 3% PFA; scale bars: 50 µm.

Besides its applicability as epithelial marker to isolate and distinguish between different phenotypes of lung cells (N. Fujino *et al.*, 2012; Hasegawa *et al.*, 2017), EpCAM has been found to be overexpressed in various carcinomas (Patriarca *et al.*, 2012) such as lung tumors (Y. Kim *et al.*, 2009; Pak *et al.*, 2012). Due to this fact, it remains unclear if the increasing amount of EpCAM-expressing mAELVi cells somehow relates to the impaired alveolar epithelial functions of the cells.

In this context, a genome-wide expression analysis of the human lung cell lines A549 and Calu-3 revealed a network of EpCAM-induced cell cycle regulators upon treatment with an EpCAM-specific antibody suggesting that EpCAM triggers several intercellular signaling pathways (Maaser & Borlak, 2008). In addition, the treatment of these cell lines with an EpCAM-specific antibody entailed a dose-dependent increase of cell proliferation rates. Taking this into account, EpCAM might possibly be involved in the mechanisms causing unlimited growth capacity of mAELVi populations which might occur concurrent with less prominent barrier function compared to primary mAEpC.

To further characterize the expression of alveolar epithelial-specific genes, cDNA sequences produced from whole-cell RNA extractions of mAELVi, mAEpC, and MLE12 cells were analyzed by PCR focusing on ATI markers (AQP5, Cav-1, T1 α , ICAM-1) and ATII markers (SP-A, SP-B, SP-C). The functions of the appropriate gene products are outlined in the following discussion. As a positive control, PCR reactions of the housekeeping gene mGAPDH (murine glyceraldehyde-3-phosphate dehydrogenase) were carried along all experiments. Reactions containing all PCR agents except the cDNA templates served as negative control to preclude contaminations. As evident from figure 19, freshly isolated mAEpC and MLE12 cells expressed all tested ATI and ATII markers displaying a heterogenous genotype. Since the isolation protocol is based on EpCAM-positive selection, freshly isolated mAEpC (day 0) could also possibly be comprised of both ATI and ATII cells, as indicated by the positive signals obtained for all tested markers. However, it is likely that *in vitro* monolayer formation is mainly performed by viable ATII cells undergoing trans-differentiation into ATI-like cells, since most of the ATI cells would not have survived the isolation procedure due to their intrinsic fragility.

In contrast, the expression profile of mAELVi.E cells was restricted to positive signals of typical ATI markers, such as AQP5, Cav-1 and ICAM-1. Thus, mAELVi cells exhibited an ATI-like genotype, while primary mAEpC and MLE12 revealed expression

Results & Discussion

profiles displaying both ATII-like and ATI-like characteristics. Gene expression details of other analyzed mAELVi populations are listed in table 11.

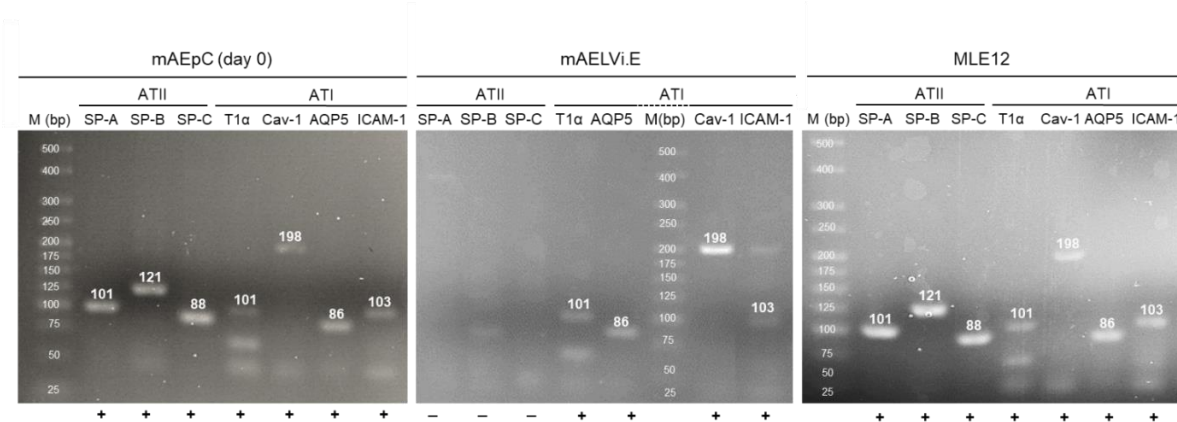


Figure 19: PCR analyses of the expression of ATI and ATII markers in mAEpC, mAELVi.E and MLE12 cells; M: Hyperladder V (Bioline) with molecular weights indicated in base pairs (bp), analyzed ATII markers: SP-A (101bp), SP-B (121bp) and SP-C (88bp); ATI markers: T1 α (101bp), AQP5 (86bp), Cav-1 (198bp) and ICAM-1 (103bp); mGAPDH and template-free samples, respectively, were run as controls (data not shown).

T1 α , also known as podoplanin, was one of the first identified ATI marker genes whose expression was shown to be restricted to type I cells of the alveolar epithelium (Cao *et al.*, 2000). Even though its importance during lung development was demonstrated by homozygous T1 α -null mice dying at birth from respiratory failure, the physiological role of the proteins in adults remains unclear (M. I. Ramirez *et al.*, 2003). Because T1 α was found to be co-expressed with aquaporins, an involvement in the regulation of fluid fluxes was proposed (Millien *et al.*, 2006). In this context, the loss of AQP5, the major ATI cell-associated water channel, was shown to cause decreased water transport upon significant molecular changes in the expression of tight junction (TJ) proteins indicating a regulatory role in TJ assembly (Kawedia *et al.*, 2007). Besides TJ complexes, ATI cells can be characterized by the presence of caveolae, invaginations of the plasma membrane coated with caveolin proteins which ATII cells are lacking (Campbell *et al.*, 1999). Thereby, Cav-1 represents the main protein component of such lipid rafts and is involved in numerous cellular processes including transport and signaling pathways as demonstrated by gene knock-out experiments (Drab *et al.*, 2001). Furthermore, Cav-1-deficient MEF (murine embryonal fibroblasts) exhibited a

hyper-proliferative phenotype when compared to wildtype MEF suggesting that Cav-1 functions as a putative tumor suppressor (Razani *et al.*, 2001).

The intercellular adhesion molecule 1, ICAM-1, is known to play a critical role in inflammatory processes and tumor cell growth in the airways (Jiang *et al.*, 1998). In normal adult rat and human lung, ICAM-1 is highly expressed in ATI cells, whereas only slight expression levels could be detected in ATII cells (Attar *et al.*, 1999). It was furthermore suggested that ICAM-1 is involved in ATI differentiation processes, hence it was included in the characterization of mAELVi populations.

As surfactant is exclusively produced by alveolar type II cells, the presence of the respective surfactant proteins SP-A, SP-B and SP-C can be used as ATII-specific markers (Mulugeta & Beers, 2006).

To further evaluate these observations regarding the functionality of the cells, mAELVi populations were analyzed due to the expression of TJ proteins and barrier properties which is described in the following.

3.4.3 Expression of TJ proteins and barrier properties of mAELVi.E and mAELVi.wt cells

To investigate the barrier properties of mAELVi monolayers in comparison with their primary counterpart, TEER measurements and immunofluorescence staining for TJ proteins were conducted. The appropriate findings are exemplary demonstrated for mAELVi.E and mAELVi.wt cells. Maximum TEER ($TEER_{max}$) and mean TEER values as well as complementary characteristics of other mAELVi populations are listed in table 11 (see 3.4.5).

To assess the TEER and optimize the cultivation conditions in view of the formation of a tight monolayer, mAELVi cells grown on Transwells® were cultivated with different media (see figure 20A) or on different coating substrates (see figure 20B). In this context, it was previously shown that the extracellular environment (e.g. medium supplements, coating substrates) *in vivo* as well as *in vitro* influences the differentiation of alveolar epithelial cells (Y. M. Lin *et al.*, 2010; Olsen *et al.*, 2005).

In case of mAELVi.E, the highest TEER peaking at $356 \Omega\text{cm}^2$ was assessed upon cultivation in CMM10 medium, whereas the TEER was lower when CMM10 was

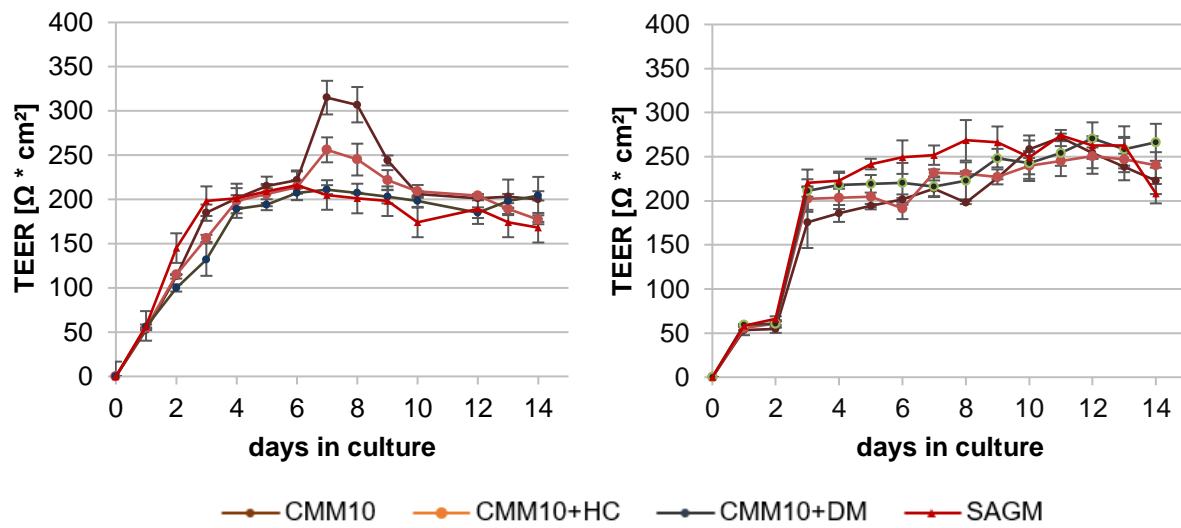
supplemented with hydrocortisone ($\text{TEER}_{\max} = 256 \Omega\text{cm}^2$) or dexamethasone ($\text{TEER}_{\max} = 211 \Omega\text{cm}^2$), respectively. Cells cultivated in SAGM medium developed TEER slightly faster but could not exceed a TEER_{\max} of $216 \Omega\text{cm}^2$. In case of mAELVi.wt, the cultivation in SAGM resulted in the highest TEER peaking at $256 \Omega\text{cm}^2$, however, all other tested medium compositions yielded in a comparable TEER development. For that reason, mAELVi cells were further cultivated in CMM10 as it is more cost effective compared to SAGM. Even though, mAEPc could also develop the highest TEER when grown in CMM10, primary cells exhibited much higher resistances peaking at $\sim 2500 \Omega\text{cm}^2$ (see figure 11).

In this context, hydrocortisone was proposed to contribute to the maintenance of an ATII-like character of isolated mAEPc *in vitro* (Rice *et al.*, 2002) corresponding to the findings obtained from this study. Accordingly, dexamethasone was suggested to play a role in the production of surfactant in primary hAEPC (J. Wang *et al.*, 2007). However, cells analyzed in the latter study were grown on a mixture of Matrigel and rat tail collagen which further influenced the differentiation processes of freshly isolated hAEPC.

For that reason, mAELVi.E and mAELVi.wt were grown on different substrates to evaluate the influence of extracellular matrix proteins on the development of TEER (see figure 21B). Hereby, the results for both mAELVi.E and mAELVi.wt demonstrate that the cells developed the highest TEER after 8 days of cultivation when grown on a combination of fibronectin (FN) and laminin-5 (LM) peaking at 305 and $264 \Omega\text{cm}^2$ for mAELVi.E and mAELVi.wt cells, respectively. TEER levels were lower when the cells were grown on a combination of fibronectin and collagen or fibronectin only. Hence, cultivation devices for mAELVi cells were coated with fibronectin and laminin-5 for further experiments consistent with the findings from primary mAEPc (see figure 10). Nonetheless, attempts to optimize the cultivation conditions of mAELVi monolayers could not increase the TEER to levels comparable with primary cells indicating that the random integration of immortalizing genes might have caused impaired barrier properties of mAELVi cells.

Results & Discussion

A Influence of medium composition on TEER development of mAELVi.E (left) and mAELVi.wt (right)



B Influence of surface coating on TEER development of mAELVi.E (left) and mAELVi.wt (right)

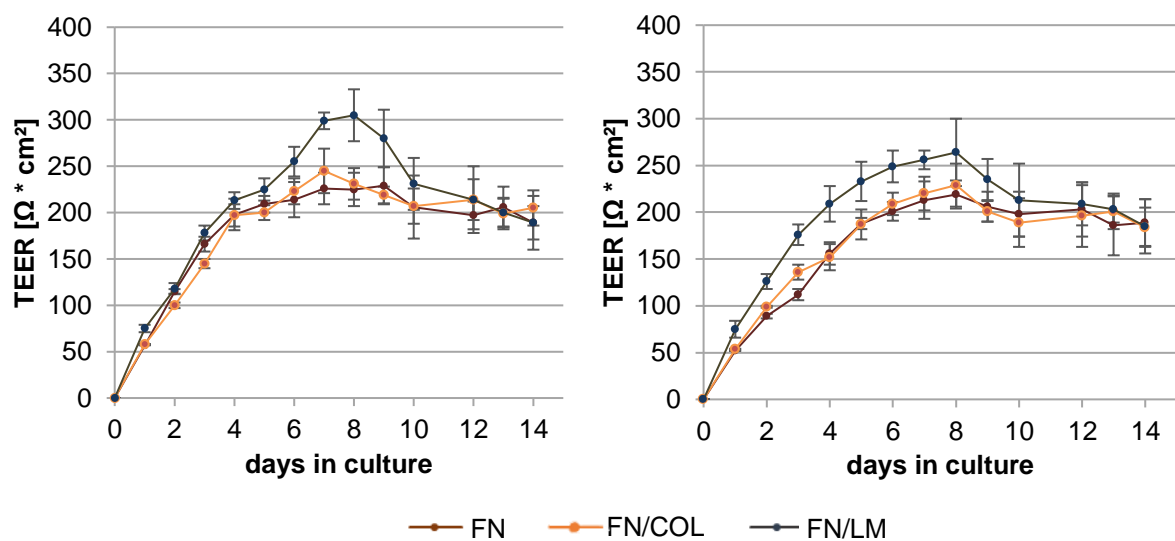


Figure 20: TEER development of mAELVi.E (left) and mAELVi.wt (right) seeded on 1.12 cm² Transwell® filter supports (pore size 0.4 µm) in CMM10 – A: Influence of medium composition (HC ≡ hydrocortisone, DM ≡ dexamethasone); B: Influence of different surface coatings (FN ≡ fibronectin; FN/COL ≡ fibronectin/collagen; FN/LM ≡ fibronectin/laminin-5); values are shown as mean ± S.D. (n = 9 from 3 independent experiments).

Results & Discussion

To better understand the decreased barrier function modulated by functional TJ, the expression of ZO-1 (see figure 21, left panel) and occludin (see figure 21, right panel) of primary mAEpC, mAELVi.E and mAELVi.wt cells was determined by immunofluorescence staining. Both TJ proteins were present in all cell types and revealed a cellular distribution restricted to cell membranes, as was observed for primary mAEpC. Despite expressing the most prominent TJ proteins ZO-1 and occludin, mAELVi cells appeared to exhibit much less pronounced barrier properties than mAEpC. These results suggest that the expression of other TJ proteins than ZO-1 and occludin might be defective causing a less sealed monolayer formation of mAELVi cells. It could also be possible that signaling pathways involved in TJ regulation and modulation processes have become dysregulated or interrupted due to the transduction of immortalizing genes (Wolburg & Lippoldt, 2002). Since functional TJ complexes are key for the maintenance of epithelial barrier functions, only analyses of all involved proteins could provide further insight in the mechanisms causing the impaired functionality of mAELVi populations when compared to primary cells.

Besides occludin, TJ complexes consist of other transmembrane core proteins, such as proteins of the Claudin family which have been discovered to form the structural backbone of TJ strands (Tsukita *et al.*, 2001). In this context, Claudin-18 as one of the most prominent TJ proteins was shown to be expressed by primary mAEpC (Demaio *et al.*, 2009). While most of these TJ proteins were found to be associated with signaling processes and anchoring to the actin cytoskeleton, recent studies have highlighted that claudins function as the major determinants of paracellular transport processes across the alveolar epithelium (Gonzalez-Mariscal *et al.*, 2003; Van Itallie & Anderson, 2006). Studies in rodent model systems revealed that claudin dysregulations might correspond to human pulmonary disorders, such as inflammation (Fang *et al.*, 2010) or sepsis (Cohen *et al.*, 2010) demonstrating the importance of functional TJ proteins and their interactions with each other and the intercellular space.

Furthermore, *Zonula Occludens* proteins, ZO-1 – 3, link the cytoplasmatic tail of occludin to the actin skeleton of the ECM and can interact with family members and other TJ-associated proteins such as Claudins and AF-6 (Fürster, 2008) whose expression should be addressed to further elucidate mAELVi cell barrier formation.

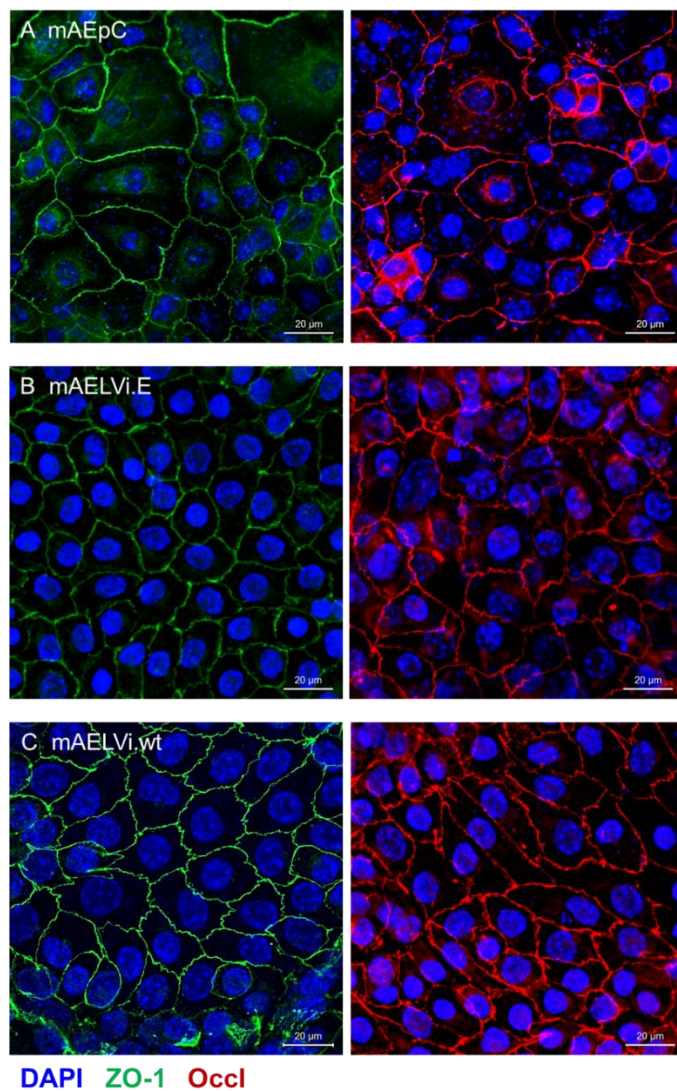


Figure 21: Expression of TJ proteins (left panel: ZO-1 in green; right panel: occludin in red); A: primary mAEpC at day 7 after isolation on 0.33 cm²-membranes; B mAELVi.E cells; C: mAELVi.wt cells; immortalized cells were stained at day 14 post seeding on 1.12 cm² membranes; cells were fixed with 3% PFA and nuclei were stained with DAPI solution; scale bars: 20 μm.

As adherens junctions mediate cell-cell adhesion promoting the formation of TJ, both types of intercellular junctions contribute to alveolar epithelial barrier functions and paracellular permeability (Ganesan *et al.*, 2013; Harris, 2012). Due to this fact, impaired mechanisms involved in the formation of functional adherens junctions could explain the less pronounced barrier properties of mAELVi populations compared to mAEpC. To elucidate the integrity of adherens junctions in mAELVi cells, further experiments are necessary. Alterations in junction assembly and function have previously also been reported to significantly impair the properties of the blood-brain barrier which is basically structured like the air-blood barrier (Stamatovic *et al.*, 2016).

In this context, the loss of junction barrier function has been outlined to play a critical role in metastatic cancers of many organs (Martin & Jiang, 2009) and inflammatory diseases such as cystic fibrosis (Coyne *et al.*, 2002).

Considering that mAELVi cells exhibited ATI-like characteristics, such as the expression of EpCAM (demonstrated by both FACS and immunofluorescence staining), typical ATI markers (demonstrated by RNA analyses) including prominent TJ proteins (see figure 21), and at the same time exhibited less pronounced barrier properties than their primary counterpart, these results appear to be contradictory. Accordingly, the question why the ability of mAELVi.E cells to build a tight monolayer with high TEER got reduced although the cells display ATI-like characteristics remains open. Quantitative transcriptome analyses of primary and immortalized cells might contribute to gain further insight in altering expression levels causing functional differences in mAELVi populations. Here, it appears that the random integration of immortalizing genes has caused a yet unsolved cellular impairment which is critical for the proper assembly of cell junctions.

3.4.4 Characterization of mAELVi.J cells

To assess the barrier properties of mAELVi.J, TEER measurements of Transwell®-grown cells were performed. Figure 22A reveals that the TEER_{max} of mAELVi.J cells was below 200 Ωcm² at any time demonstrating lacking barrier properties. In consistence with this result, light microscopy of mAELVi.J (Figure 22B) revealed that the cells built a leaky monolayer with cells appearing to be just slightly attached to each other. Consequently, mAELVI.J cells were not included in paracellular transport studies and toxicity prediction experiments in this work.

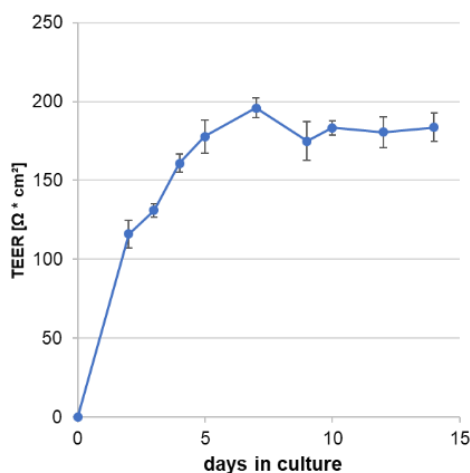
Nevertheless, this immortalization outcome provides further evidence that the long-term expression of TAg, as single immortalizing gene, leads to severe alterations of the cell's phenotype, as previously described for other epithelial cell types (Bae *et al.*, 1998; Nitta *et al.*, 2001; Yamasaki *et al.*, 2009). Upon other TAg immortalization attempts, at least some *in vivo*-like cell characteristics could be retained. As an example, the Murine Lung Epithelial (MLE) cell line was produced from lung tumors induced in transgenic mice expressing TAg under the control of the lung-specific SP-

Results & Discussion

C promotor (Wikenheiser *et al.*, 1992). These cell lines grew rapidly, lacked contact inhibition but could demonstrate some ATII-like features (Wikenheiser *et al.*, 1993).

In this context, *in vitro* models like the hereby described mAELVi.J cells could be applied for studies addressing the molecular mechanisms of tumorigenesis and cancer progression as TAg signatures were also found in tumors from human patients suffering from the most aggressive breast, lung or prostate cancers (Deeb *et al.*, 2007; Gazdar *et al.*, 2002).

A TEER measurement



B Light microscopy

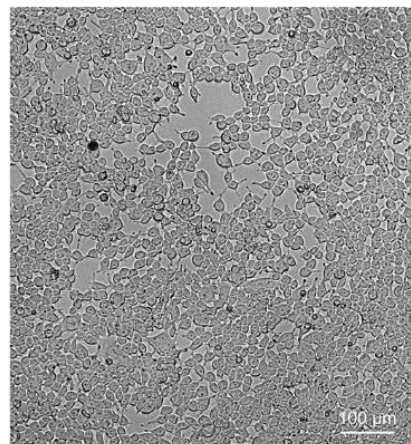


Figure 22: Characterization of mAELVi.J cells regarding barrier properties - A: TEER development; values are shown as mean \pm S.D (n=9 from 3 independent experiments). B: LM picture; scale bar: 100 μm .

3.4.5 Tabular characterization summary of mAELVi populations

Table 11: Characterization overview of mAELVi cells, primary mAEpC and MLE12; cells were characterized regarding the pattern of integrated lentiviral genes, ATI and ATII-like marker expression (PCR data), percentage of EpCAM-positive cells (FACS analyses; performed at cell passages 17 - 21) and TEER (mean and maximum in Ωcm^2).

Cells	Immortalization features	Integrated immortalizing genes	Marker expression (PCR data)		EpCAM-positive cells (FACS)	TEER (Ωcm^2)	
			ATI-like	ATII-like		mean	maximum
mAELVi.A	CI-SCREEN gene library 200 μ l + polybrene	Ezh2, Fos, Id3, Id4, Klf4, Rex	T1 α Cav-1 ICAM-1 AQP5	/	77.05%	187	205
mAELVi.B	CI-SCREEN gene library w/o E6, E7, Nanog 200 μ l + polybrene	Ezh2, Fos, Id3	T1 α Cav-1 ICAM-1 AQP5	/	86.65%	189	199
mAELVi.C	CI-SCREEN gene library 200 μ l + polybrene clonal formation	E7, Fos, Id3, RhoA, Nfe2L2	T1 α Cav-1 ICAM-1 AQP5	/	96.23%	211	244
mAELVi.D	CI-SCREEN gene library 150 μ l + polybrene	Bmi1, E7, Id2, Id3, Nanog, RhoA, Nfe2L2	T1 α Cav-1 ICAM-1 AQP5	SP-A	91.71%	201	216
mAELVi.E	CI-SCREEN gene library 100 μ l + polybrene clonal formation	Bmi1, Fos, Id2, Id3, RhoA	T1 α Cav-1 ICAM-1 AQP5	/	91.77%	248	356
mAELVi.F	CI-SCREEN gene library 100 μ l + polybrene	Nanog, RhoA, Nfe2L2	T1 α AQP5	/	73.44%	189	210
mAELVi.G	CI-SCREEN gene library 100 μ l + polybrene clonal formation	Bmi1, E6, Id2, Id3, Myc	T1 α Cav-1 AQP5	SP-A	83.94%	206	268
mAELVi.H	CI-SCREEN gene library 100 μ l + polybrene	Ezh2, Id3, RhoA	T1 α Cav-1 AQP5	/	93.56%	199	234
mAELVi.J	JSARLT vector 150 μ l + polybrene	SV40 TAg (conditional expression)	T1 α Cav-1 ICAM-1 AQP5	SP-B	92.11%	177	198
mAELVi.wt	minimal set (9/33) of immortalizing genes from CI-SCREEN gene library 200 μ l lentivirus + polybrene	E6, Fos, Id2, Id3, Nanog	T1 α AQP5 Cav-1 I-CAM1	SP-B	94.53%	213	259
primary mAEpC	N/A	N/A	T1 α , AQP5, Cav-1, ICAM-1	SP-A SP-B SP-C	98.67%	1800	2500
MLE12	N/A	SV40 TAg	T1 α , AQP5, Cav-1, ICAM-1	SP-A SP-B SP-C	88.45%	190	216

3.5 Transport studies

The pulmonary route is being thoroughly investigated not only for local drug administration to treat lung diseases but also as a non-invasive alternative to systemic drug delivery. During preclinical studies, it is thus of utmost importance to examine the biopharmaceutical and pharmacological aspects of the interactions between the alveolar lining and a certain compound or drug formulation, respectively. Besides transporter- or receptor-mediated transport, ions and larger molecules might enter the blood stream via the paracellular route mainly modulated by TJ complexes as major rate-limiting barrier (Rubas *et al.*, 1996). For this purpose, pulmonary epithelial cell culture models are key to predict transport rates and evaluate apparent permeability coefficients (P_{app}) of a specific cell type for a defined molecule.

In this context, the absorption kinetics and TEER of cell monolayers were determined by performing permeability studies and comparing the resulting P_{app} values for the transport of fluorescent model tracers with different molecular weight (MW). Thereby, the transport rates of the hydrophilic molecule sodium fluorescein (Na-Flu; MW 400°Da) were assessed either in the absence or presence of the TJ modulator EDTA (M. A. Deli, 2009a) for mAEpC, mAELVi.E, mAELVi.wt and MLE12 monolayers (see figure 23A). Furthermore, the bidirectional transport of FITC-dextran (FD3000; MW 3000 Da) was determined for monolayers of mAEpC, mAELVi.E and mAELVi.wt (see figure 23B). TEER was measured before and after each experiment.

The Na-Flu- P_{app} coefficients of immortalized cells (mAELVi.E, mAELVi.wt) and MLE12 were comparable, but were almost 10-fold higher than those of mAEpC. In the presence of EDTA, a more than two-fold increase in the permeability of the tightly-joined primary cells was observed, whereas this effect was less apparent for the leakier immortalized and MLE12 cells (see figure 23A, left panel). As expected, the TEER, and thus, the barrier function of mAEpC, significantly declined in a dose-dependent manner in the presence of EDTA. This effect was less obvious for mAELVi and MLE12 cells (see figure 23A, right panel). These results give evidence that primary cells exhibited functional TJs, but that these were lacking in all the other tested cells. In contrast, mAEpC exhibited P_{app} values comparable to those recently described for immortalized hAELVi cells (Kuehn *et al.*, 2016; Kletting *et al.*, 2017). However, the findings of mAEpC clearly demonstrate that the chelator EDTA can be applied to

Results & Discussion

enhance drug absorption as the depletion of Ca^{2+} ions and Mg^{2+} ions causes the reversible opening of TJ (X. Wang *et al.*, 2016).

The transport rate of FD3000 was assessed in apical-to-basolateral ($a \rightarrow b$) and in basolateral-to-apical ($b \rightarrow a$) direction (see figure 23B, left panel). Mean P_{app} values ranged between 1×10^{-6} and 2.5×10^{-6} cm/second, and were of a similar scale for all cell types tested. The lack of any preferred directionality points to passive transport, without the involvement of any active transporter or efflux system. As mentioned above, the TEER was independent of the transport direction remaining well above $1000 \Omega\text{cm}^2$ for mAEpC, while mAELVi.E and mAELVi.wt showed comparable but lower TEER values remaining at $\sim 250 \Omega\text{cm}^2$ (see figure 23B, right panel). However, in contrast to the Na-Flu permeability, the FD3000- P_{app} coefficients of primary and immortalized cells exhibited similar levels. This indicates that, in spite a higher permeability for the lower MW Na-Flu and relatively remote TEER ($\sim 250 \Omega\text{cm}^2$), monolayers of the latter two cell populations effectively represented an absorption barrier for the higher MW FD3000.

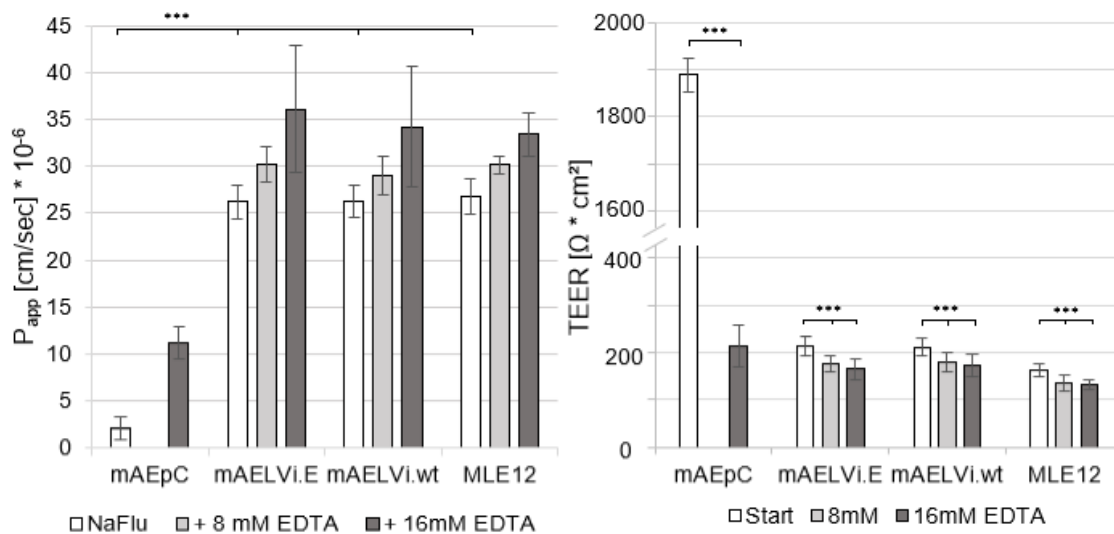
Taken together, these results provide evidence that mAELVi cells could successfully be applied to assess the transport rates of high-MW compounds and probably also the transport of nanoparticles. The primary mAEpC, with their tighter TJ, are more suitable for use in pulmonary absorptions studies of low-MW compounds. Since primary cultures of alveolar epithelial cells from pigs (Steimer *et al.*, 2007), rats (Cheek *et al.*, 1989; K. J. Kim *et al.*, 2001; Matsukawa *et al.*, 1997) and humans (Bur *et al.*, 2006; Elbert *et al.*, 1999) could successfully be applied for the assessment of transport fluxes, the results of the studies of mAEpC complete the spectrum of suitable *in vitro* models of the air-blood barrier.

To overcome the limitations of primary models and to diminish the number of animals used in this context in line with the 3R principle, various cell lines have been employed for the predication of cell permeability (Sarmento *et al.*, 2012). Thereby, high TEER of monolayers represent a major prerequisite to mimic the *in vivo* situation of the peripheral lung (Srinivasan *et al.*, 2015). Since the herein described mAELVi populations exhibited less pronounced barrier properties than their primary counterpart, the cell's applicability for the evaluation of permeabilities is limited.

Results & Discussion

Similarly, the human alveolar cell lines TT1 and A549, respectively, have been used in drug transport studies despite lacking diffusional barrier properties (van den Bogaard *et al.*, 2009; Z. Wang & Zhang, 2004). In contrast, the previously described ATI-like hAELVi cells providing high TEER represent a promising tool in these premises (Kuehn *et al.*, 2016). Furthermore, cell lines of bronchial epithelial origin such as NHBC (H. Lin *et al.*, 2007) and Calu-3 cells (Foster *et al.*, 2000; Z. Wang & Zhang, 2004) form tight monolayers and constitute suitable models to study drug adsorption in early drug development stages. Besides, novel advancements towards a more realistic *in vivo* simulation of the air-blood barrier such as co-cultures of distinct lung cells (Lehmann *et al.*, 2011; Pan *et al.*, 2015) and three-dimensional models (Horvath *et al.*, 2015) are currently being investigated.

A Transport of Na-fluorescein (mw = 400Da) ± EDTA



B Bidirectional transport of FD3000 (mw = 3000Da)

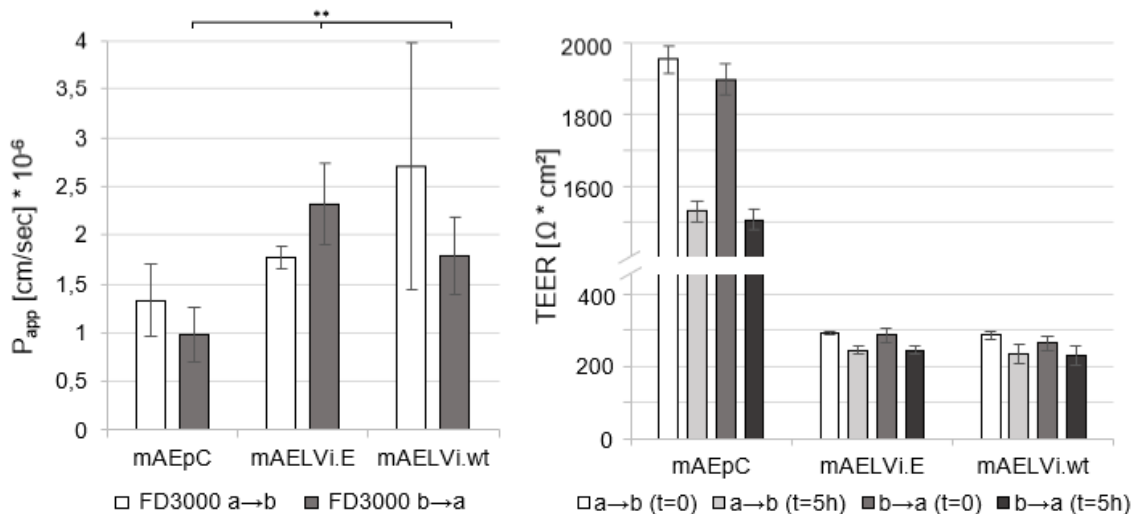


Figure 23: Assessment of transport properties by determination of permeability and barrier integrity (TEER) – A: Transport of Na-fluorescein (mw = 400Da) in the absence or presence of the TJ modulator EDTA; TEER values were assessed before and after the transport experiments; B: Bidirectional (a→b and b→a) transport of FITC-dextran (FD3000; mw = 3000Da) and the corresponding TEER values. Data was determined in triplicate and is shown as mean ± S.D. (n = 9 from 3 individual experiments); *p < 0.05, **p < 0.01, ***p < 0.001.

3.6 Cytotoxicity studies

Inhaled particles from gases, vapors or aerosols with the ability to overcome natural respiratory barriers including surfactant, alveolar macrophages and the tight epithelial cells, can induce a wide range of local or systemic adverse health effects which must be precluded in terms of risk and safety assessment of a certain compound (Hayes & Bakand, 2010). Up to today, these toxic effects are tested in animals prompting the need for alternative *in vitro* test systems consistent with the 3R principle. Based on available LC₅₀ data from animal testing (lethal concentration causing 50% mortality within 2 weeks after 4 hours inhalation exposure), chemically different substances of known single-dose inhalation toxicity were assigned to one of the five acute inhalation toxicity hazard categories in terms of the United Nation's Globally Harmonized System (GHS) of Classification and Labelling of Chemicals according to the United Nations (2011). In this context, the cytotoxic effects of 17 of such compounds on different cell culture systems, i.e. ATII-like A549 and non-specific NIH3T3 control cells, were previously investigated to evaluate their applicability as potential routine *in vitro* models to predict acute inhalation toxicity (U. G. Sauer *et al.*, 2013).

To determine if mAELVi.E, mAELVi.wt, MLE12 and the human hAELVi cells (Kuehn *et al.*, 2016) can be applied accordingly, the effects of a small set of compounds from different GHS categories, which are listed in table 12, were assessed for these cells by determining IC₅₀ values and subsequent comparison with the corresponding GHS category (see figure 23). To be compliant with the 3R principle, primary cells were excluded from these experiments. The results from individual experiments of hAELVi cells did not offer adequate consistency to allow an evaluation of cytotoxic effects (data not shown).

Although there was no direct correlation between the GHS categories 1 - 4 (with category 1 representing the highest toxicity) and IC₅₀ values, the actual IC₅₀ values obtained were very similar across all three tested cell lines. Importantly, for GHS category 5 compounds (which are the least toxic) the calculated IC₅₀ were higher than 10 mg/ml (log10 threshold) for all substances, except a single outlier in the case of ethanol, indicating relatively low hazard. These findings are in line with those reported by Sauer *et. al.* (2013), who suggested four GHS-corresponding *in vitro* hazard categories. Here, IC₅₀ ≤ 10 mg/ml were categorized into *in vitro* hazard category 4 which correlates to low hazard compounds of GHS category 5.

Results & Discussion

All three cell populations were thus able to distinguish between GHS category 5 and GHS category 4 or lower. Thus, these results demonstrated that immortalized murine cells could be useful for preliminary estimations of the potential inhalation toxicity of substances.

Table 12: Test substances of different GHS categories applied for cytotoxicity assessment and corresponding hazard and GHS labelling information according to a previous work (U. G. Sauer *et al.*, 2013).

GHS category	Test substance	Hazard information	GHS labelling
2	Formaldehyde (FA) 37%	Human carcinogen causing respiratory irritation and sensitization as well as adverse changes in the upper respiratory tract (Checkoway <i>et al.</i> , 2011; Lefebvre <i>et al.</i> , 2012)	“fatal if inhaled”
	Glutaraldehyde (GA) 25%	Respiratory irritant causing sensitization and occupational asthma (Gannon <i>et al.</i> , 1995)	
3	Sodium dodecylsulfate (SDS)	Respiratory irritant causing surfactant changes in cellular permeability and cell lysis (Singer & Tjeerdema, 1993)	“toxic if inhaled”
5	Ethanol	Respiratory irritant causing low hazard at any feasible exposure concentration according to http://echa.europa.eu/	“maybe harmful if inhaled”
	Acetone	Respiratory irritant with fast adsorption into the blood causing central nervous effects (A. Fujino <i>et al.</i> , 1992)	
(5)	Lactose	Control substance w/o known respiratory toxicity	N/A

In principle, the validity of such an *in vitro* test system is limited, due to the set-up itself (Landsiedel *et al.*, 2014) and to the fact that it can only address some of the reasons for toxicity (Scherliess, 2011), such as tissue damage or possible transport that eventually leads to systemic effects.

In this context, the mAELVi model might be further improved, in order to achieve a more realistic reflection of the *in vivo* situation, e.g. by implementing ALI conditions, as suggested previously (Hein *et al.*, 2011; Hittinger M, 2017). Other approaches to enhance existing *in vitro* models of the deep lung further include non-cellular barriers, such as mucus (Gandhi & Vliagostis; Murgia *et al.*, 2016) or surfactant (Raesch *et al.*,

2015). Furthermore, a range of promising *in vitro* exposure techniques have recently been developed which offer great potential to assess the biological activities of aerosolized substances (Murgia *et al.*, 2017).

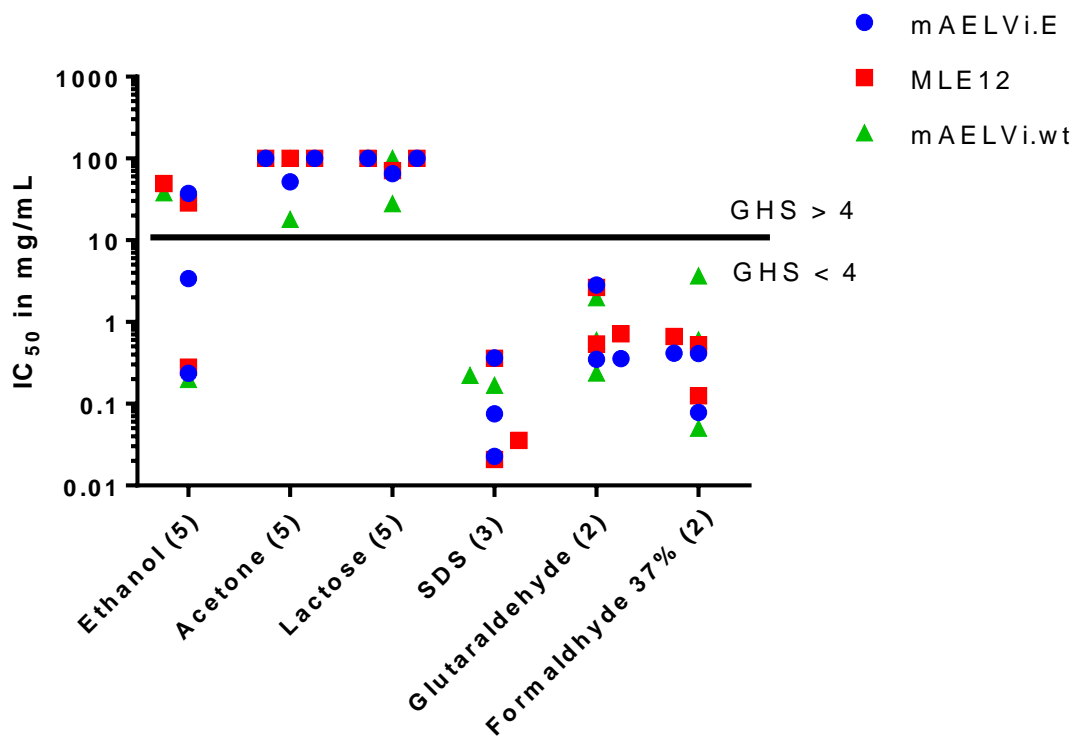


Figure 24: Cytotoxic effects of substances from different GHS categories – three independent experiments were performed to calculate specific IC_{50} values for ethanol, acetone, lactose, SDS, glutaraldehyde (GA) and formaldehyde (FA) for mAELVi.E, mAELVi.wt and MLE 12 cells. In each experiment ($n = 3$), decreasing serial dilutions (100, 10, 1, -0.1, -0.01, -0.001, -0.0001 and -0.00001 mg/ml) were analyzed using MTT assay. Each point in the graph represents the mean IC_{50} . Substances and their corresponding GHS category are listed on the x-axis. The horizontal line indicates the *in vitro* threshold for substances of GHS category ≤ 4, as described by U. G. Sauer *et al.* (2013).

4 Conclusion & Outlook

Reflecting the *in vivo* situation, primary mAEpC isolated from mouse lungs trans-differentiate *in vitro* into ATI-like cells featuring crucial properties of the air-blood barrier. Therefore, an efficient isolation method for mAEpC which grow as a monolayer and develop high TEER by expressing functional tight junction complexes was established. This primary *in vitro* model could demonstrate its applicability for the assessment of paracellular transport rates and offers great opportunities towards advanced investigations of the alveolar epithelium. As an example, primary mAEpC were previously applied to study immune responses upon *Pseudomonas aeruginosa* infection in correlation with corresponding *in vivo* experiments (Wolf & Sapich *et al.*, 2016). In this context, the option to correlate *in vitro* and *in vivo* data generated from murine models provides an asset over human cell culture systems. As an alternative to isolate primary AEpC from lung tissue, previous and recent advances to differentiate either murine Clara cells (Zheng *et al.*, 2017), murine embryonal (Ali *et al.*, 2002; Samadikuchaksaraei & Bishop, 2006) or human (Huang *et al.*, 2014; Jacob *et al.*, 2017) stem cells into alveolar epithelial cells, respectively, have been described. However, experimental designs using primary cells are substantially limited mainly due to their restricted availability, lifespan and ethical concerns failing to comply with the 3R principle.

Since animal testing remains indispensable for many routine research areas such as drug development and safety assessment, this study aimed at the generation of novel *in vitro* systems reflecting alveolar epithelial features in compliance with the 3R principle. Thus, primary mAEpC from heterozygous RosaConL mice were transduced with a lentiviral library consisting of 33 proliferation-promoting genes to establish a reliable immortalization protocol. By this approach, 8 genetically distinct mAELVi cell populations (mAELVi.A – H) with unlimited growth capacity could be achieved. Apart from this, transgenic mAELVi cells generated from RosaConL mice exhibit a Luciferase gene and could be useful for engraftment experiments, e.g. to investigate lung repair mechanisms or cell regeneration after bleomycin exposure as previously demonstrated using murine ATII cells (Hoffman & Ingenito, 2012; P. M. Wang & Martin, 2013).

Furthermore, a set of rather ATI-specific immortalizing genes could be defined and confirmed by the establishment of the wildtype cell population mAELVi.wt. In this respect, the immortalization protocol can further be applied to obtain mAELVi cells from mice with a defined genetic background, e.g. a specific knock-out strain to resolve a certain pathway or the pathogenesis of lung diseases, which can possibly be correlated to appropriate *in vivo* data of the same mouse model, as mentioned above.

The obtained mAELVi populations were subsequently characterized regarding alveolar epithelial features in comparison with primary mAEpC and partly MLE12 cells. Even though mAEpC could be immortalized in a way that the resultant mAELVi populations can easily be handled and grown in almost infinite quantities, monolayers of immortalized cells developed much less pronounced barrier properties than their primary counterpart. Remarkably, mAELVi cells expressed the prominent TJ proteins ZO-1 and occluding demonstrated by immunofluorescent staining revealing a distribution pattern restricted to the cell membranes, as expected. Thus, the assembly or functionality of the TJ complexes formed by mAELVi populations must have been impaired due to immortalization-related processes upon the random integration of genes, whereby the underlying mechanisms remain unsolved. Most likely, alterations in signaling pathways are accountable for aberrant growth control mechanism and thus, cellular characteristics are strongly influenced, as outlined before. On this account, the establishment of controllable expression systems to transduce immortalizing genes could reduce the likelihood of acquiring new mutations or genetic instability (May *et al.*, 2007; May *et al.*, 2005). However, it was not possible to achieve such an inducible expression system upon the herein described immortalization of mAEpC.

In this regard, pursuing analysis of the gene expression profile of mAELVi cells could provide further elucidation of the cell's impaired TJ functionality, e.g. by investigating other relevant proteins associated with tight and adherens junctions. Apart from this, the chromosomal integrity as well as the transformation status of mAELVi cells upon engraftment in mice should be addressed to evaluate the cell's capability to proliferate anchorage dependently (Chang *et al.*, 2000). At best, non-transformed immortalized cells would remain non-tumorigenic and show cell contact inhibited proliferation (Lipps *et al.*, 2013).

Since mAELVi cells lack the development of high TEER, permeability studies confirmed that the cells do not build a barrier for the low-MW tracer compound Na-Flu while primary cells clearly demonstrated integer barrier function. In this regard, the permeability of mAEPc was significantly enhanced upon treatment with the TJ modulator and Ca²⁺-chelator EDTA validating functional TJ complexes. Accordingly, TEER of mAEPc was significantly reduced when EDTA was present, whereas, this effect was less obvious for mAELVi and MLE12 cells.

In contrast to low-MW compounds, the assessment of transport rates of FD3000 disclosed that mAEPc and mAELVi exhibited comparable permeabilities for this high-MW compound. Thus, mAELVi cells might be applied as a model to predict pulmonary absorption of molecules bigger than 3 kDa contributing to the challenge to reduce the number of animals used during drug development following the 3R principle. However, it was previously shown that molecules bigger than 3.5 Da are certainly precluded from entering the paracellular route (Rubas *et al.*, 1996) which narrows the possible applications of mAELVi cells in these premises. In addition to the paracellular transport, further studies of mAELVi cells could address transporter-mediated drug adsorption, e.g. by analyses of active efflux systems such as the P-glycoprotein (Endter *et al.*, 2007) or the activities of metabolizing enzymes present (I. I. Forbes, 2000; Sakamoto *et al.*, 2015; Z. Wang & Zhang, 2004).

However, cytotoxicity assays of a small set of GHS-categorized compounds known as acute inhalation toxicity hazard demonstrated that immortalized mAELVi and MLE12 cells allow an initial estimation of potential toxic effects. This could be shown by the fact that the tested cell lines were able to distinguish between substances of GHS category 5 and those of GHS category 4 or lower and thus, might contribute to the 3R principle by reducing the numbers of mice used for the risk and safety assessment of chemicals and drug molecules. Further development of the mAELVi model towards an enhanced imitation of the organotypic situation of the distal lung, such as the use of dose-controlled air-interface deposition systems (Bitterle *et al.*, 2006; Mühlhopt *et al.*, 2016) or co-cultivation with surfactant-producing cells or alveolar macrophages (Hittinger *et al.*, 2016a; Lehmann *et al.*, 2011) could improve this *in vitro* cytotoxicity testing strategy.

As mAELVi cells could be cultivated at the ALI, the model could eventually be applied for nanoparticle uptake studies, as described for A549 cells (Blank *et al.*, 2006). The

development and use of nanoparticle-based drug delivery systems enables specific cell targeting and might contribute to novel therapies to treat respiratory tract disorders (Fytianos *et al.*, 2016). In this regard, gene therapy approaches are currently investigated for a variety of acute and chronic pulmonary diseases such as the autosomal recessive disorder CF (Griesenbach *et al.*, 2004). Since attempts to transfer genes to AEPC using viral and non-viral (e.g. nanoparticle carriers) vehicles have not been fully successful in recent years, mAELVi cells could be applied to evaluate different transduction and transfection methods. Similarly, a lentiviral SP-C-specific GFP reporter expression construct could effectively transduce MLE12 cells providing the chance to facilitate ATII-specific gene therapy (Wunderlich *et al.*, 2008). In this study, the commercially available cell line MLE12 was used as a reference to investigate potential benefits compared to primary and immortalized mAELVi cells. However, MLE12 cells were not able to develop a functional absorption barrier and their use did not convey any benefit over the use of other tested cells.

Moreover, mAELVi cells may be suitable to study specific virus-host interactions, e.g. virus-induced cellular damage of the alveolar epithelium. Here, primary cultures of the murine alveolar epithelium provided robust *in vitro* models which can be correlated with *in vivo* findings to identify viral and host factors contributing to the severity of a respiratory virus-induced disease (Kebaabetswe *et al.*, 2013). In this regard, it was recently pointed out that primary porcine respiratory epithelial cells retained high TEER upon Influenza infection. This fact indicates that research on pulmonary virus infections could be implemented independently from barrier properties providing a possible application for mAELVi cells (Wu *et al.*, 2016).

Since the airway epithelium responds to inhaled pathogens with an increased release of mediators of the innate immune system such as chemokines, cytokines and antimicrobial peptides, the mechanisms behind the recognition of pathogens by alveolar epithelial cells are crucial to coordinate protective immune responses. In this context, pattern-recognizing molecules mediating direct cell signaling such as Toll-like receptors (TLR) play an important role. Various TLR were shown to be expressed by airways epithelial cells mediating responses to bacterial, fungal and viral particles (Bals & Hiemstra, 2004). Analyses of the TLR expression and signaling in mAELVi cells could thus contribute to the development of novel therapies for infectious or inflammatory lung diseases (John *et al.*, 2010).

Conclusion & Outlook

As the mAELVi cell model has not yet been fully adapted to a specific application, many barrier-independent investigations and further advancements could potentially be considered. As an example, the human ATI-like cell line TT1 lacking a diffusional barrier were successfully used to study the alveolar inflammatory response to lipopolysaccharide (LPS) and might be useful for toxicity studies (van der Bogaard et al., 2009). In contrast to mAELVi cells, the TT1 cell line was established by transduction of primary ATII cells with hTERT and SV40 TAg. Both mAELVi and TT1 cells displayed an ATI-like character but not develop into monolayers with high TEER.

Taken together, the generation of mAELVi populations by transduction of primary mAEpC could contribute to the development of novel *in vitro* models of the alveolar epithelium offering great potential to be applied for a variety of barrier-independent investigations addressing basic, pharmaceutical-relevant and disease-related question pursuant to the 3R principle. However, advancement and adaptions of the immortalized model to a specific application must be further investigated and validated.

5 Appendix

5.1 List of abbreviations

3R	Reduce, refine, replace
α	Alpha
Ab	Antibody
ADMET	adsorption, distribution, metabolism, excretion, toxicity
Ag	Antigen
ALI	Air-liquid interface
AQP5	Aquaporin 5
ATI/II	Alveolar epithelial type I/II cells
bp	DNA base pairs
BSA	Bovine serum albumin
Cav-1	Caveolin-1 protein
cDNA	<i>complementary DNA</i>
CF	Cystic fibrosis
CFTR	Cystic fibrosis transmembrane conductance regulator
CLSM	Confocal Laser Scanning Microscopy
COL	Collagen
COPD	Chronic obstructive pulmonary disease
CMM	Complete mouse medium
DM	Dexamethasone
DMEM	Dulbecco's Modified Eagle Medium
DMSO	Dimethyl sulfoxide
DNA	Desoxyribonucleic acid
EBV	Epstein-Barr virus
EDTA	Ethylendiaminetetraacetic acid
EpCAM	Epithelial cell adhesion molecule
EtOH	Ethanol
EVOM	Epithelial voltohmometer
FA	Formaldehyde
FACS	Fluorescence-activated cell sorting
FBS	Fetal bovine serum
FITC	Fluorescein isothiocyanate

FD	FITC-labeled dextran
FDA	Food and Drug Administration
FN	Fibronectin
GA	Glutaraldehyde
GFP	Green fluorescent protein
GHS	Globally Harmonized System
hAELVi	Human alveolar epithelial lentivirus immortalized cells
hAEpC	Human alveolar epithelial cells
HBBS	Hank's balanced salt solution
HC	Hydrocortisone
H/E	Hematoxylin/Eosin
HEPES	4-(2-hydroxyethyl)-1-piperazineethanesulfonic acid
HPV	Human papilloma virus
hTert	Human telomerase reverse transcriptase
IC ₅₀	50% of the maximum inhibitory concentration
ICAM-1	Intracellular adhesion molecule-1
kb	Kilobase pairs
kDa	Kilo-Dalton
KRB	Krebs-Ringer buffer
LC ₅₀	Lethal concentration, 50%
LCC	Liquid-covered conditions
LM	Laminin
mAEpC	Murine alveolar epithelial cells
mAELVi	Murine alveolar epithelial lentivirus immortalized cells
MEF	Mouse embryonic fibroblasts
mGAPDH	Murine glyceraldehyde-3-phosphate dehydrogenase
MLE12	Murine Lung Epithelial cell line 12
MTT	3-(4,5-dimethylthiazol-2-yl)-2,5-diphenyltetrazolium bromide
mRNA	Messenger RNA
N/A	Not applicable
Na-Flu	Sodium fluorescein
NCBI	National Center for Biotechnology Information
NEAA	Non-essential amino acids
Occl	Occludin
PADDOCC	Pharmaceutical Aerosol Deposition Device on Cell Cultures

P _{app}	Apparent permeability coefficient
PBS	Phosphate buffered saline
PCR	Polymerase chain reaction
PFA	Paraformaldehyde
PKC	Protein kinase C
P/S	Penicillin/streptomycin
RNA	Ribonucleic acid
rpm	rounds per minute
RT	Room temperature
SAGM	Small airway growth medium
S.D.	Standard deviation
SDS	Sodium dodecyl sulfate
SP-A/B/C	Surfactant protein A, B or C
SV40	Simian virus 40
TAg	Large T antigen
TEER	Transepithelial electrical resistance
TEM	Transmission electron microscopy
TJ	Tight junction(s)
TLR	Toll-like receptor
VSV-G	Vesicular stomatitis virus glycoprotein
v/v	Volume per volume
w/o	without
w/v	Weight per volume
ZO-1	Zonula Occludens protein 1

5.2 List of figures

- Figure 1** **Structure of the airway epithelia** and main cell types occurring at the 3 principal levels of the respiratory system: the trachea/bronchi, bronchioles and alveoli; adapted and modified from Klein *et al.* (2011).
- Figure 2** **A - Organization of the human respiratory system** emphasizing the anatomy of the lung and the air-conducting structures terminating in alveolar sacs; **B - The alveoli and comprising cell types** of the area of the alveolar epithelium and capillary endothelium displaying the air-blood barrier as the site of gas exchange; illustrations were adapted and modified from Mescher (2016).
- Figure 3** **Scheme of the two main ways of transport across the air-blood barrier** – the paracellular and the transcellular route. Paracellular uptake occurs through the intercellular space of adjacent ATI cells and is regulated by junctional complexes (tight, adherens, gap junctions and desmosomes, shown schematically). In contrast, transcellular uptake through the cell membranes is mediated either by transporter proteins or transcytosis.
- Figure 4** **Scheme of immortalization strategy** using 33 different lentiviral vector, each constitutively expressing a potential immortalizing gene (CI-SCREEN gene library; Lipps *et al.*, 2018) to transduce primary mAEpC. Upon transduction, the random integration of certain genes triggered cell proliferation while other integrated gene combinations had no growth-inducing effect. Proliferating cells were expanded and characterized in terms of the integration pattern and alveolar epithelial features.
- Figure 5** **Illustrated overview of the mAEpC isolation procedure** according to a previous work (Wolf & Sapich *et al.*, 2016); Images were modified from (K. A. Sauer *et al.*, 2006).
- Figure 6** **Schematic overview of the lentivirus production procedure** by co-transfection of HEK293T cells, virus harvesting and the subsequent lentiviral transduction of primary mAEpC.
- Figure 7** **Flow cytometric determination of EpCAM-positive cells** assessed by FACS analysis before (a, left) and after (b, right) MACS magnetic beads cell separation during the isolation procedure of mAEpC.
- Figure 8** **Trans-differentiation of primary mAEpC** – immunofluorescent staining of mAEpC was performed at different time points post isolation; the expression of proSP-C protein (ATII marker) is shown in the upper panel; the expression of ZO-1protein (both ATI and TJ marker) is shown in the lower panel (both proteins shown in green); cells were fixed on 0.33 cm²-membranes with 3% PFA and nuclei were stained with DAPI solution (shown in blue); scale bars: 20 µm.
- Figure 9** **Ultrastructure of primary mAEpC** cultivated for 8 days on Transwell® membranes at a.) the air-liquid interface or b.) liquid-covered conditions. Green circles indicate desmosomal structures, blue circles indicate tight junction complexes; cells were grown on 0.4 µm thick Transwell® filters with a pore size of 0.4 µm and stained with H/E; scale bars: 500 nm.

- Figure 10** **Influence of different cultivation conditions on the TEER development of mAEpC monolayers** – A: mAEpC seeded on FN/LM-coated Transwells® at different cell densities; B: mAEpC seeded in a density of 1.5×10^6 cells/cm² on different coating combinations (FN/COL ≡ Fibronectin/Collagen or FN/LM ≡ Fibronectin/Laminin) and cultivated in either CMM or SAGM; values are shown as mean ± S.D. (n = 9 from 3 independent experiments).
- Figure 11** **Comparison of the TEER development of primary mAEpC grown under liquid-covered conditions (LCC) or at the air-liquid interface (ALI)**; values are shown as mean ± S.D. (n=18 from 6 independent mAEpC isolation procedures).
- Figure 12** **Barrier properties and trans-differentiation of hAEpC** – A: TEER development of primary hAEpC cultivated in either CMM or SAGM; values are shown as mean ± S.D. with (n=6 from 2 independent hAEpC isolation procedures: HIPS#629 and HIPS#631). B: Immunofluorescence of proSP-C (green) at day 1 post isolation; C: Immunofluorescence of ZO-1 (green) at day 7 post isolation; hAEpC were fixed with 3% PFA on 0.33 cm²-Transwell® membranes and nuclei were stained with DAPI solution (blue); scale bars: 20μm.
- Figure 13** **Growth curve of mAELVi.J cells** at passage 21 assessed over 10 days either at induced conditions (Dox) or uninduced conditions (w/o Dox); numbers of cells are shown as mean ± S.D. (n=3).
- Figure 14** **Formation of proliferating mAELVi.E cells at passage 6** after lentiviral transduction; cells with distinct morphology were separated from surrounding cells by a shifted two-step trypsinization and the cell population was maintained as mAELVi.E, scale bars: 100μm.
- Figure 15** **Light microscopic images** of primary mAEpC and different immortalized mAELVi cell populations, as indicated; cells were cultured on fibronectin/laminin-5-coated plastic; scale bars: 100μm.
- Figure 16** **Histological cross sections of mAELVi.E and mAELVi.wt** grown on fibronectin/laminin-5-coated 10 μm-thick Transwells® with 0.4 μm pore size; membrane sections were stained with H/E; images were captured with an inverted light microscope.
- Figure 17** **Percentage of EpCAM-positive cells of mAELVi** cell populations assessed with a monoclonal anti-EpCAM PE antibody by FACS analyses. Results from early (passages 1 – 4) and late (passages 17 – 21) passages are compared.
- Figure 18** **Expression of EpCAM in mAELVi.E cells** at passage 33 (left: DAPI-stained nuclei, middle: EpCAM distribution, right: merge); cells were fixed on fibronectin/laminin-5-coated chamberslides with 3% PFA; scale bars: 50 μm.
- Figure 19** **PCR analyses of the expression of ATI and ATII markers in mAEpC, mAELVi.E and MLE12 cells**; M: Hyperladder V (Bioline) with molecular weights indicated in base pairs (bp), analyzed ATII markers: SP-A (101bp), SP-B (121bp) and SP-C (88bp); ATII markers: T1α (101bp), AQP5 (86bp), Cav-1 (198bp) and ICAM-1 (103bp); mGAPDH and template-free samples, respectively, were run as controls (data not shown).

Figure 20 **TEER development of mAELVi.E (left) and mAELVi.wt (right)** seeded on 1.12 cm² Transwell® filter supports (pore size 0.4 µm) in CMM10 – A: Influence of medium composition (HC ≡ hydrocortisone, DM ≡ dexamethasone); B: Influence of different surface coatings (FN ≡ fibronectin; COL ≡ collagen; LM ≡ laminin-5); values are shown as mean ± S.D. (n = 9 from 3 independent experiments).

Figure 21 **Expression of TJ proteins** (left panel: ZO-1 in green; right panel: occludin in red); A: primary mAEPc at day 7 after isolation on 0.33 cm²-membranes; B mAELVi.E cells; C: mAELVi.wt cells; immortalized cells were stained at day 14 post seeding on 1.12 cm² membranes; cells were fixed with 3% PFA and nuclei were stained with DAPI solution; scale bars: 20 µm.

Figure 22 **Characterization of mAELVi.J cells regarding barrier properties** - A: TEER development; values are shown as mean ± S.D (n=9 from 3 independent experiments). B: LM picture; scale bar: 100 µm.

Figure 23 **Assessment of transport properties by determination of permeability and barrier integrity (TEER)** – A: Transport of Na-fluorescein (mw = 400Da) in the absence or presence of the TJ modulator EDTA; TEER values were assessed before and after the transport experiments; B: Bidirectional (a→b and b→a) transport of FITC-dextran (FD3000; mw = 3000Da) and the corresponding TEER values. Data was determined in triplicate and is shown as mean ± S.D. (n = 9 from 3 individual experiments); *p < 0.05, **p < 0.01, ***p < 0.001.

Figure 24 **Cytotoxic effects of substances from different GHS categories** – three independent experiments were performed to calculate specific IC₅₀ values for ethanol, acetone, lactose, SDS, glutaraldehyde (GA) and formaldehyde (FA) for mAELVi.E, mAELVi.wt and MLE 12 cells. In each experiment (n = 3), decreasing serial dilutions (100, 10, 1, -0.1, -0.01, -0.001, -0.0001 and -0.00001 mg/ml) were analyzed using MTT assay. Each point in the graph represents the mean IC₅₀. Substances and their corresponding GHS category are listed on the x-axis. The horizontal line indicates the *in vitro* threshold for substances of GHS category ≤ 4, as described by U. G. Sauer *et al.* (2013).

5.3 List of tables

- Table 1** Composition of buffer solutions and respective applications.
- Table 2** Origin and description of cell lines and primary cells in alphabetical order.
- Table 3** Composition of cell cultivation media for cells of murine and human origin.
- Table 4** PCR program to analyze the gene integration pattern of mAELVi cells.
- Table 5** Reverse primer sequences of the CI-SCREEN library (Lipps *et al.*, 2018) to analyze the pattern of integrated immortalizing genes in mAELVi cells performing 33 independent PCR reactions. The forward primer binds within the SV40 promotor region of the immortalizing gene expression cassette and was used for all PCR reactions (SV40-Forward primer sequence: 5' GGAGGCCTAGGCTTTGCAA 3').
- Table 6** Volumes of cultivation medium for apical and basolateral compartments of 0.33 cm and 1.12 cm² Transwell® inserts to set either LCC or ALI conditions.
- Table 7** Primer sequences to analyze lung cell-specific marker expression by PCR.
- Table 8** PCR program to analyze the expression of lung-specific marker genes.
- Table 9** Overview of start volumes (of the Transwells®) and sample/KRB volumes (to transfer to the 96-well plate) in dependence on the growing size of the Transwell® insert and the transport direction.
- Table 10** Pattern of integrated genes from CI-SCREEN gene library upon lentiviral transduction of mAEpC which resulted in expandable mAELVi cells (mAELVi.A-H); *mAELVi.wt were transduced with a set of 9 out of 33 immortalizing genes; the results are based on PCR-analysis of mAELVi DNA extractions; green boxes indicate positive PCR products for the respective gene; mGAPDH was used as internal control of the PCR.
- Table 11** Characterization overview of mAELVi cells, primary mAEpC and MLE12; cells were characterized regarding the pattern of integrated lentiviral genes, ATI and ATII-like marker expression (PCR data), percentage of EpCAM-positive cells (FACS analyses; performed at cell passages 17 - 21) and TEER (mean and maximum in Ωcm²).
- Table 12** Test substances of different GHS categories applied for cytotoxicity assessment and corresponding hazard and GHS labelling information according to a previous work (U. G. Sauer, 2013).

References

- Aarbiou**, J., Ertmann, M., van Wetering, S., van Noort, P., Rook, D., Rabe, K. F., et al. (2002). Human neutrophil defensins induce lung epithelial cell proliferation in vitro. *J Leukoc Biol*, 72(1), 167-174.
- Agrahari**, V., Agrahari, V., & Mitra, A. K. (2016). Nanocarrier fabrication and macromolecule drug delivery: challenges and opportunities. *Ther Deliv*, 7(4), 257-278. doi:10.4155/tde-2015-0012
- Ali**, N. N., Edgar, A. J., Samadikuchaksaraei, A., Timson, C. M., Romanska, H. M., Polak, J. M., et al. (2002). Derivation of type II alveolar epithelial cells from murine embryonic stem cells. *Tissue Eng*, 8(4), 541-550. doi:10.1089/107632702760240463
- Anastassiadis**, K., Rostovskaya, M., Lubitz, S., Weidlich, S., & Stewart, A. F. (2010). Precise conditional immortalization of mouse cells using tetracycline-regulated SV40 large T-antigen. *Genesis*, 48(4), 220-232. doi:10.1002/dvg.20605
- Angel**, P., & Karin, M. (1991). The role of Jun, Fos and the AP-1 complex in cell-proliferation and transformation. *Biochim Biophys Acta*, 1072(2-3), 129-157.
- Attar**, M. A., Bailie, M. B., Christensen, P. J., Brock, T. G., Wilcoxon, S. E., & Paine, R., 3rd. (1999). Induction of ICAM-1 expression on alveolar epithelial cells during lung development in rats and humans. *Exp Lung Res*, 25(3), 245-259.
- Bae**, V. L., Jackson-Cook, C. K., Maygarden, S. J., Plymate, S. R., Chen, J., & Ware, J. L. (1998). Metastatic sublines of an SV40 large T antigen immortalized human prostate epithelial cell line. *Prostate*, 34(4), 275-282.
- Balda**, M. S., & Matter, K. (2000). Transmembrane proteins of tight junctions. *Semin Cell Dev Biol*, 11(4), 281-289. doi:10.1006/scdb.2000.0177
- Balls**, M., Goldberg, A. M., Fentem, J. H., Broadhead, C. L., Burch, R. L., Festing, M. F., et al. (1995). The three Rs: the way forward: the report and recommendations of ECVAM Workshop 11. *Altern Lab Anim*, 23(6), 838-866.
- Bantikassegn**, A., Song, X., & Politi, K. (2015). Isolation of Epithelial, Endothelial, and Immune Cells from Lungs of Transgenic Mice with Oncogene-Induced Lung Adenocarcinomas. *American Journal of Respiratory Cell and Molecular Biology*, 52(4), 409-417. doi:10.1165/rcmb.2014-0312MA
- Barkauskas**, C. E., Cronce, M. J., Rackley, C. R., Bowie, E. J., Keene, D. R., Stripp, B. R., et al. (2013). Type 2 alveolar cells are stem cells in adult lung. *J Clin Invest*, 123(7), 3025-3036. doi:10.1172/JCI68782
- Barton**, A. D., & Lourenco, R. V. (1973). Bronchial secretions and mucociliary clearance. Biochemical characteristics. *Arch Intern Med*, 131(1), 140-144.
- Bhaskaran**, M., Kolliputi, N., Wang, Y., Gou, D., Chintagari, N. R., & Liu, L. (2007). Trans-differentiation of alveolar epithelial type II cells to type I cells involves autocrine signaling by transforming growth factor beta 1 through the Smad pathway. *J Biol Chem*, 282(6), 3968-3976. doi:10.1074/jbc.M609060200

References

- Bitterle**, E., Karg, E., Schroepel, A., Kreyling, W. G., Tippe, A., Ferron, G. A., *et al.* (2006). Dose-controlled exposure of A549 epithelial cells at the air-liquid interface to airborne ultrafine carbonaceous particles. *Chemosphere*, 65(10), 1784-1790. doi:10.1016/j.chemosphere.2006.04.035
- Blank**, F., Rothen-Rutishauser, B. M., Schurch, S., & Gehr, P. (2006). An optimized in vitro model of the respiratory tract wall to study particle cell interactions. *J Aerosol Med*, 19(3), 392-405. doi:10.1089/jam.2006.19.392
- Bocker**, W., Yin, Z., Drosse, I., Haasters, F., Rossmann, O., Wierer, M., *et al.* (2008). Introducing a single-cell-derived human mesenchymal stem cell line expressing hTERT after lentiviral gene transfer. *J Cell Mol Med*, 12(4), 1347-1359. doi:10.1111/j.1582-4934.2008.00299.x
- Bur**, M., Huwer, H., Lehr, C. M., Hagen, N., Guldbrandt, M., Kim, K. J., *et al.* (2006). Assessment of transport rates of proteins and peptides across primary human alveolar epithelial cell monolayers. *Eur J Pharm Sci*, 28(3), 196-203. doi:10.1016/j.ejps.2006.02.002
- Bur**, M., & Lehr, C. M. (2008). Pulmonary cell culture models to study the safety and efficacy of innovative aerosol medicines. *Expert Opin Drug Deliv*, 5(6), 641-652. doi:10.1517/17425247.5.6.641
- Camelo**, A., Dunmore, R., Sleeman, M. A., & Clarke, D. L. (2014). The epithelium in idiopathic pulmonary fibrosis: breaking the barrier. *Front Pharmacol*, 4, 173. doi:10.3389/fphar.2013.00173
- Campbell**, L., Hollins, A. J., Al-Eid, A., Newman, G. R., von Ruhland, C., & Gumbleton, M. (1999). Caveolin-1 expression and caveolae biogenesis during cell transdifferentiation in lung alveolar epithelial primary cultures. *Biochem Biophys Res Commun*, 262(3), 744-751. doi:10.1006/bbrc.1999.1280
- Cao**, Y. X., Jean, J. C., & Williams, M. C. (2000). Cytosine methylation of an Sp1 site contributes to organ-specific and cell-specific regulation of expression of the lung epithelial gene t1alpha. *Biochem J*, 350 Pt 3, 883-890.
- Castellani**, S., Guerra, L., Favia, M., Di Gioia, S., Casavola, V., & Conese, M. (2012). NHERF1 and CFTR restore tight junction organisation and function in cystic fibrosis airway epithelial cells: role of ezrin and the RhoA/ROCK pathway. *Lab Invest*, 92(11), 1527-1540. doi:10.1038/labinvest.2012.123
- Castleman**, W. L., Northrop, P. J., & McAllister, P. K. (1991). Replication of parainfluenza type-3 virus and bovine respiratory syncytial virus in isolated bovine type-II alveolar epithelial cells. *Am J Vet Res*, 52(6), 880-885.
- Castro-Gamero**, A. M., Borges, K. S., Lira, R. C., Andrade, A. F., Fedatto, P. F., Cruzeiro, G. A., *et al.* (2013). Chromosomal heterogeneity and instability characterize pediatric medulloblastoma cell lines and affect neoplastic phenotype. *Cytotechnology*, 65(5), 871-885. doi:10.1007/s10616-012-9529-z
- Chang**, B. D., Watanabe, K., Broude, E. V., Fang, J., Poole, J. C., Kalinichenko, T. V., *et al.* (2000). Effects of p21Waf1/Cip1/Sdi1 on cellular gene expression: implications for carcinogenesis, senescence, and age-related diseases. *Proc Natl Acad Sci U S A*, 97(8), 4291-4296.

References

- Checkoway**, H., Ray, R. M., Lundin, J. I., Astrakianakis, G., Seixas, N. S., Camp, J. E., et al. (2011). Lung cancer and occupational exposures other than cotton dust and endotoxin among women textile workers in Shanghai, China. *Occup Environ Med*, 68(6), 425-429. doi:10.1136/oem.2010.059519
- Cheek**, J. M., Kim, K. J., & Crandall, E. D. (1989). Tight monolayers of rat alveolar epithelial cells: bioelectric properties and active sodium transport. *Am J Physiol*, 256(3 Pt 1), C688-693.
- Chen**, F. F., Liu, Y., Wang, F., Pang, X. J., Zhu, C. D., Xu, M., et al. (2015). Effects of upregulation of Id3 in human lung adenocarcinoma cells on proliferation, apoptosis, mobility and tumorigenicity. *Cancer Gene Ther*, 22(9), 431-437. doi:10.1038/cgt.2015.38
- Chen**, J., Chen, Z., Narasaraju, T., Jin, N., & Liu, L. (2004). Isolation of highly pure alveolar epithelial type I and type II cells from rat lungs. *Lab Invest*, 84(6), 727-735. doi:10.1038/labinvest.3700095
- Cohen**, T. S., Gray Lawrence, G., & Margulies, S. S. (2010). Cultured alveolar epithelial cells from septic rats mimic in vivo septic lung. *PLoS One*, 5(6), e11322. doi:10.1371/journal.pone.0011322
- Corti**, M., Brody, A. R., & Harrison, J. H. (1996). Isolation and primary culture of murine alveolar type II cells. *Am J Respir Cell Mol Biol*, 14(4), 309-315. doi:10.1165/ajrcmb.14.4.8600933
- Coyne**, C. B., Vanhook, M. K., Gambling, T. M., Carson, J. L., Boucher, R. C., & Johnson, L. G. (2002). Regulation of airway tight junctions by proinflammatory cytokines. *Mol Biol Cell*, 13(9), 3218-3234. doi:10.1091/mbc.E02-03-0134
- Crandall**, E. D., & Matthay, M. A. (2001). Alveolar epithelial transport. Basic science to clinical medicine. *Am J Respir Crit Care Med*, 163(4), 1021-1029. doi:10.1164/ajrccm.163.4.2006116
- Crapo**, J. D., Barry, B. E., Gehr, P., Bachofen, M., & Weibel, E. R. (1982). Cell number and cell characteristics of the normal human lung. *Am Rev Respir Dis*, 125(6), 740-745. doi:10.1164/arrd.1982.125.6.740
- Damia**, G., & D'Incalci, M. (2010). Genetic instability influences drug response in cancer cells. *Curr Drug Targets*, 11(10), 1317-1324.
- Daum**, N., Kuehn, A., Hein, S., Schaefer, U. F., Huwer, H., & Lehr, C. M. (2012). Isolation, cultivation, and application of human alveolar epithelial cells. *Methods Mol Biol*, 806, 31-42. doi:10.1007/978-1-61779-367-7_3
- de Souza Carvalho**, C., Daum, N., & Lehr, C. M. (2014). Carrier interactions with the biological barriers of the lung: advanced in vitro models and challenges for pulmonary drug delivery. *Adv Drug Deliv Rev*, 75, 129-140. doi:10.1016/j.addr.2014.05.014
- Deeb**, K. K., Michalowska, A. M., Yoon, C. Y., Krummey, S. M., Hoenerhoff, M. J., Kavanaugh, C., et al. (2007). Identification of an integrated SV40 T/t-antigen cancer signature in aggressive human breast, prostate, and lung carcinomas with poor prognosis. *Cancer Res*, 67(17), 8065-8080. doi:10.1158/0008-5472.CAN-07-1515
- Deli**, M. A. (2009a). Potential use of tight junction modulators to reversibly open membranous barriers and improve drug delivery. *Biochim Biophys Acta*, 1788(4), 892-910. doi:10.1016/j.bbamem.2008.09.016

References

- Deli**, M. A. (2009b). Potential use of tight junction modulators to reversibly open membranous barriers and improve drug delivery. *Biochimica et Biophysica Acta (BBA) - Biomembranes*, 1788(4), 892-910. doi:<https://doi.org/10.1016/j.bbamem.2008.09.016>
- Demaior**, L., Tseng, W., Balverde, Z., Alvarez, J. R., Kim, K. J., Kelley, D. G., et al. (2009). Characterization of mouse alveolar epithelial cell monolayers. *Am J Physiol Lung Cell Mol Physiol*, 296(6), L1051-1058. doi:10.1152/ajplung.00021.2009
- Dobbs**, L. G., Johnson, M. D., Vanderbilt, J., Allen, L., & Gonzalez, R. (2010). The great big alveolar TI cell: evolving concepts and paradigms. *Cell Physiol Biochem*, 25(1), 55-62. doi:10.1159/000272063
- Drab**, M., Verkade, P., Elger, M., Kasper, M., Lohn, M., Lauterbach, B., et al. (2001). Loss of caveolae, vascular dysfunction, and pulmonary defects in caveolin-1 gene-disrupted mice. *Science*, 293(5539), 2449-2452. doi:10.1126/science.1062688
- Elbert**, K. J., Schafer, U. F., Schafers, H. J., Kim, K. J., Lee, V. H., & Lehr, C. M. (1999). Monolayers of human alveolar epithelial cells in primary culture for pulmonary absorption and transport studies. *Pharm Res*, 16(5), 601-608.
- Endter**, S., Becker, U., Daum, N., Huwer, H., Lehr, C. M., Gumbleton, M., et al. (2007). P-glycoprotein (MDR1) functional activity in human alveolar epithelial cell monolayers. *Cell Tissue Res*, 328(1), 77-84. doi:10.1007/s00441-006-0346-6
- Fang**, X., Neyrinck, A. P., Matthay, M. A., & Lee, J. W. (2010). Allogeneic human mesenchymal stem cells restore epithelial protein permeability in cultured human alveolar type II cells by secretion of angiopoietin-1. *J Biol Chem*, 285(34), 26211-26222. doi:10.1074/jbc.M110.119917
- Flemming**, R. G., Murphy, C. J., Abrams, G. A., Goodman, S. L., & Nealey, P. F. (1999). Effects of synthetic micro- and nano-structured surfaces on cell behavior. *Biomaterials*, 20(6), 573-588.
- Foldbjerg**, R., Dang, D. A., & Autrup, H. (2011). Cytotoxicity and genotoxicity of silver nanoparticles in the human lung cancer cell line, A549. *Arch Toxicol*, 85(7), 743-750. doi:10.1007/s00204-010-0545-5
- Forbes**, B., & Ehrhardt, C. (2005). Human respiratory epithelial cell culture for drug delivery applications. *Eur J Pharm Biopharm*, 60(2), 193-205. doi:10.1016/j.ejpb.2005.02.010
- Forbes**, I. I. (2000). Human airway epithelial cell lines for in vitro drug transport and metabolism studies. *Pharm Sci Technolo Today*, 3(1), 18-27.
- Förster**, C. (2008). Tight junctions and the modulation of barrier function in disease. *Histochemistry and Cell Biology*, 130(1), 55-70. doi:10.1007/s00418-008-0424-9
- Foster**, K. A., Avery, M. L., Yazdanian, M., & Audus, K. L. (2000). Characterization of the Calu-3 cell line as a tool to screen pulmonary drug delivery. *Int J Pharm*, 208(1-2), 1-11.
- Foster**, K. A., Oster, C. G., Mayer, M. M., Avery, M. L., & Audus, K. L. (1998). Characterization of the A549 cell line as a type II pulmonary epithelial cell model for drug metabolism. *Exp Cell Res*, 243(2), 359-366. doi:10.1006/excr.1998.4172
- Fuchs**, S., Hollins, A. J., Laue, M., Schaefer, U. F., Roemer, K., Gumbleton, M., et al. (2003). Differentiation of human alveolar epithelial cells in primary culture: morphological characterization and synthesis of caveolin-1 and surfactant protein-C. *Cell Tissue Res*, 311(1), 31-45. doi:10.1007/s00441-002-0653-5

References

- Fujino**, A., Satoh, T., Takebayashi, T., Nakashima, H., Sakurai, H., Higashi, T., *et al.* (1992). Biological monitoring of workers exposed to acetone in acetate fibre plants. *Br J Ind Med*, 49(9), 654-657.
- Fujino**, N., Kubo, H., Ota, C., Suzuki, T., Suzuki, S., Yamada, M., *et al.* (2012). A novel method for isolating individual cellular components from the adult human distal lung. *Am J Respir Cell Mol Biol*, 46(4), 422-430. doi:10.1165/rcmb.2011-0172OC
- Fytianos**, K., Drasler, B., Blank, F., von Garnier, C., Seydoux, E., Rodriguez-Lorenzo, L., *et al.* (2016). Current in vitro approaches to assess nanoparticle interactions with lung cells. *Nanomedicine (Lond)*, 11(18), 2457-2469. doi:10.2217/nmm-2016-0199
- Gandhi**, V. D., & Vliagoftis, H. (2015). Airway epithelium interactions with aeroallergens: role of secreted cytokines and chemokines in innate immunity. *Front Immunol*, 6, 147. doi:10.3389/fimmu.2015.00147
- Ganesan**, S., Comstock, A. T., & Sajjan, U. S. (2013). Barrier function of airway tract epithelium. *Tissue Barriers*, 1(4), e24997. doi:10.4161/tibb.24997
- Gannon**, P. F., Bright, P., Campbell, M., O'Hickey, S. P., & Burge, P. S. (1995). Occupational asthma due to glutaraldehyde and formaldehyde in endoscopy and x ray departments. *Thorax*, 50(2), 156-159.
- Garrod**, D., & Chidgey, M. (2008). Desmosome structure, composition and function. *Biochimica et Biophysica Acta (BBA) - Biomembranes*, 1778(3), 572-587. doi:<http://dx.doi.org/10.1016/j.bbamem.2007.07.014>
- Gazdar**, A. F., Butel, J. S., & Carbone, M. (2002). SV40 and human tumours: myth, association or causality? *Nat Rev Cancer*, 2(12), 957-964. doi:10.1038/nrc947
- Gereke**, M., Autengruber, A., Grobe, L., Jeron, A., Bruder, D., & Stegemann-Koniszewski, S. (2012). Flow cytometric isolation of primary murine type II alveolar epithelial cells for functional and molecular studies. *J Vis Exp*(70). doi:10.3791/4322
- Gerlach**, J. C., & Zeilinger, K. (2002). Adult stem cell technology--prospects for cell based therapy in regenerative medicine. *Int J Artif Organs*, 25(2), 83-90.
- Gonzalez-Mariscal**, L., Betanzos, A., Nava, P., & Jaramillo, B. E. (2003). Tight junction proteins. *Prog Biophys Mol Biol*, 81(1), 1-44.
- Gonzalez**, R., Yang, Y. H., Griffin, C., Allen, L., Tigue, Z., & Dobbs, L. (2005). Freshly isolated rat alveolar type I cells, type II cells, and cultured type II cells have distinct molecular phenotypes. *Am J Physiol Lung Cell Mol Physiol*, 288(1), L179-189. doi:10.1152/ajplung.00272.2004
- Gossen**, M., & Bujard, H. (1992). Tight control of gene expression in mammalian cells by tetracycline-responsive promoters. *Proc Natl Acad Sci U S A*, 89(12), 5547-5551.
- Graham**, F. L., Smiley, J., Russell, W. C., & Nairn, R. (1977). Characteristics of a human cell line transformed by DNA from human adenovirus type 5. *J Gen Virol*, 36(1), 59-74. doi:10.1099/0022-1317-36-1-59
- Griesenbach**, U., Geddes, D. M., & Alton, E. W. (2004). Gene therapy for cystic fibrosis: an example for lung gene therapy. *Gene Ther*, 11 Suppl 1, S43-50. doi:10.1038/sj.gt.3302368

References

- Groneberg**, D. A., Eynott, P. R., Doring, F., Dinh, Q. T., Oates, T., Barnes, P. J., et al. (2002). Distribution and function of the peptide transporter PEPT2 in normal and cystic fibrosis human lung. *Thorax*, 57(1), 55-60.
- Gunzel**, D., & Yu, A. S. (2013). Claudins and the modulation of tight junction permeability. *Physiol Rev*, 93(2), 525-569. doi:10.1152/physrev.00019.2012
- Hansen**, T., Blickwede, M., & Borlak, J. (2006). Primary rat alveolar epithelial cells for use in biotransformation and toxicity studies. *Toxicol In Vitro*, 20(5), 757-766. doi:10.1016/j.tiv.2005.10.011
- Hansen**, T., Chougule, A., & Borlak, J. (2014). Isolation and cultivation of metabolically competent alveolar epithelial cells from A/J mice. *Toxicol In Vitro*, 28(5), 812-821. doi:10.1016/j.tiv.2014.03.009
- Harris**, T. J. (2012). An introduction to adherens junctions: from molecular mechanisms to tissue development and disease. *Subcell Biochem*, 60, 1-5. doi:10.1007/978-94-007-4186-7_1
- Hartsock**, A., & Nelson, W. J. (2008). Adherens and Tight Junctions: Structure, Function and Connections to the Actin Cytoskeleton. *Biochimica et biophysica acta*, 1778(3), 660-669. doi:10.1016/j.bbamem.2007.07.012
- Hasegawa**, K., Sato, A., Tanimura, K., Uemasu, K., Hamakawa, Y., Fuseya, Y., et al. (2017). Fraction of MHCII and EpCAM expression characterizes distal lung epithelial cells for alveolar type 2 cell isolation. *Respir Res*, 18(1), 150. doi:10.1186/s12931-017-0635-5
- Hayes**, A., & Bakand, S. (2010). Inhalation toxicology. *EXS*, 100, 461-488.
- Hein**, S., Bur, M., Schaefer, U. F., & Lehr, C. M. (2011). A new Pharmaceutical Aerosol Deposition Device on Cell Cultures (PADDCC) to evaluate pulmonary drug absorption for metered dose dry powder formulations. *Eur J Pharm Biopharm*, 77(1), 132-138. doi:10.1016/j.ejpb.2010.10.003
- Herold**, S., Gabrielli, N. M., & Vadasz, I. (2013). Novel concepts of acute lung injury and alveolar-capillary barrier dysfunction. *Am J Physiol Lung Cell Mol Physiol*, 305(10), L665-681. doi:10.1152/ajplung.00232.2013
- Hittinger** M, B. S., Siebenbürger L, Zäh K, Gress A, Guenther S, Wiegand B, Boerger C, Berger M, Krebs T, Groß H, Lehr C. (2017). Proof of Concept of the VITROCELL Dry Powder Chamber: A New In Vitro Test System for the Controlled Deposition of Aerosol Formulations. *RDD Europe 2017*, 2, 283-288.
- Hittinger**, M., Janke, J., Huwer, H., Scherliess, R., Schneider-Daum, N., & Lehr, C. M. (2016a). Autologous co-culture of primary human alveolar macrophages and epithelial cells for investigating aerosol medicines. Part I: model characterisation. *Altern Lab Anim*, 44(4), 337-347.
- Hittinger**, M., Juntke, J., Kletting, S., Schneider-Daum, N., de Souza Carvalho, C., & Lehr, C. M. (2015). Preclinical safety and efficacy models for pulmonary drug delivery of antimicrobials with focus on in vitro models. *Adv Drug Deliv Rev*, 85, 44-56. doi:10.1016/j.addr.2014.10.011
- Hittinger**, M., Mell, N. A., Huwer, H., Loretz, B., Schneider-Daum, N., & Lehr, C. M. (2016b). Autologous co-culture of primary human alveolar macrophages and epithelial cells for investigating aerosol medicines. Part II: evaluation of IL-10-loaded microparticles for the treatment of lung inflammation. *Altern Lab Anim*, 44(4), 349-360.

References

- Hoffman**, A. M., & Ingenito, E. P. (2012). Alveolar epithelial stem and progenitor cells: emerging evidence for their role in lung regeneration. *Curr Med Chem*, 19(35), 6003-6008.
- Hollenhorst**, M. I., Richter, K., & Fronius, M. (2011). Ion transport by pulmonary epithelia. *J Biomed Biotechnol*, 2011, 174306. doi:10.1155/2011/174306
- Horvath**, L., Umehara, Y., Jud, C., Blank, F., Petri-Fink, A., & Rothen-Rutishauser, B. (2015). Engineering an in vitro air-blood barrier by 3D bioprinting. *Sci Rep*, 5, 7974. doi:10.1038/srep07974
- Huang**, S. X. L., Islam, M. N., O'Neill, J., Hu, Z., Yang, Y.-G., Chen, Y.-W., et al. (2014). Efficient generation of lung and airway epithelial cells from human pluripotent stem cells. *Nat Biotech*, 32(1), 84-91. doi:10.1038/nbt.2754
- Hubbard**, K., & Ozer, H. L. (1999). Mechanism of immortalization. *Age (Omaha)*, 22(2), 65-69. doi:10.1007/s11357-999-0008-1
- Isakson**, B. E., Evans, W. H., & Boitano, S. (2001a). Intercellular Ca²⁺ signaling in alveolar epithelial cells through gap junctions and by extracellular ATP. *Am J Physiol Lung Cell Mol Physiol*, 280(2), L221-228.
- Isakson**, B. E., Lubman, R. L., Seedorf, G. J., & Boitano, S. (2001b). Modulation of pulmonary alveolar type II cell phenotype and communication by extracellular matrix and KGF. *Am J Physiol Cell Physiol*, 281(4), C1291-1299.
- Jacob**, A., Morley, M., Hawkins, F., McCauley, K. B., Jean, J. C., Heins, H., et al. (2017). Differentiation of Human Pluripotent Stem Cells into Functional Lung Alveolar Epithelial Cells. *Cell Stem Cell*, 21(4), 472-488.e410. doi:10.1016/j.stem.2017.08.014
- Jiang**, Z., Woda, B. A., Savas, L., & Fraire, A. E. (1998). Expression of ICAM-1, VCAM-1, and LFA-1 in adenocarcinoma of the lung with observations on the expression of these adhesion molecules in non-neoplastic lung tissue. *Mod Pathol*, 11(12), 1189-1192.
- John**, G., Yildirim, A. Ö., Rubin, B. K., Gruenert, D. C., & Henke, M. O. (2010). TLR-4–Mediated Innate Immunity Is Reduced in Cystic Fibrosis Airway Cells. *American Journal of Respiratory Cell and Molecular Biology*, 42(4), 424-431. doi:10.1165/rcmb.2008-0408OC
- Kamalian**, L., Forootan, S. S., Bao, Z. Z., Zhang, Y., Gosney, J. R., Foster, C. S., et al. (2010). Inhibition of tumourigenicity of small cell lung cancer cells by suppressing Id3 expression. *Int J Oncol*, 37(3), 595-603.
- Kawedia**, J. D., Nieman, M. L., Boivin, G. P., Melvin, J. E., Kikuchi, K., Hand, A. R., et al. (2007). Interaction between transcellular and paracellular water transport pathways through Aquaporin 5 and the tight junction complex. *Proc Natl Acad Sci U S A*, 104(9), 3621-3626. doi:10.1073/pnas.0608384104
- Kebaabetswe**, L. P., Haick, A. K., & Miura, T. A. (2013). Differentiated phenotypes of primary murine alveolar epithelial cells and their susceptibility to infection by respiratory viruses. *Virus Res*, 175(2), 110-119. doi:10.1016/j.virusres.2013.04.008
- Kemp**, S. J., Thorley, A. J., Gorelik, J., Seckl, M. J., O'Hare, M. J., Arcaro, A., et al. (2008). Immortalization of human alveolar epithelial cells to investigate nanoparticle uptake. *Am J Respir Cell Mol Biol*, 39(5), 591-597. doi:10.1165/rcmb.2007-0334OC
- Kim**, K. J., Borok, Z., & Crandall, E. D. (2001). A useful in vitro model for transport studies of alveolar epithelial barrier. *Pharm Res*, 18(3), 253-255.

References

- Kim**, Y., Kim, H. S., Cui, Z. Y., Lee, H. S., Ahn, J. S., Park, C. K., et al. (2009). Clinicopathological implications of EpCAM expression in adenocarcinoma of the lung. *Anticancer Res*, 29(5), 1817-1822.
- Klein**, S. G., Hennen, J., Serchi, T., Blomeke, B., & Gutleb, A. C. (2011). Potential of coculture in vitro models to study inflammatory and sensitizing effects of particles on the lung. *Toxicol In Vitro*, 25(8), 1516-1534. doi:10.1016/j.tiv.2011.09.006
- Kreja**, L., & Seidel, H. J. (2002). On the cytotoxicity of some microbial volatile organic compounds as studied in the human lung cell line A549. *Chemosphere*, 49(1), 105-110.
- Kuehn**, A., Kletting, S., de Souza Carvalho-Wodarz, C., Repnik, U., Griffiths, G., Fischer, U., et al. (2016). Human alveolar epithelial cells expressing tight junctions to model the air-blood barrier. *ALTEX*. doi:10.14573/altex.1511131
- Landsiedel**, R., Sauer, U. G., Ma-Hock, L., Schnekenburger, J., & Wiemann, M. (2014). Pulmonary toxicity of nanomaterials: a critical comparison of published in vitro assays and in vivo inhalation or instillation studies. *Nanomedicine (Lond)*, 9(16), 2557-2585. doi:10.2217/nnm.14.149
- Lee**, E. J., Vunjak-Novakovic, G., Wang, Y., & Niklason, L. E. (2009). A biocompatible endothelial cell delivery system for in vitro tissue engineering. *Cell Transplant*, 18(7), 731-743. doi:10.3727/096368909X470919
- Lefebvre**, M. A., Meuling, W. J., Engel, R., Coroama, M. C., Renner, G., Pape, W., et al. (2012). Consumer inhalation exposure to formaldehyde from the use of personal care products/cosmetics. *Regul Toxicol Pharmacol*, 63(1), 171-176. doi:10.1016/j.yrtph.2012.02.011
- Lehmann**, A. D., Daum, N., Bur, M., Lehr, C. M., Gehr, P., & Rothen-Rutishauser, B. M. (2011). An in vitro triple cell co-culture model with primary cells mimicking the human alveolar epithelial barrier. *Eur J Pharm Biopharm*, 77(3), 398-406. doi:10.1016/j.ejpb.2010.10.014
- Leighton**, J., & Kline, I. (1954). Studies on human cancer using sponge matrix tissue culture. II. Invasion of connective tissue by carcinoma (strain HeLa). *Tex Rep Biol Med*, 12(4), 865-873.
- Lestari**, F., Hayes, A. J., Green, A. R., & Chattopadhyay, G. (2012). In vitro cytotoxicity and morphological assessment of smoke from polymer combustion in human lung derived cells (A549). *Int J Hyg Environ Health*, 215(3), 320-332. doi:10.1016/j.ijeh.2011.12.006
- Lian**, J. B., Stein, G. S., Bortell, R., & Owen, T. A. (1991). Phenotype suppression: a postulated molecular mechanism for mediating the relationship of proliferation and differentiation by Fos/Jun interactions at AP-1 sites in steroid responsive promoter elements of tissue-specific genes. *J Cell Biochem*, 45(1), 9-14. doi:10.1002/jcb.240450106
- Lin**, H., Li, H., Cho, H.-J., Bian, S., Roh, H.-J., Lee, M.-K., et al. (2007). *Air-Liquid Interface (ALI) culture of human bronchial epithelial cell monolayers as an in vitro model for airway drug transport studies* (Vol. 96).
- Lin**, Y. M., Zhang, A., Rippon, H. J., Bismarck, A., & Bishop, A. E. (2010). Tissue engineering of lung: the effect of extracellular matrix on the differentiation of embryonic stem cells to pneumocytes. *Tissue Eng Part A*, 16(5), 1515-1526. doi:10.1089/ten.TEA.2009.0232
- Lindl**, T. (1996). Development of human monoclonal antibodies: A review. *Cytotechnology*, 21(3), 183-193. doi:10.1007/BF00365341

References

- Lipps**, C., Klein, F., Wahlicht, T., Seiffert, V., Butueva, M., Zauers, J., et al. (2018). Expansion of functional personalized cells with specific transgene combinations. *Nat Commun*, 9(1), 994. doi:10.1038/s41467-018-03408-4
- Lipps**, C., May, T., Hauser, H., & Wirth, D. (2013). Eternity and functionality - rational access to physiologically relevant cell lines. *Biol Chem*, 394(12), 1637-1648. doi:10.1515/hsz-2013-0158
- Liu**, D., Mei, X., Wang, L., & Yang, X. (2017). RhoA inhibits apoptosis and increases proliferation of cultured SPCA1 lung cancer cells. *Molecular Medicine Reports*, 15(6), 3963-3968. doi:10.3892/mmr.2017.6545
- Louis**, N., Evelegh, C., & Graham, F. L. (1997). Cloning and sequencing of the cellular-viral junctions from the human adenovirus type 5 transformed 293 cell line. *Virology*, 233(2), 423-429. doi:10.1006/viro.1997.8597
- Maaser**, K., & Borlak, J. (2008). A genome-wide expression analysis identifies a network of EpCAM-induced cell cycle regulators. *British Journal of Cancer*, 99(10), 1635-1643. doi:10.1038/sj.bjc.6604725
- Martin**, T. A., & Jiang, W. G. (2009). Loss of tight junction barrier function and its role in cancer metastasis. *Biochimica et Biophysica Acta (BBA) - Biomembranes*, 1788(4), 872-891. doi:<https://doi.org/10.1016/j.bbamem.2008.11.005>
- Martinez**, E., Engel, E., Planell, J. A., & Samitier, J. (2009). Effects of artificial micro- and nano-structured surfaces on cell behaviour. *Ann Anat*, 191(1), 126-135. doi:10.1016/j.aanat.2008.05.006
- Matsukawa**, Y., Lee, V. H., Crandall, E. D., & Kim, K. J. (1997). Size-dependent dextran transport across rat alveolar epithelial cell monolayers. *J Pharm Sci*, 86(3), 305-309. doi:10.1021/js960352x
- May**, T., Butueva, M., Bantner, S., Markusic, D., Seppen, J., MacLeod, R. A., et al. (2010). Synthetic gene regulation circuits for control of cell expansion. *Tissue Eng Part A*, 16(2), 441-452. doi:10.1089/ten.TEA.2009.0184
- May**, T., Hauser, H., Klein, F., Zauers, J., & Schucht, R. (2016). Methods and vectors for cell immortalisation: Google Patents.
- May**, T., Hauser, H., & Wirth, D. (2004). Transcriptional control of SV40 T-antigen expression allows a complete reversion of immortalization. *Nucleic Acids Res*, 32(18), 5529-5538. doi:10.1093/nar/gkh887
- May**, T., Hauser, H., & Wirth, D. (2006). Current status of transcriptional regulation systems. *Cytotechnology*, 50(1-3), 109-119. doi:10.1007/s10616-006-9007-6
- May**, T., Hauser, H., & Wirth, D. (2007). In vitro expansion of tissue cells by conditional proliferation. *Methods Mol Med*, 140, 1-15.
- May**, T., Mueller, P. P., Weich, H., Froese, N., Deutsch, U., Wirth, D., et al. (2005). Establishment of murine cell lines by constitutive and conditional immortalization. *J Biotechnol*, 120(1), 99-110. doi:10.1016/j.jbiotec.2005.03.027
- McDowell**, E. M., Barrett, L. A., Glavin, F., Harris, C. C., & Trump, B. F. (1978). The respiratory epithelium. I. Human bronchus. *J Natl Cancer Inst*, 61(2), 539-549.
- Mescher**, A. (2016). *Junqueira's Basic Histology Text & Atlas* (14th ed.).

References

- Messier**, E. M., Mason, R. J., & Kosmider, B. (2012). Efficient and rapid isolation and purification of mouse alveolar type II epithelial cells. *Exp Lung Res*, 38(7), 363-373. doi:10.3109/01902148.2012.713077
- Mignotte**, B., Larcher, J. C., Zheng, D. Q., Esnault, C., Coulaud, D., & Feunteun, J. (1990). SV40 induced cellular immortalization: phenotypic changes associated with the loss of proliferative capacity in a conditionally immortalized cell line. *Oncogene*, 5(10), 1529-1533.
- Millien**, G., Spira, A., Hinds, A., Wang, J., Williams, M. C., & Ramirez, M. I. (2006). Alterations in gene expression in T1 alpha null lung: a model of deficient alveolar sac development. *BMC Dev Biol*, 6, 35. doi:10.1186/1471-213X-6-35
- Milyavsky**, M., Shats, I., Erez, N., Tang, X., Senderovich, S., Meerson, A., et al. (2003). Prolonged culture of telomerase-immortalized human fibroblasts leads to a premalignant phenotype. *Cancer Res*, 63(21), 7147-7157.
- Moiani**, A., Paleari, Y., Sartori, D., Mezzadra, R., Miccio, A., Cattoglio, C., et al. (2012). Lentiviral vector integration in the human genome induces alternative splicing and generates aberrant transcripts. *The Journal of Clinical Investigation*, 122(5), 1653-1666. doi:10.1172/JCI61852
- Mülhopt**, S., Dilger, M., Diabaté, S., Schlager, C., Krebs, T., Zimmermann, R., et al. (2016). Toxicity testing of combustion aerosols at the air-liquid interface with a self-contained and easy-to-use exposure system. *Journal of Aerosol Science*, 96, 38-55. doi:<https://doi.org/10.1016/j.jaerosci.2016.02.005>
- Mulugeta**, S., & Beers, M. F. (2006). Surfactant protein C: its unique properties and emerging immunomodulatory role in the lung. *Microbes Infect*, 8(8), 2317-2323. doi:10.1016/j.micinf.2006.04.009
- Munger**, K., Baldwin, A., Edwards, K. M., Hayakawa, H., Nguyen, C. L., Owens, M., et al. (2004). Mechanisms of human papillomavirus-induced oncogenesis. *J Virol*, 78(21), 11451-11460. doi:10.1128/JVI.78.21.11451-11460.2004
- Murgia**, X., Pawelzyk, P., Schaefer, U. F., Wagner, C., Willenbacher, N., & Lehr, C. M. (2016). Size-Limited Penetration of Nanoparticles into Porcine Respiratory Mucus after Aerosol Deposition. *Biomacromolecules*, 17(4), 1536-1542. doi:10.1021/acs.biomac.6b00164
- Murgia**, X., Yasar, H., Carvalho-Wodarz, C., Loretz, B., Gordon, S., Schwarzkopf, K., et al. (2017). Modelling the bronchial barrier in pulmonary drug delivery: A human bronchial epithelial cell line supplemented with human tracheal mucus. *Eur J Pharm Biopharm*, 118, 79-88. doi:10.1016/j.ejpb.2017.03.020
- Nickel**, S., Clerkin, C. G., Selo, M. A., & Ehrhardt, C. (2016). Transport mechanisms at the pulmonary mucosa: implications for drug delivery. *Expert Opin Drug Deliv*, 13(5), 667-690. doi:10.1517/17425247.2016.1140144
- Nitta**, M., Katabuchi, H., Otake, H., Tashiro, H., Yamaizumi, M., & Okamura, H. (2001). Characterization and tumorigenicity of human ovarian surface epithelial cells immortalized by SV40 large T antigen. *Gynecol Oncol*, 81(1), 10-17. doi:10.1006/gyno.2000.6084
- O'Hare**, M. J., Bond, J., Clarke, C., Takeuchi, Y., Atherton, A. J., Berry, C., et al. (2001). Conditional immortalization of freshly isolated human mammary fibroblasts and endothelial cells. *Proc Natl Acad Sci U S A*, 98(2), 646-651. doi:10.1073/pnas.98.2.646

References

- Olsen**, C. O., Isakson, B. E., Seedorf, G. J., Lubman, R. L., & Boitano, S. (2005). Extracellular matrix-driven alveolar epithelial cell differentiation in vitro. *Exp Lung Res*, 31(5), 461-482.
- Pak**, M. G., Shin, D. H., Lee, C. H., & Lee, M. K. (2012). Significance of EpCAM and TROP2 expression in non-small cell lung cancer. *World J Surg Oncol*, 10, 53. doi:10.1186/1477-7819-10-53
- Pan**, F., Han, L., Zhang, Y., Yu, Y., & Liu, J. (2015). Optimization of Caco-2 and HT29 co-culture in vitro cell models for permeability studies. *Int J Food Sci Nutr*, 66(6), 680-685. doi:10.3109/09637486.2015.1077792
- Patil**, J. S., & Sarasija, S. (2012). Pulmonary drug delivery strategies: A concise, systematic review. *Lung India : Official Organ of Indian Chest Society*, 29(1), 44-49. doi:10.4103/0970-2113.92361
- Patriarca**, C., Macchi, R. M., Marschner, A. K., & Mellstedt, H. (2012). Epithelial cell adhesion molecule expression (CD326) in cancer: a short review. *Cancer Treat Rev*, 38(1), 68-75. doi:10.1016/j.ctrv.2011.04.002
- Patton**, J. S., & Byron, P. R. (2007). Inhaling medicines: delivering drugs to the body through the lungs. *Nat Rev Drug Discov*, 6(1), 67-74. doi:10.1038/nrd2153
- Qian**, Z., Travanty, E. A., Oko, L., Edeen, K., Berglund, A., Wang, J., et al. (2013). Innate immune response of human alveolar type II cells infected with severe acute respiratory syndrome-coronavirus. *Am J Respir Cell Mol Biol*, 48(6), 742-748. doi:10.1165/rcmb.2012-0339OC
- Quintana**, A. M., Landolt, G. A., Annis, K. M., & Hussey, G. S. (2011). Immunological characterization of the equine airway epithelium and of a primary equine airway epithelial cell culture model. *Vet Immunol Immunopathol*, 140(3-4), 226-236. doi:10.1016/j.vetimm.2010.12.008
- R. Mathias**, N., Yamashita, F., & Lee, V. (1996). *Respiratory epithelial cell culture models for evaluation of ion and drug transport* (Vol. 22).
- Raesch**, S. S., Tenzer, S., Storck, W., Rurainski, A., Selzer, D., Ruge, C. A., et al. (2015). Proteomic and Lipidomic Analysis of Nanoparticle Corona upon Contact with Lung Surfactant Reveals Differences in Protein, but Not Lipid Composition. *ACS Nano*, 9(12), 11872-11885. doi:10.1021/acsnano.5b04215
- Ramirez**, M. I., Millien, G., Hinds, A., Cao, Y., Seldin, D. C., & Williams, M. C. (2003). T1alpha, a lung type I cell differentiation gene, is required for normal lung cell proliferation and alveolus formation at birth. *Dev Biol*, 256(1), 61-72.
- Ramirez**, R. D., Sheridan, S., Girard, L., Sato, M., Kim, Y., Pollack, J., et al. (2004). Immortalization of human bronchial epithelial cells in the absence of viral oncoproteins. *Cancer Res*, 64(24), 9027-9034. doi:10.1158/0008-5472.CAN-04-3703
- Razani**, B., Engelmann, J. A., Wang, X. B., Schubert, W., Zhang, X. L., Marks, C. B., et al. (2001). Caveolin-1 null mice are viable but show evidence of hyperproliferative and vascular abnormalities. *J Biol Chem*, 276(41), 38121-38138. doi:10.1074/jbc.M105408200
- Rice**, W. R., Conkright, J. J., Na, C. L., Ikegami, M., Shannon, J. M., & Weaver, T. E. (2002). Maintenance of the mouse type II cell phenotype in vitro. *Am J Physiol Lung Cell Mol Physiol*, 283(2), L256-264. doi:10.1152/ajplung.00302.2001

References

- Robertson**, D. M., Li, L., Fisher, S., Pearce, V. P., Shay, J. W., Wright, W. E., et al. (2005). Characterization of growth and differentiation in a telomerase-immortalized human corneal epithelial cell line. *Invest Ophthalmol Vis Sci*, 46(2), 470-478. doi:10.1167/iovs.04-0528
- Rokicki**, W., Rokicki, M., Wojtacha, J., & Dżelijjili, A. (2016). The role and importance of club cells (Clara cells) in the pathogenesis of some respiratory diseases. *Kardiochirurgia i Torakochirurgia Polska = Polish Journal of Cardio-Thoracic Surgery*, 13(1), 26-30. doi:10.5114/kitp.2016.58961
- Roth**, F. D., Quintar, A. A., Leimgruber, C., Garcia, L., Uribe Echevarria, E. M., Torres, A. I., et al. (2013). Restoration of the normal Clara cell phenotype after chronic allergic inflammation. *Int J Exp Pathol*, 94(6), 399-411. doi:10.1111/iep.12041
- Rubas**, W., Cromwell, M. E., Shahrokh, Z., Villagran, J., Nguyen, T. N., Wellton, M., et al. (1996). Flux measurements across Caco-2 monolayers may predict transport in human large intestinal tissue. *J Pharm Sci*, 85(2), 165-169. doi:10.1021/jf950267+
- Saha**, P., Kim, K. J., & Lee, V. H. (1996). A primary culture model of rabbit conjunctival epithelial cells exhibiting tight barrier properties. *Curr Eye Res*, 15(12), 1163-1169.
- Sakamoto**, A., Matsumaru, T., Yamamura, N., Suzuki, S., Uchida, Y., Tachikawa, M., et al. (2015). Drug Transporter Protein Quantification of Immortalized Human Lung Cell Lines Derived from Tracheobronchial Epithelial Cells (Calu-3 and BEAS2-B), Bronchiolar-Alveolar Cells (NCI-H292 and NCI-H441), and Alveolar Type II-like Cells (A549) by Liquid Chromatography-Tandem Mass Spectrometry. *J Pharm Sci*, 104(9), 3029-3038. doi:10.1002/jps.24381
- Salomon**, J. J., & Ehrhardt, C. (2012). Organic cation transporters in the blood-air barrier: expression and implications for pulmonary drug delivery. *Ther Deliv*, 3(6), 735-747.
- Samadikuchaksaraei**, A., & Bishop, A. E. (2006). Derivation and Characterization of Alveolar Epithelial Cells From Murine Embryonic Stem Cells In Vitro. In K. Turksen (Ed.), *Embryonic Stem Cell Protocols: Volume 2: Differentiation Models* (pp. 233-248). Totowa, NJ: Humana Press.
- Sanders**, N., Rudolph, C., Braeckmans, K., De Smedt, S. C., & Demeester, J. (2009). Extracellular barriers in respiratory gene therapy. *Adv Drug Deliv Rev*, 61(2), 115-127. doi:10.1016/j.addr.2008.09.011
- Sandhu**, U., Cebula, M., Behme, S., Riemer, P., Wodarczyk, C., Metzger, D., et al. (2011). Strict control of transgene expression in a mouse model for sensitive biological applications based on RMCE compatible ES cells. *Nucleic Acids Res*, 39(1), e1. doi:10.1093/nar/gkq868
- Sapich**, S., Hittinger, M., Hendrix-Jastrzebski, R., Repnik, U., Griffiths, G., May, T., et al. (2018). Murine alveolar epithelial cells and their lentivirus-mediated immortalisation. *Altern Lab Anim*, 46(2), 73-89.
- Sarmento**, B., Andrade, F., Silva, S. B. d., Rodrigues, F., das Neves, J., & Ferreira, D. (2012). Cell-based in vitro models for predicting drug permeability. *Expert Opinion on Drug Metabolism & Toxicology*, 8(5), 607-621. doi:10.1517/17425255.2012.673586
- Sauer**, K. A., Scholtes, P., Karwot, R., & Finotto, S. (2006). Isolation of CD4+ T cells from murine lungs: a method to analyze ongoing immune responses in the lung. *Nat Protoc*, 1(6), 2870-2875. doi:10.1038/nprot.2006.435

References

- Sauer**, U. G., Vogel, S., Hess, A., Kolle, S. N., Ma-Hock, L., van Ravenzwaay, B., *et al.* (2013). In vivo-in vitro comparison of acute respiratory tract toxicity using human 3D airway epithelial models and human A549 and murine 3T3 monolayer cell systems. *Toxicol In Vitro*, 27(1), 174-190. doi:10.1016/j.tiv.2012.10.007
- Scherliess**, R. (2011). The MTT assay as tool to evaluate and compare excipient toxicity in vitro on respiratory epithelial cells. *Int J Pharm*, 411(1-2), 98-105. doi:10.1016/j.ijpharm.2011.03.053
- Schmidt**, H., Michel, C., Braubach, P., Fauler, M., Neubauer, D., Thompson, K. E., *et al.* (2017). Water Permeability Adjusts Resorption in Lung Epithelia to Increased Apical Surface Liquid Volumes. *Am J Respir Cell Mol Biol*, 56(3), 372-382. doi:10.1165/rccb.2016-0161OC
- Schmitz**, M., Driesch, C., Beer-Grondke, K., Jansen, L., Runnebaum, I. B., & Durst, M. (2012). Loss of gene function as a consequence of human papillomavirus DNA integration. *Int J Cancer*, 131(5), E593-602. doi:10.1002/ijc.27433
- Schneeberger**, E. E., & Lynch, R. D. (2004). The tight junction: a multifunctional complex. *Am J Physiol Cell Physiol*, 286(6), C1213-1228. doi:10.1152/ajpcell.00558.2003
- Schwerk**, J., Koster, M., Hauser, H., Rohde, M., Fulde, M., Hornef, M. W., *et al.* (2013). Generation of mouse small intestinal epithelial cell lines that allow the analysis of specific innate immune functions. *PLoS One*, 8(8), e72700. doi:10.1371/journal.pone.0072700
- Seluanov**, A., Vaidya, A., & Gorbunova, V. (2010). Establishing primary adult fibroblast cultures from rodents. *J Vis Exp*(44). doi:10.3791/2033
- Singer**, M. M., & Tjeerdema, R. S. (1993). Fate and effects of the surfactant sodium dodecyl sulfate. *Rev Environ Contam Toxicol*, 133, 95-149.
- Sinha**, M., & Lowell, C. A. (2016). Isolation of Highly Pure Primary Mouse Alveolar Epithelial Type II Cells by Flow Cytometric Cell Sorting. *Bio Protoc*, 6(22). doi:10.21769/BioProtoc.2013
- Spitzer**, D., Hauser, H., & Wirth, D. (1999). Complement-protected amphotropic retroviruses from murine packaging cells. *Hum Gene Ther*, 10(11), 1893-1902. doi:10.1089/10430349950017572
- Srinivasan**, B., Kolli, A. R., Esch, M. B., Abaci, H. E., Shuler, M. L., & Hickman, J. J. (2015). TEER measurement techniques for in vitro barrier model systems. *J Lab Autom*, 20(2), 107-126. doi:10.1177/2211068214561025
- Stamatovic**, S. M., Johnson, A. M., Keep, R. F., & Andjelkovic, A. V. (2016). Junctional proteins of the blood-brain barrier: New insights into function and dysfunction. *Tissue Barriers*, 4(1), e1154641. doi:10.1080/21688370.2016.1154641
- Steimer**, A., Franke, H., Haltner-Ukomado, E., Laue, M., Ehrhardt, C., & Lehr, C. M. (2007). Monolayers of porcine alveolar epithelial cells in primary culture as an in vitro model for drug absorption studies. *Eur J Pharm Biopharm*, 66(3), 372-382. doi:10.1016/j.ejpb.2006.11.006
- Steimer**, A., Haltner, E., & Lehr, C. M. (2005). Cell culture models of the respiratory tract relevant to pulmonary drug delivery. *J Aerosol Med*, 18(2), 137-182. doi:10.1089/jam.2005.18.137

References

- Steimer**, A., Laue, M., Franke, H., Haltner-Ukomado, E., & Lehr, C. M. (2006). Porcine alveolar epithelial cells in primary culture: morphological, bioelectrical and immunocytochemical characterization. *Pharm Res*, 23(9), 2078-2093. doi:10.1007/s11095-006-9057-7
- Stevens**, J. B., Horne, S. D., Abdallah, B. Y., Ye, C. J., & Heng, H. H. (2013). Chromosomal instability and transcriptome dynamics in cancer. *Cancer Metastasis Rev*, 32(3-4), 391-402. doi:10.1007/s10555-013-9428-6
- Stevenson**, M. (2002). Molecular biology of lentivirus-mediated gene transfer. *Curr Top Microbiol Immunol*, 261, 1-30.
- Susewind**, J., de Souza Carvalho-Wodarz, C., Repnik, U., Collnot, E. M., Schneider-Daum, N., Griffiths, G. W., et al. (2016). A 3D co-culture of three human cell lines to model the inflamed intestinal mucosa for safety testing of nanomaterials. *Nanotoxicology*, 10(1), 53-62. doi:10.3109/17435390.2015.1008065
- Tam**, A., Wadsworth, S., Dorscheid, D., Man, S. F., & Sin, D. D. (2011). The airway epithelium: more than just a structural barrier. *Ther Adv Respir Dis*, 5(4), 255-273. doi:10.1177/1753465810396539
- Thorley**, A. J., Ruenraroengsak, P., Potter, T. E., & Tetley, T. D. (2014). Critical determinants of uptake and translocation of nanoparticles by the human pulmonary alveolar epithelium. *ACS Nano*, 8(11), 11778-11789. doi:10.1021/nn505399e
- Todaro**, G. J., & Green, H. (1963). Quantitative studies of the growth of mouse embryo cells in culture and their development into established lines. *J Cell Biol*, 17, 299-313.
- Tomita**, M., Hayashi, M., & Awazu, S. (1996). Absorption-enhancing mechanism of EDTA, caprate, and decanoylcarnitine in Caco-2 cells. *J Pharm Sci*, 85(6), 608-611. doi:10.1021/js9504604
- Traggiai**, E. (2012). Immortalization of human B cells: analysis of B cell repertoire and production of human monoclonal antibodies. *Methods Mol Biol*, 901, 161-170. doi:10.1007/978-1-61779-931-0_10
- Trzpis**, M., McLaughlin, P. M., de Leij, L. M., & Harmsen, M. C. (2007). Epithelial cell adhesion molecule: more than a carcinoma marker and adhesion molecule. *Am J Pathol*, 171(2), 386-395. doi:10.2353/ajpath.2007.070152
- Tsicopoulos**, A., de Nadai, P., & Glineur, C. (2013). Environmental and genetic contribution in airway epithelial barrier in asthma pathogenesis. *Curr Opin Allergy Clin Immunol*, 13(5), 495-499. doi:10.1097/ACI.0b013e328364e9fe
- Tsukita**, S., Furuse, M., & Itoh, M. (2001). Multifunctional strands in tight junctions. *Nat Rev Mol Cell Biol*, 2(4), 285-293. doi:10.1038/35067088
- Uchenna Agu**, R., Ikechukwu Ugwoke, M., Armand, M., Kinget, R., & Verbeke, N. (2001). The lung as a route for systemic delivery of therapeutic proteins and peptides. *Respiratory Research*, 2(4), 198-209. doi:10.1186/rr58
- United Nations**, N. U. (2011). Globally Harmonized System of Categorization and Labelling of Chemicals (GHS). *Fourth revised edition*.

References

- Urlinger**, S., Baron, U., Thellmann, M., Hasan, M. T., Bujard, H., & Hillen, W. (2000). Exploring the sequence space for tetracycline-dependent transcriptional activators: novel mutations yield expanded range and sensitivity. *Proc Natl Acad Sci U S A*, 97(14), 7963-7968. doi:10.1073/pnas.130192197
- van den Bogaard**, E. H., Dailey, L. A., Thorley, A. J., Tetley, T. D., & Forbes, B. (2009). Inflammatory response and barrier properties of a new alveolar type 1-like cell line (TT1). *Pharm Res*, 26(5), 1172-1180. doi:10.1007/s11095-009-9838-x
- Van Driessche**, W., Kreindler, J. L., Malik, A. B., Margulies, S., Lewis, S. A., & Kim, K. J. (2007). Interrelations/cross talk between transcellular transport function and paracellular tight junctional properties in lung epithelial and endothelial barriers. *Am J Physiol Lung Cell Mol Physiol*, 293(3), L520-524. doi:10.1152/ajplung.00218.2007
- Van Itallie**, C. M., & Anderson, J. M. (2006). Claudins and epithelial paracellular transport. *Annu Rev Physiol*, 68, 403-429. doi:10.1146/annurev.physiol.68.040104.131404
- Wang**, J., Edeen, K., Manzer, R., Chang, Y., Wang, S., Chen, X., et al. (2007). Differentiated human alveolar epithelial cells and reversibility of their phenotype in vitro. *Am J Respir Cell Mol Biol*, 36(6), 661-668. doi:10.1165/rcmb.2006-0410OC
- Wang**, J., Nikrad, M. P., Phang, T., Gao, B., Alford, T., Ito, Y., et al. (2011). Innate immune response to influenza A virus in differentiated human alveolar type II cells. *Am J Respir Cell Mol Biol*, 45(3), 582-591. doi:10.1165/rcmb.2010-0108OC
- Wang**, P. M., & Martin, W. J. (2013). Evidence of donor epithelial type 2 cell engraftment in bleomycin-injured murine lung after airway delivery. *The FASEB Journal*, 27(1 Supplement), 1166.1116.
- Wang**, S., & Hubmayr, R. D. (2011). Type I Alveolar Epithelial Phenotype in Primary Culture. *American Journal of Respiratory Cell and Molecular Biology*, 44(5), 692-699. doi:10.1165/rcmb.2009-0359OC
- Wang**, X., Wang, N., Yuan, L., Li, N., Wang, J., & Yang, X. (2016). Exploring tight junction alteration using double fluorescent probe combination of lanthanide complex with gold nanoclusters. *Sci Rep*, 6, 32218. doi:10.1038/srep32218
- Wang**, Z., & Zhang, Q. (2004). Transport of proteins and peptides across human cultured alveolar A549 cell monolayer. *Int J Pharm*, 269(2), 451-456.
- Weibel**, E. R. (2011). *Lung Cell Biology Comprehensive Physiology*: John Wiley & Sons, Inc.
- Wikenheiser**, K. A., Clark, J. C., Linnoila, R. I., Stahlman, M. T., & Whitsett, J. A. (1992). Simian virus 40 large T antigen directed by transcriptional elements of the human surfactant protein C gene produces pulmonary adenocarcinomas in transgenic mice. *Cancer Res*, 52(19), 5342-5352.
- Wikenheiser**, K. A., Vorbroker, D. K., Rice, W. R., Clark, J. C., Bachurski, C. J., Oie, H. K., et al. (1993). Production of immortalized distal respiratory epithelial cell lines from surfactant protein C/simian virus 40 large tumor antigen transgenic mice. *Proc Natl Acad Sci U S A*, 90(23), 11029-11033.
- Winter**, M. J., Nagtegaal, I. D., van Krieken, J. H. J. M., & Litvinov, S. V. (2003). The Epithelial Cell Adhesion Molecule (Ep-CAM) as a Morphoregulatory Molecule Is a Tool in Surgical Pathology. *The American Journal of Pathology*, 163(6), 2139-2148.

References

- Wolburg**, H., & Lippoldt, A. (2002). Tight junctions of the blood-brain barrier: development, composition and regulation. *Vascul Pharmacol*, 38(6), 323-337.
- Wolf** L., Sapich S., Honecker, A., Jungnickel, C., Seiler, F., Bischoff, M., Wonnenberg, B., et al. (2016). IL-17A-mediated expression of epithelial IL-17C promotes inflammation during acute *Pseudomonas aeruginosa* pneumonia. *Am J Physiol Lung Cell Mol Physiol*, 311(5), L1015-L1022. doi:10.1152/ajplung.00158.2016
- Wright**, J. R. (2005). Immunoregulatory functions of surfactant proteins. *Nat Rev Immunol*, 5(1), 58-68. doi:10.1038/nri1528
- Wu**, N. H., Yang, W., Beineke, A., Dijkman, R., Matrosovich, M., Baumgartner, W., et al. (2016). The differentiated airway epithelium infected by influenza viruses maintains the barrier function despite a dramatic loss of ciliated cells. *Sci Rep*, 6, 39668. doi:10.1038/srep39668
- Wunderlich**, S., Gruh, I., Winkler, M. E., Beier, J., Radtke, K., Schmiedl, A., et al. (2008). Type II pneumocyte-restricted green fluorescent protein expression after lentiviral transduction of lung epithelial cells. *Hum Gene Ther*, 19(1), 39-52. doi:10.1089/hum.2006.0180
- Yacobi**, N. R., Malmstadt, N., Fazlollahi, F., DeMaio, L., Marchelletta, R., Hamm-Alvarez, S. F., et al. (2010). Mechanisms of alveolar epithelial translocation of a defined population of nanoparticles. *Am J Respir Cell Mol Biol*, 42(5), 604-614. doi:10.1165/rcmb.2009-0138OC
- Yacobi**, N. R., Phuleria, H. C., Demaio, L., Liang, C. H., Peng, C. A., Sioutas, C., et al. (2007). Nanoparticle effects on rat alveolar epithelial cell monolayer barrier properties. *Toxicol In Vitro*, 21(8), 1373-1381. doi:10.1016/j.tiv.2007.04.003
- Yamasaki**, K., Kawasaki, S., Young, R. D., Fukuoka, H., Tanioka, H., Nakatsukasa, M., et al. (2009). Genomic aberrations and cellular heterogeneity in SV40-immortalized human corneal epithelial cells. *Invest Ophthalmol Vis Sci*, 50(2), 604-613. doi:10.1167/iovs.08-2239
- Yin**, H., & Kassner, M. (2016). In Vitro High-Throughput RNAi Screening to Accelerate the Process of Target Identification and Drug Development. *Methods Mol Biol*, 1470, 137-149. doi:10.1007/978-1-4939-6337-9_11
- Zhang**, D., Zhang, J. Y., Dai, S. D., Liu, S. L., Liu, Y., Tang, N., et al. (2014). Co-expression of delta-catenin and RhoA is significantly associated with a malignant lung cancer phenotype. *Int J Clin Exp Pathol*, 7(7), 3724-3732.
- Zheng**, D., Soh, B. S., Yin, L., Hu, G., Chen, Q., Choi, H., et al. (2017). Differentiation of Club Cells to Alveolar Epithelial Cells In Vitro. *Sci Rep*, 7, 41661. doi:10.1038/srep41661

Scientific output

Articles published in Peer-reviewed Journals

- **Murine alveolar epithelial cells and their lentivirus-mediated immortalization** (Sapich et al., 2018)

Alternatives to Laboratory Animals (ATLA)
Volume 46, Issue 2 – May 2018, pages 73-89.

Sapich, Hittinger, Hendrix-Jastrzebski, Repnik, Griffiths, May, Wirth, Bals, Schneider-Daum, Lehr.

IL-17A-mediated expression of epithelial IL-17C promotes inflammation during acute *Pseudomonas aeruginosa* pneumonia

American Journal Physiology - Lung Cellular and Molecular Physiology
Volume 311, Issue 5 – November 2016, pages L1015-L1022.

Wolf*, **Sapich***, Honecker, Jungnickel, Seiler, Bischoff, Wonnenberg, Herr, Schneider-Daum, Lehr, Bals, Beisswenger.

*equally contributing first authors

Oral presentations

- **6th HZI Annual PhD retreat and ESR Symposium**
December 15 – 17, 2014 in Goslar-Hahnenklee, Germany
- **HZI Graduate School – 6th International PhD Symposium**
December 12, 2013 in Braunschweig, Germany

Poster presentations

- **International Society of Aerosols in Medicine Congress**
20. ISAM 2015 Congress, May 30 – June 3, 2015 in Munich, Germany
- **Lung Regeneration and beyond - BREATH meets REBIRTH**
3rd International DZL Symposium, May 8 – 10, 2014 in Hannover, Germany
- **Biological Barriers - 10th International Congress and Workshop**
February 16 – 21, 2014 in Saarbrücken, Germany
- **Pharmaceutical sciences devoted to infection research**
3rd International HIPS Symposium, June 18, 2013 in Saarbrücken, Germany
- **HZI Graduate School – 6th International PhD Symposium**
December 12, 2013 in Braunschweig, Germany

Curriculum vitae

PERSONAL INFORMATION

Name Sandra Sapich
Date of birth December 9, 1986
Place of birth Zweibrücken, Germany

EDUCATION

- | | |
|-------------------|---|
| 08/2012 – 11/2018 | Doctoral thesis
Helmholtz Institute for Pharmaceutical Research Saarland
and Helmholtz Centre for Infection Research
Saarbrücken and Braunschweig, Germany
Title: Primary and immortalized murine alveolar epithelial
cells as novel <i>in vitro</i> systems for preclinical studies
Supervision: Prof. Dr. Claus-Michael Lehr |
| 06/2011 – 04/2012 | Diploma thesis (M. sc. equivalent)
Center of Human and Molecular Biology
Institute of Virology
Saarland University Medical Center, Homburg, Germany
Title: Target gene identification of deregulated microRNAs in
prostate cancer
Supervision: Prof. Dr. Friedrich Grässer |
| 10/2006 – 06/2011 | Study of Human and Molecular Biology
Majors: Virology & Immunology, Cell Biology and
Pharmacology
Saarland University, Saarbrücken, Germany |
| 08/1997 – 03/2006 | Abitur (University Entrance Qualification)
Helmholtz-Gymnasium Zweibrücken, Germany |

WORK EXPERIENCE & STAYS ABROAD

- | | |
|-------------------|---|
| 08/2016 – 06/2017 | Trainee in Communication & Process Improvement
Pharmaceutical Development Unit
for parenteral, topical & ophthalmic dosage forms
Technical Research & Development
Novartis Pharma AG, Basel, Switzerland |
| 06/2010 – 12/2010 | Laboratory internship
Department of Biotechnology
Universidade Estadual Paulista
Assis, São Paulo, Brazil |

Danksagung

Allen voran bedanke ich mich bei meinem Doktorvater Prof. Dr. Claus-Michael Lehr und meiner Betreuerin Dr. Nicole Schneider-Daum für die Bereitstellung meines Themas, interessante und motivierende Diskussionen, sowie für eure Geduld und Unterstützung in der „heißen Phase“ für den erfolgreichen Abschluss dieser Arbeit und das Publizieren des entsprechenden Manuskripts. Nicole, dir danke ich außerdem für das Korrekturlesen dieser Arbeit und die perfektionistische Arbeitsweise, die du mir vermittelt hast!

Des Weiteren bedanke ich mich recht herzlich bei Herrn Prof. Dr. Robert Bals für die Anfertigung des Zweitgutachtens, sowie bei der gesamten Prüfungskommission.

Ein großes Dankeschön geht auch an Dagmar Wirth und Tobias May vom Helmholtz-Zentrum für Infektionsforschung bzw. InSCREENeX in Braunschweig, wo ich in mehr als eineinhalb Jahren essentielle Ergebnisse und Erkenntnisse für diese Arbeit erzielen konnte. Danke für die Betreuung und herzliche Aufnahme in euren Arbeitskreis!

Natürlich danke ich auch allen Kollegen der „DDEL“-Gruppe am HIPS, der „MSYS“-Gruppe am HZI und des Instituts für Biopharmazie der Universität des Saarlandes, die mich in irgendeiner Form unterstützt und begleitet haben. In allen drei Institutionen herrschte stets eine angenehme Arbeitsatmosphäre und eine helfende Hand ließ nie lange auf sich warten. Besonders möchte ich mich bei Marius bedanken, der mir vor allem beim Planen, Verfassen und Publizieren des Manuskripts mit vollem Einsatz zur Seite gestanden hat.

Mein ganz besonderer Dank gilt auch den lieben Menschen aus meinem privaten Umfeld, die mich auf dem Weg zum Doktortitel begleitet, motiviert, gepusht und aufgebaut haben. Ohne eure Unterstützung könnte ich diese Zeilen heute nicht schreiben!

An mein Zuhause in den weltbesten WGs in Saarbrücken und Braunschweig sowie an die wunderbaren Leute, die ich in dieser Zeit kennenlernen durfte, werde ich immer gerne zurückdenken!

Danke an Chrissi, Anna, Katja, Regina, Bernadette, Jenny, Evelyn, Lieblingsnachbar Yassin und allen WG-Besuchern für unzählige gemeinsame Küchenabende, weltbewegende Gespräche, die verrücktesten Motto-Partys, unfassbar viel Spaß und die aufbauenden Worte, wenn es mal nicht so lief...

– good times and crazy friends make the best memories!

In diesem Sinne gebührt dir, liebe Chrissi, ein megagroßes Dankeschön. Du hast mich vom ersten bis zum letzten Tag am HIPS und darüber hinaus begleitet - als Kollegin, Mitbewohnerin, aber vor allem als wertvolle Freundin - an guten, wie an schlechten Tagen. Außerdem durfte ich durch dich auch die Wuppertal-Crew kennen und lieben lernen!

Nina, dir danke ich für die positiven „vibes“ während des Schreibens, den Rückenwind und ganz besonders für die durchtanzten Nächte, musikalischen Highlights und einfach schöne Zeiten an den verschiedensten Orten dieser Welt, durch die ich dem Doktoranden-Alltag auch mal entfliehen konnte!

Wolf, mein größter Schatz, auch du hast mich über die letzten Jahre hinweg begleitet und wir haben dabei eine besondere Geschichte geschrieben, deren Wendung mich unfassbar glücklich macht! Ich danke dir von ganzem Herzen, dass du dein Reich mit mir (und meinen Launen) teilst, mich motivierst die Dinge stets positiv anzugehen und mich in meinen Vorhaben unterstützt!!! Mit dem Abschluss dieser Arbeit steht auch uns ein neues Kapitel bevor und ich freue mich sehr dich an meiner Seite zu haben! Ich liebe dich!

Der größte Dank kommt zum Schluss und geht an meine Eltern und Familie, die immer und ausnahmslos für mich da waren und ohne die ich nicht der Mensch geworden wäre, der ich heute bin – eure konstante Unterstützung hat mir den nötigen Rückhalt gegeben, um durchzuhalten und mich immer wieder aufs Neue zu motivieren!

In Gedanken widme ich diese Arbeit meiner verstorbenen Oma und danke ihr von ganzem Herzen für die Zeit, die ich mit ihr verbringen durfte, für ihre bedingungslose Liebe und den unaufhörlichen Glauben an mich, auch wenn ich ihn selbst verloren hatte.

♥♥♥ DANKE ♥♥♥